



APPLICATION OF NANOFUID IN AUTOMOTIVE ENGINE RADIATORS

A THESIS

**SUBMITTED TO THE DEPARTMENT OF MECHANICAL ENGINEERING
TECHNIQUES OF POWER**

**IN PARTIAL FULFILLMENT OF THE REQUIREMENTS FOR THE
DEGREE OF MASTER THERMAL TECHNOLOGIES IN MECHANICAL
ENGINEERING TECHNIQUES OF POWER (M.TECH.)**

BY

KARAAR MAHDI SALEH

Supervised by

Prof. Dr. Dhafer Manea Hicham

Asst. Prof. Dr. Montader Almoussawi

July /2021

DECLARATION

I hereby declare that the work in this thesis is my own except for quotations and summaries, which have been duly acknowledged.

Signature:

Name: Karaar Mahdi Saleh

Date: / /2021

COMMITTEE REPORT

We certify that we have read this thesis titled " **APPLICATION OF NANOFLUID IN AUTOMOTIVE ENGINE RADIATORS** " submitted by Karaar Mahdi Saleh as examining committee, examined the student in its contents. In our opinion, the thesis is adequate for an award of the degree of Master degree of Technical Thermal Engineering.

Signature:
Name: **Prof. Dr. Dhafer M. Hachim**

(Supervisor)
Date: / / 2021

Signature:
Name: **Assist Prof. Dr. Montader Almoussawi**

(Co-Supervisor)
Date: / / 2021

Signature:
Name: **Assist Prof. Dr. Hyder H. Balla**

(Member)
Date: / / 2021

Signature:
Name: **Assist Prof. Dr. Sattar Aljabair**

(Member)
Date: / / 2021

Signature:
Name: **Prof. Dr. Akram W. Ezzat**
(Chairman)
Date: / / 2021

Approval of the Engineering Technical college – Najaf

Signature:
Name: **Ass. Prof. Dr. Hassanain G. Hameed**
Dean of Engineering Technical college – Najaf

Date: / / 2021

SUPERVISOR CERTIFICATION

I certify that this thesis entitled " **APPLICATION OF NANOFUID IN AUTOMOTIVE ENGINE RADIATORS** ", which is submitted by **Karaar Mahdi Saleh**, has been prepared under my supervision at the mechanic Techniques Engineering of Power Department, Engineering Technical College-Najaf, AL-Furat Al-Awsat Technical University, as partialfulfilment of the requirements for the Master degree of Technical Thermal Engineering.

Signature:
Name: **Prof. Dr. Dhafer M. Hachim**

(Supervisor)

Date: / / 2021

Signature:
Name: **Assist Prof. Dr. Montader Almoussawi**

(Supervisor)

Date: / / 2021

In view of the available recommendation, I forward this thesis for debateby the examining committee.

Signature:

Name: **Prof. Dr. Dhafer M. Hachim**

(Head Mechanical. Eng. Tech. of
Power Dept.)

Date: / / 2021

LINGUISTIC CERTIFICATION

This is to certify that this thesis entitled “**APPLICATION OF NANOFUID IN AUTOMOTIVE ENGINE RADIATORS**” was reviewed linguistically. Its language was amended to meet the style of the English language.

Signature:

Name: Asst Prof. Ameer Ali Hussein

Date:

ACKNOWLEDGEMENT

I would like to extend my deep respect and gratitude to the supervisors of Prof. Dr. Dhafer Manea Hicham and Asst. Prof. Dr. Montader Almoussawi for their support during the research period and their guidance to complete this study.

I extend my sincere thanks to the Dean (Ass. Prof. Dr Hassanain G. Hameed) of the Technical College of Engineering, Najaf, and the esteemed head of Mechanical. Eng. Tech. of Power Department (Prof. Dr Dhafer M. Hachim) to provide possible assistance to facilitate the study process. Special thanks go to the members of the Department for their assistance.

Thank you to my dear parents, brothers and wife for their patience, support and encouragement throughout my life.

Karaar Mahdi Saleh

2021

ABSTRACT

The performance of automotive engines can be improved by removing the amount of heat generated from internal combustion through the radiators by enhancement of coolant fluid. The use of nanofluids was one of the reasons to reduce the amount of heat and increase the thermal performance of the engine. Most base fluids have low thermal performance. However, their thermal efficiency can be increased by using nanoparticles, Nanofluids are colloidal fluids consisting of nano-sized particles <100 nm mixed with a base fluid. The aim of the study is to reduce the size of the radiator and study the economic analysis of the use of nanofluids in automobile radiators .In this work, the effect of nanofluids on the thermal performance of automotive radiators has been studied numerically and experimentally. The numerical study was done using the COMSOL Multiphysics software V.5.4 on three types of nanofluids (Al₂O₃, CuO and MWCNT) at different volume concentrations 0.5, 1, 2 % and at different flow rates 4, 6, 8 L/min with an inlet temperature of 60, 70 and 80 °C. Experiments were performed on two different automotive radiators, the regular size the smaller size by 35% approximately from the regular size radiator. The three types of nanofluids have been tested on the radiator to compare their thermal performance with respect to the base fluid. The current results were compared with previous studies with high sobriety to verify the numerical results, where we found a good agreement of 6.2% approximately, and to verify the experimental results, the results were compared with correlations representing laminar flow within the tubes, and the results showed a good agreement of 6.7% approximately. The numerical results showed that the best thermal performance was an MWCNT nanofluid, where the highest percentage of heat transfer enhancement was obtained for the Nusselt number of 25.83%, 42.37%,

and 59.7% at a volume concentration of 0.5, 1, and 2 %, respectively. The experiment results showed that the nanofluids operate with higher thermal performance than the base fluids. The highest Nusselt number when using MWCNT nanofluid was 26.6%, 42% at a volume concentration of 0.5, 1% compared to the base fluid. The economic analysis of the experimental study showed that it is possible to reduce the volume of the Automotive radiator by 35% approximately, as well as give an additional area and a decrease in the amount of coolant when using MWCNT nanofluid at a flow rate of 4 L/min and 80 °C.

LIST OF CONTENTS

DECLARATION.....	i
COMMITTEE REPORT	ii
SUPERVISOR CERTIFICATION	iii
LINGUISTIC CERTIFICATION	iv
ACKNOWLEDGEMENT	v
ABSTRACT.....	vi
LIST OF CONTENTS.....	viii
LIST OF TABLES	xi
LIST OF FIGURES	xii
CHAPTER ONE.....	2
INTRODUCTION.....	2
1.1 General	2
1.2 Heat Exchanger	3
1.2.1 Automotive Radiators	4
1.3 Nanofluids.....	5
1.4 Thermal Conductivity of Nanofluid.....	6
1.5 Types of Nanoparticles	7
1.5.1 Alumina.....	7
1.5.2 Copper Oxide (CuO)	7
1.5.6 Multi-Walled Carbon Nanotubes (MWCNT)	7
1.6 Surfactants	8
1.7 Nanofluid Preparation	9
1.7.1 The One-Step Method:.....	9
1.7.2 The Two-Step Method:	9
1.8 Advantages and Disadvantages of Nanofluids	10
Study Objectives.....	11
CHAPTER TWO.....	13
LITERATURE REVIEW.....	13
2.1 Introduction	13
2.2 Experimental Study of the of flow and heat transfer mechanism of nanofluids in automobile radiators.....	13
2.2 Numerical Study of Flow and Heat Transfer mechanism of nanofluids in automobile radiators.....	20

2.3 Summary of Literature Review	22
2.4 Scope of study	23
CHAPTER THREE.....	36
THEORETICAL ANALYSIS AND NUMERICAL SIMULATION	36
3.1 Introduction	36
3.2 Mathematical Modelling.....	36
3.2.1 Assumption for Numerical Simulation.....	36
3.2.2 Geometry.....	37
3.2.3 Governing Equations	40
3.2.4 Initial and Boundary Conditions	41
3.2.5 COMSOL Multiphysics.....	42
3.2.6 Mesh Independency	42
3.2.7 Thermophysical Properties of Nanofluid.....	44
3.2.8 Data Extraction.....	45
CHAPTER FOUR.....	49
EXPERIMENTAL WORK.....	49
4.1 Introduction	49
4.2 Experimental Setup	49
4.2.1 Radiators	51
4.2.2 Cooling Fan.....	52
4.2.3 Water Pump.....	53
4.2.4 Water Tank.....	55
4.2.5 Water Heater	55
4.2.6 Rotameter	56
4.6.7 Thermocouples	57
4.3 Nanofluid Preparation	57
4.3 Nanofluid Properties Measurement.....	60
CHAPTER FIVE.....	64
RESULTS AND DISCUSSION	64
5.1 Introduction	64
5.2 Numerical Results.....	64
5.1.1 CFD Model's Verification	64
5.1.2 Effect of Distilled Water Flow Rate in Radiators With Different Inlet Temperatures	66

5.1.3 Effect of Nanofluid Flow Rate in Radiators With Different Inlet Temperatures	70
5.2 Experimental Result	86
5.2.1 Verification of The Experimental Setup	86
5.2.2 The Effect of The Nanofluid on The Performance of Regular Size Radiator	87
5.2.3 Effect The Nanofluid Performance on Smaller Size Radiator With MWCNT	97
5.3. Comparing The Numerical Results With The Experimental Results of Nanofluids	101
5.4 Economic Analysis Using For Nanofluid in Radiators.....	102
CHAPTER SIX.....	105
CONCLUSIONS AND RECOMMENDATIONS	105
6.1 Conclusions	105
6.2 Recommendations.....	107
References	108
APPENDIX - A	119
THERMOCOUPLE’S CALIBRATION.....	119
APPENDIX – B.....	125
NANOPARTICLE’S PROPERTIES.....	125
APPENDIX – C.....	128
APPENDIX – D	131
BLOCK DIAGRAM FOR OUR STUDY	131
APPENDIX - E.....	132
WIND SPEED CALIBRATION.....	132
APPENDIX – F	133
LIST OF PUBLICATIONS	133
الخلاصه	135

LIST OF TABLES

Table 1.1 Materials of nanoparticles.....	3
Table 1.2 The thermal conductivity of common nanomaterials [12]	6
Table 1.3 Advantages and Disadvantages of Nano-Fluid.....	10
Table 2.1 Summary of experimental study for Alumina or Aluminum Oxide (Al_2O_3) Nanoparticles.....	24
Table 2.2 Summary of experimental study for Copper (Cu) Nanoparticles.....	26
Table 2.3 Summary of experimental study for Copper Oxide (CuO) Nanoparticles.....	27
Table 2.4 Summary of experimental study for Iron Oxide (Fe_2O_3) Nanoparticles.....	28
Table 2.5 Summary of experimental study for magnesium Oxide (MgO) Nanoparticles.....	29
Table 2.6 Summary of experimental study for Multi Welded Carbon Nanotube (MWCNT) Nanoparticles	29
Table 2.7 Summary of experimental study for Silica (SiO_2) Nanoparticles.....	31
Table 2.8 Summary of experimental study for Zinc oxide (ZnO) Nanoparticles.....	32
Table 2.9 Summary of experimental study for Titanium Oxide (TiO_2) Nanoparticles.....	33
Table 2.10 Summary of experimental study for Hybrid Nanoparticles..	34
Table 3.1 show the dimension of geometry in this study measured experimentally	39
Table 4.1 The specification of radiators	52
Table 5.1 Comparison of the thermal properties obtained using of experimental test with the recommended correlations	70
Table 5.2 Table for summarizing the results of improvement in the Nusselt number at 4 L/min.....	85
Table 5.2 Cost of radiators and nanofluid.....	103
Table 5.3 Cost of nanoparticles.....	103

LIST OF FIGURES

Figure 1.1 Parts of the cooling system in automotive.....	5
Figure 1.2 Structural of the surfactants.....	8
Figure 1.3 Nanofluid Preparation by The Two-Step Method.....	10
Figure 3.1 Variation of flow velocity in all tubes.....	37
Figure 3.2 The 3-D geometry of the flat tube with fins.....	38
Figure 3.3 Flat tube with dimensions.....	39
Figure 3.4 The 3D mesh model tetrahedra type used for numerical simulations	43
Figure 3.5 Mesh independency curve with outlet temperature.....	44
Figure 4.1 the schematic diagram of an experimental setup.....	50
Figure 4.2 photograph of the experimental setup	50
Figure 4.3 Radiators used in the study.....	51
Figure 4.4 the cooling fan used in the study	53
Figure 4.5 Anemometer to measure airflow velocity	53
Figure 4.6 Centrifugal pump.....	54
Figure 4.7 Ls frequency converter	54
Figure 4.8 cylindrical water tank	55
Figure 4.9 water heater and thermostat.....	56
Figure 4.10 Flowmeter and beaker	56
Figure 4.11 Distribution of thermocouples on the radiator	57
Figure 4.13 Ultrasonic device	58
Figure 4.14 Nanofluids stability with surfactant Gum Arabic (C ₁₅ H ₂₀ NNaO ₄).....	59
Figure 4.15 Sensitive scale.....	59
Figure 4.16 Thermal conductivity measurement device.....	60
Figure 4.17 viscosity measurement device	61
Figure 5.1 Comparison of the numerical results of the current study with the experimental results of Hussein et al.[90].....	65
Figure 5.2 Comparison of the numerical results of the current study with the Elsebay et al. [91].....	66
Figure 5.3 variation of the Nusselt number for distilled water.....	68
Figure 5.4 Temperature variation of distilled water with a different flow	68
Figure 5.5 fins and the tube with the temperature variation flow rate and temp.....	69
Figure 5.6 Nusselt number varied with different flow rates at 60 ° C....	72

Figure 5.7 Nusselt number varied with different flow rates at 70 ° C....	72
Figure 5.8 Nusselt number varied with different flow rates at 80 ° C....	73
Figure 5.9 Enhancement of Nusselt number for Numerical result	73
Figure 5.10 Heat transfer rate varied with different flow rates at 60 ° C	75
Figure 5.11 Heat transfer rate varied with different flow rates at 70 ° C	75
Figure 5.12 Heat transfer rate varied with different flow rates at 80 ° C	76
Figure 5.13 Enhancement of heat transfer rate for Numerical result	76
Figure 5.14 Temperature variation of the flat tube with fins at 0.5 vol%	
.....	78
Figure 5.15 Temperature variation of the flat tube with fins 1 vol%	78
Figure 5.16 Temperature variation of the flat tube with fins at 2 vol% .	79
Figure 5.17 Temperature variation of distilled water flow along the flat tube	80
Figure 5.18 Temperature variation Al ₂ O ₃ flow along the flat tube	80
Figure 5.19 Temperature variation of CuO flow along the flat tube	81
Figure 5.20 Temperature variation of MWCNT flow along the flat tube	81
Figure 5.21 the pumping power of the water and nanofluid.....	83
Figure 5.22 Fluid Velocity profile for the tube with the different flow rate	83
Figure 5.23 Fluid temperature profile for the tube with the different flow rate	84
Figure 5.24 Velocity profile as an arrow along the tube	84
Figure 5.25 Streamline of the fluid along the tube	85
Figure 5.26 Verification of the experimental setup	86
Figure 5.27 Variation of the Nusselt number of Al ₂ O ₃ nanofluid at 80 °C	88
Figure 5.28 Variation of the heat transfer rate of Al ₂ O ₃ nanofluid at 80 °C.....	89
Figure 5.29 Variation of the outlet temperature of Al ₂ O ₃ nanofluid at 80 °C.....	89
Figure 5.30 Variation of the Nusselt number of CuO nanofluid at 80 °C	91
Figure 5.31 Variation of the heat transfer rate of CuO nanofluid at 80 °C	91
Figure 5.32 Variation of the outlet temperature of CuO nanofluid at 80 °C.....	92

Figure 5.33 Variation of the Nusselt number of MWCNT nanofluid at 80 °C.....	93
Figure 5.34 Variation of the heat transfer rate of MWCNT nanofluid at 80 °C.....	94
Figure 5.35 Variation of the outlet temperature of MWCNT nanofluid at 80 °C.....	94
Figure 5.36 Variation of the Nusselt number of Al ₂ O ₃ , CuO, and MWCNT nanofluid at 80 °C.....	96
Figure 5.37 Variation of the heat transfer rate of Al ₂ O ₃ , CuO, and MWCNT nanofluid at 80 °C.....	96
Figure 5.38 Variation of the outlet temperature of Al ₂ O ₃ , CuO, and MWCNT nanofluid at 80 °C.....	97
Figure 5.39 Variation of the Nusselt number of MWCNT nanofluid for a small radiator at 80 °C	99
Figure 5.40 Variation of the heat transfer rate of MWCNT nanofluid for a small radiator at 80 °C.....	99
Figure 5.41 Variation of the outlet temperature of MWCNT nanofluid for a small radiator at 80 °C	100
Figure A2. Thermocouple's calibrations and data logger.....	120

CHAPTER ONE
INTRODUCTION

CHAPTER ONE

INTRODUCTION

1.1 General

One reason for global warming can be attributed to the harmful gases emitted from the automotive engine exhaust. The Kyoto Protocol was adopted in 1997 to reduce greenhouse gas emissions [1]. This has encouraged many researchers to find an alternative technique to reduce these gases' emissions. Energy consumption of automotive engines can be reduced by improving the performance of the engine cooling system. Heat transfer is an essential process in industrial and consumer products in many industrial applications. If the engine temperature is too high, there will be a chance of engine wear and an increase in the fuel's heat and lubricating efficiency, which may affect the engine's performance. The acceptable temperature ranged from 90 to 105 °C [2] should be maintained to increase engine efficiency and reduce fuel consumption. However, the efficiency of traditional coolant fluids such as water, engine oil, ethylene glycol, etc., has to be enhanced. Therefore, there is a need for a fluid with higher heat transfer performance. Modern technologies are nanofluids, mixtures of base fluids and nanoparticles with sizes ranging from 1 to 100 nanometers prepared as a suspension by ultrasonic waves. By using different types of nanoparticles such as (Minerals, metal oxides, ceramics oxide, metal carbides, carbon in various forms, metal nitrides) [3] as shown in Table 1.1, to increase the heat transfer rate of the heat exchangers, these particles can improve the heat transfer in the coolant at a specific concentration compared to the base fluid. It can be inferred that an enhancement in the heat transfer by

more than 50% in real-time applications can be achieved using a low concentration of nanoparticles [4].

Table 1.1 Materials of nanoparticles

Minerals	gold, copper
metal oxides	alumina, silica, zirconia, titania
oxide ceramics	Al_2O_3 , CuO, TiO_2
metal carbides	SiC
carbon in various forms	Carbon nanotubes, diamond, graphite
metal nitrides	AlN, SiN

1.2 Heat Exchanger

A heat exchanger is a device that changes the temperature of a fluid by transferring it through tubes that run through another material. Heat exchange is the process of transferring heat from one medium to another. Energy, chemicals, food industries, air conditioners, and freezers are used for heat exchangers. The automobile sector, as well as domestic appliances such as chillers, refrigerators, and water heaters, are the most conventional heat exchanger applications that may be found. Heat exchangers are also utilized in the oil and gas sector to chill and preheat liquid, as well as in power plants to condense steam or preheat boiler liquid intake. Other practical applications for heat exchangers are solar collectors, aviation, electronic devices, etc. [5][6]. Heat exchangers that are both efficient and cost-effective are required in this field. The primary objectives of heat exchanger research are to lower the size of heat exchangers while maintaining the same thermal performance and

minimizing pumping power. Many efforts have been made in recent decades to increase heat transfer efficiency in heat exchangers by boosting the heat transfer coefficient of the fluids. Heat exchangers employ fluids to transport heat throughout the system. Thermal conductivity, viscosity, density, and specific heat are all factors that affect their ability to exchange heat [7]. Nanofluids (NFs) are heat transfer fluids that can improve the thermal performance of heat exchangers.

1.2.1 Automotive Radiators

Radiators are used to transfer thermal energy from one mode to another for cooling and heating. Radiators work in automotive, buildings and PC electronics, where radiators lose most of their heat through convection. Coolant act as a cooling source for an automotive engine because the temperature in the engine cylinder reaches 2000 to 2500 °C [8]. If the coolant fluid has high-temperature differences, this may cause engine components to be deformed. When heat is not dissipated from the engine, the material cylinder may malfunction. Radiators can reduce the chances of piston crashes and keep the temperature to a minimum.

Nowadays, aluminium radiators are used extensively, especially in automotive; they usually include a jacket part, installed at the top to allow coolant entry. The other is installed at the bottom to let the coolant out. The radiator is consisted of tubes installed in a parallel arrangement, whereas; the aluminium fins are connected to all tubes. In a radiator, coolant flows from inlet to outlet through several tubes installed in a parallel arrangement, and hot water enters through the inlet port. A fan is installed behind the radiator for the cooling air for dissipate the heat cooling in the radiator pipe to the surrounding. Usually, a mixture of water and antifreeze (ethylene glycol or propylene glycol) in automotive

radiators are used as a liquid coolant. Figure 1.1 shows the parts of the cooling system in vehicles [9].

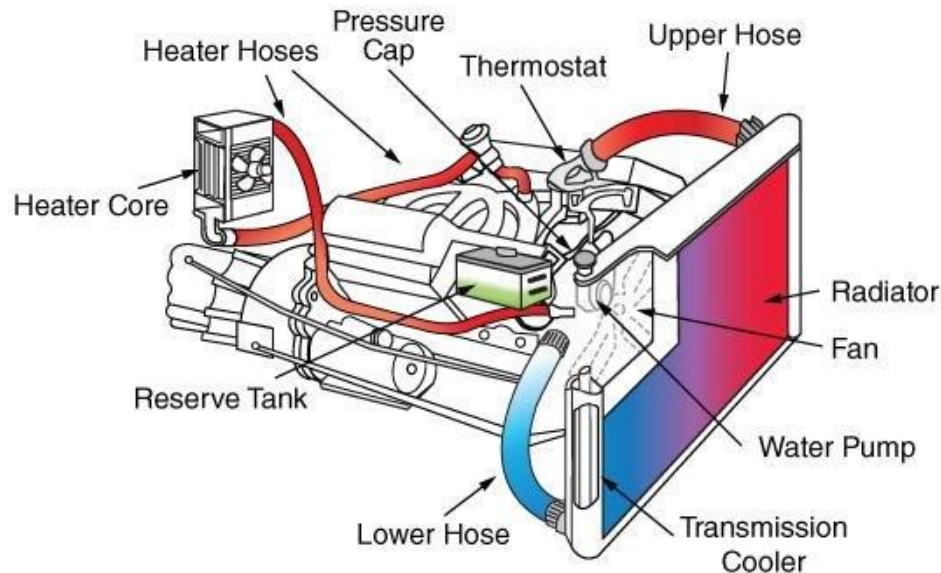


Figure 1.1 Parts of the cooling system in automotive

1.3 Nanofluids

Heat transfer has been enhanced by adding nano-sized particles to many base fluids to increase the thermal conductivity and heat transfer coefficient. For the first time, Choi has established a mixture of nanoparticles with a base fluid to form a colloidal mixture called (nanofluid) at Argonne National Laboratory, Argonne, Illinois, in 1995. [10]. This fluid showed better thermal properties than the micro-size fluids due to the nanoparticles' more extensive surface area and higher momentum. Showed higher stability compared to the micros-size particles. Due to the high thermal conductivity of the mixture of nanoparticles mixed with the base fluid, these fluids are considered a promising method for many uses in many thermal applications such as solar energy. That act as heat exchangers to cool down the solar cells to

increase their efficiency. Nanoparticles are made of several materials, including metals, metal oxides, ceramic oxides, semiconductors, various carbon forms, and many nanoparticles. Xuan and Li [7] suggested a mechanism to suspend these nanoparticles using ultrasonic and magnetic mixing devices; the stability has been enhanced by adding surfactants.

1.4 Thermal Conductivity of Nanofluid

Conductive heat transfer occurs between two objects in contact with each other. Most metals are good conductors of heat, and the better the conductor, the faster the heat transfer. When a substance is heated, the particles vibrate, raising the energy inside, and thermal conduction occurs. The nanomaterials' conductivity depends on many factors, including the base fluid's conductivity and the nanoparticle concentration ratio in the nanofluid [11]. The thermal conductivity values of the most common nanoparticles are shown in Table 1.2.

Table 1.2 The thermal conductivity of common nanomaterials [12]

Materials	Thermal conductivity W.K/m²
Diamond	3300
MWCNT	3000
Copper oxide (CuO)	76
Alumina (Al ₂ O ₃)	40
Titanium dioxide (TiO ₂)	8.4
Water (base fluid)	0.613

1.5 Types of Nanoparticles

1.5.1 Alumina

Alumina or Aluminum oxide is a Chemical composition with the formula Al_2O_3 . It exists in the form of two patterns that differ from each other in the crystal structure, and thus they also differ in physical and chemical properties and the applications, which are the alpha (α) type and the gamma (γ) type [13]. Aluminum oxide nanoparticles can be synthesized by many techniques including ball milling, sol-gel, pyrolysis, sputtering, hydrothermal, and laser ablation. The laser ablation is a commonly used technique to produce nanoparticles, since it can be synthesized in gas, vacuum or liquid. The technique offers several advantages such as rapid and high purity process compared with other methods It occurred in spherical or nearly spherical nanoparticles and directed or undirected fibers. Small particle fiber diameter (2-10nm) and Specific high surface area $> 100 \text{ m}^2 / \text{g}$ [14].

1.5.2 Copper Oxide (CuO)

Copper oxide (CuO) nanoparticle powder is black-brown, containing 79.87% copper and 20.10% oxygen. The physical properties are the density of 6.31 g/cm^3 and a molar mass of 79.55 g/mol [15]. Copper oxide nanoparticles can be synthesized using the aqueous precipitation method. In this method, copper acetate is used as a precursor and sodium hydroxide as a stabilizing agent. They are used in thermo-optical applications and ceramic resistors with ample magnetic storage because they are high-tech superconductors.

1.5.6 Multi-Walled Carbon Nanotubes (MWCNT)

Multi-walled carbon nanotubes (MWCNTs) are hollow, cylindrically shaped allotropes of carbon that have a high aspect ratio (length to diameter ratio) Their name is derived from their structure consisting of overlapping single-walled carbon nanotubes. [16] these

tubes are very similar to the long, straight, parallel, and cylindrical carbon layers around a hollow tube. MWCNTs are sometimes used to refer to double and triple-walled carbon nanotubes [17].

1.6 Surfactants

Surfactants are substances that have an active surfactant agent consisting of hydrophilic groups that help reduce the biphasic tension of a two-phase system, such as (liquid-solid) and another hydrophobic group as how in Figure 1.2. It is classified into four groups (cationic, anionic, amphoteric, and non-ionic). Common types of surfactants are (sodium dodecylbenzene sulfonate, Gum Arabic, sodium dodecyl sulfate, and Triton X-100) [18]. This material is used to increase the stability of nanofluids, which are used in many applications for an extended period of more than six months [19].

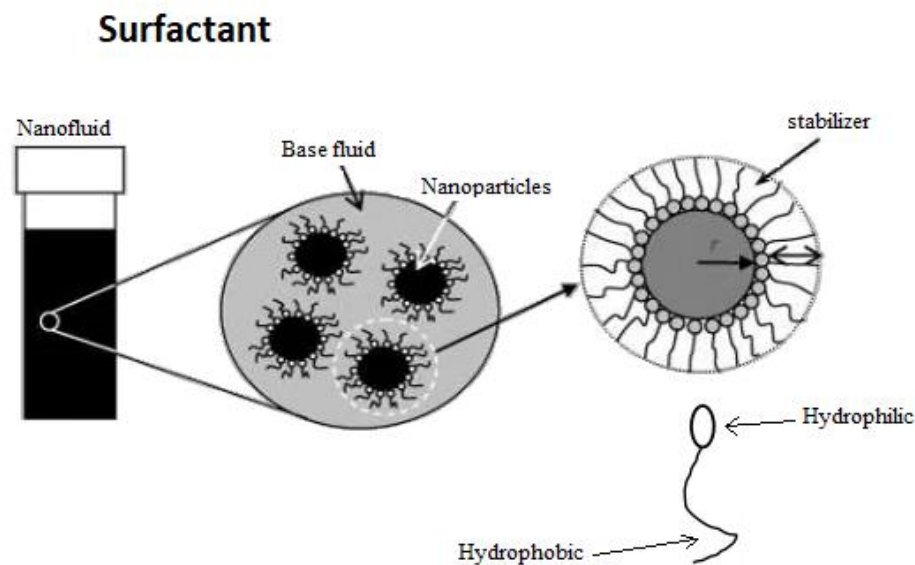


Figure 1.2 Structural of the surfactants

1.7 Nanofluid Preparation

Two ways to prepare the nanofluid are usually used, the one-step method and the two-step method. Each method has a specific procedure, and each technique depends on the availability and materials used.

1.7.1 The One-Step Method:

The stability of nanoparticles characterizes them due to the little agglomeration of the particles inside the fluid. It includes synthesizing particles and their dispersion with the base fluid by chemical and physical methods such as physical and chemical depositing vapour. **Eastman et al.** [20] have performed a direct condensation procedure of metallic vapour into nanoparticles on ethylene glycol. **Lo et al.** [21] and others used an electric arc to melt and evaporate pure metallic rods, which were subsequently condensed in deionized water to obtain an extremely stable nanofluid. One of the disadvantages of this method is the high production cost. Thus, it is not possible to produce large quantities with this method. This method was not used because of the high cost of synthesizing a nanofluid with good specifications and the difficulty of producing large quantities with it.

1.7.2 The Two-Step Method:

This technique is the most widely used [22]. It is possible to produce large quantities of nanoparticles in this way, where the particles are made in the form of dry powders. It can be dispersed with the base fluid after several different methods, including magnetic mixing, ultrasonic, and homogenization. one of the disadvantages of this method is the aggregation of the nanoparticles in the base fluid. Figure 1.3 shows how to prepare nanofluids using the two-step method.



Figure 1.3 Nanofluid Preparation by The Two-Step Method

1.8 Advantages and Disadvantages of Nanofluids

In addition to a small boost in cooling efficiency relative to pure liquid, the nanoparticles usefulness increases the heat transfer coefficient by improving the nano-fluids thermal conductivity. There are, however, some significant disadvantages that raise questions about the use of nano-fluid in automotive radiators. Table 2 shows the most common advantages and disadvantages of nano-fluid.

Table 1.3 Advantages and Disadvantages of Nano-Fluid

Advantages	Disadvantages
Enhanced heat transfer coefficient to higher thermal conductivity, mainly of laminar flow	It has to raise the pumping power because of the significantly decreased pressure.
It is possible to make miniature devices available because of the improved heat transfer.	The high-cost suspension of nanoparticles, especially those requiring the addition of substances such as surfactants to improve stability [23]
	The accumulation of particles when the fluid is in a state of stagnation for a long time causing the flow pathways to close

Study Objectives

The main objectives of the current study can be listed as:

- 1- Numerically and experimentally investigate study the nanofluids effect on the thermal performance in automotive radiator.
- 2- Reducing the size of the radiator by using nanofluids that have better thermal performance than the rest to be used in the small radiator to provide additional space under the hood.
- 3- Economic analysis of nanofluids in automobile radiators, in terms of thermal performance and reasonable cost compared to the rest of nanofluids.

CHAPTER TWO
LITERATURE REVIEW

CHAPTER TWO

LITERATURE REVIEW

2.1 Introduction

This chapter presents a review of the previous work carried out on the automotive radiator thermal performance using nanofluids (nanoparticles added to the base fluids, usually distilled water and ethylene glycol).

2.2 Experimental Study of the of flow and heat transfer mechanism of nanofluids in automobile radiators

Many studies have been presented to increase the thermal performance of automotive radiators. One technique to improve the thermal performance is adding nanoparticles (Al_2O_3 , CuO , MgO , SiO_2 , ZnO , MWCNT, etc.) to the base fluids. Previous experimental research on the nanofluids added to the automotive radiator is listed below.

Goudarzi and Jamali 2017 [13] Studied the effect of inserting the coil wire of different shapes inside the automotive radiator pipe, and the Al_2O_3 nanofluid was tested with varying volume concentrations, the Nusselt number at Reynolds number ($18,500 < \text{Re} < 22,700$) with the wire is higher compared to EG without wire inserts. **Subhedar et al.** 2018 [24] added nanoparticles of (Al_2O_3) with water and ethyl alcohol with a mixing ratio of 50:50 and with a concentration of nanoparticles (0.2-0.8) vol% and a temperature range of (65-85) °C. It was found that the improvement in heat transfer at a concentration of 0.2 vol % was 30% compared to the base fluid. The results suggested the availability of reduction in the automotive radiator size and thus in fuel consumption. **Elsaid** 2019 [25] concluded from the experimental results that cobalt

oxide is more efficient than aluminium oxide nanoparticles in heat exchangers. The Nusselt number increases with the increase in the temperature of the nanofluid. **Said et al.** 2019 [26] carried out an experimental study on the automotive radiator by adding nanoparticles (Al_2O_3 , TiO_2) to enhance the thermal performance. With a concentration of (0.05-0.3) vol % and flow rate of (0.5-3) L/min, it was found that the increase in Nusselt number was 24.21% at 0.3 vol% for Al_2O_3 and 14.99% at 0.3 vol% for TiO_2 .

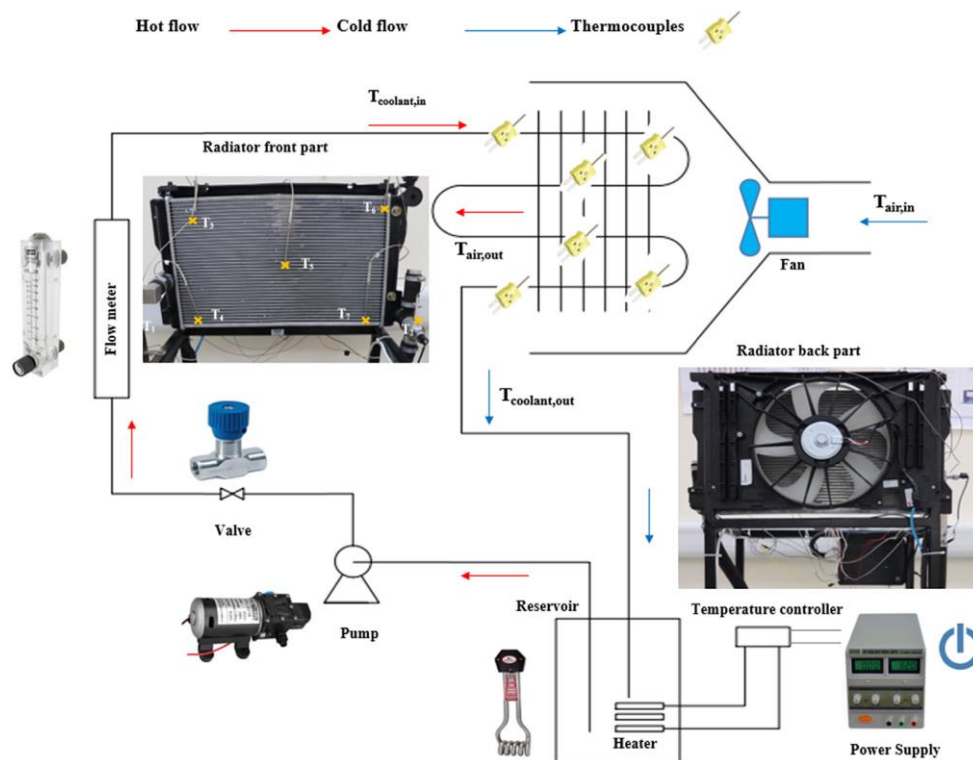


Figure 2.1 Schematic representation for **Said et al.** 2019 [26]

M. Gajendiran, E. Saravanakumar 2016 [27] carried out an experimental study using transformer oil as a base fluid with copper nanoparticles. The heat transfer results increased by 15% more than water and 66% more than the transformer oil coolant. **Ravisankar et al.** 2018 [28] used copper nanoparticles with water. The results showed an

increase in the heat transfer coefficient compared to the base fluid by 16% at a concentration of 0.025% - 0.05% and 19 % at a concentration of 0.05% - 0.075. **Naraki et al.** 2013 [29] carried out an experimental study on nanoparticles of CuO with a size of 60 nm, a purity of 98% and at a concentration of 0.04 vol % at a laminar flow, and a Reynolds number ($100 < Re < 1000$) and PH 10.1. The results showed an improvement in the heat transfer coefficient by (6-8) %. **Heris et al.** 2014 [30] carried out an experimental study by using CuO nanoparticles with a concentration (0.05-0.8)%vol and a flow rate of (4-8) L/min. They obtained the highest Nusselt number of 55% at a concentration of 0.8%, and the Nusselt number was found to increase when increasing the flow rate of the nanofluid and the temperature. **Samira et al.** 2015 [31] studied the pressure drop in the automotive radiator by using copper oxide (CuO) nanoparticles of 60 nm diameter with (water and Ethylene glycol in a ratio of 60: 40) and a concentration (0.05-0.8)%. The nanofluid was prepared using the mechanical mixing of the liquid with the nanoparticles for 14 hours and an ultrasonic treatment for two hours. The results showed that with the increase in the inlet temperature of the fluid, the viscosity of the nanofluid decreased, which in turn led to a decrease in the pressure and the friction factor, the increase in the fluid temperature by 19 °C has led to a reduction of the pressure by 13.17%. **Hamad.** 2016 [32] carried out an experimental investigation of the heat transfer performance using nanoparticles of copper oxide (CuO) and titanium oxide (TiO₂) with (Water + EG) as a base fluid with a volume concentration from (0.5-5) %. The results showed an increase in the heat transfer enhancement of 12.4% for CuO and 9.52% for TiO₂ at a concentration of 5% compared to the base fluid. The heat transfer coefficient of copper oxide was more significant than the heat transfer coefficient of titanium oxide.

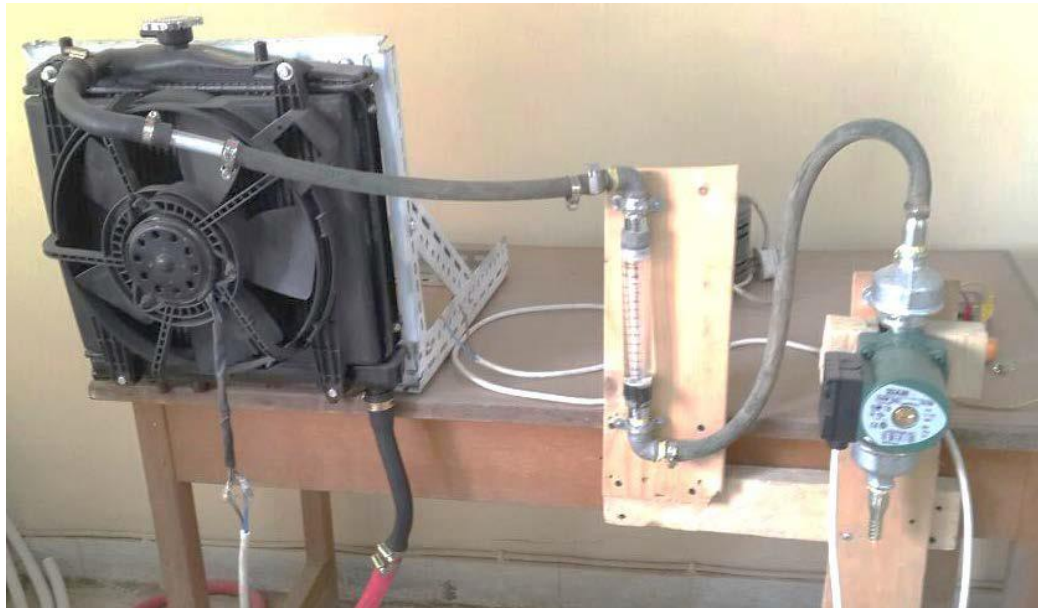


Figure 2.2 Experimental setup for **Hamad**, 2016 [32]

Vermahmoudi et al. 2014 [33] applied an experimental investigation on the (HTP) heat transfer performance using iron oxide (Fe_2O_3) as nanoparticles and water as a base fluid at concentrations of (0.15, 0.4, 0.65) vol%. The nanofluid was prepared by the two-step method, and the nanofluid was more stable at pH 11.1 for more than two days. Experiments showed an improvement of 13% in the heat transfer performance at a volume concentration of 0.65 vol%. **Tafakhori et al.** 2020 [34] have calculated the effect of magnetite iron oxide Fe_3O_4 , purity of 99% nanoparticles with a concentration of 0.9% and a diameter of 28 nm in distilled water. They found that an increase in the thermal conductivity of 55.73% has been achieved compared to the base fluid; it is also found that after using the nanofluid, the coefficient of friction has increased as a result of the increase in the cooling fluid viscosity.

Hamzah and Al-amir 2017 [35] studied the effect of magnesium oxide (MgO) nanoparticles mixed with distilled water as a base fluid with a concentration range (0.125-2) vol% and with a fluid flow rate (1-10) L/min. The results showed an increase in the heat transfer rate of 6% at 0.125 vol % concentration and 40% at volume concentration 2%. **Kumar Rai et al.** 2018 [36] carried out an experimental study on mixing MgO nanoparticles with base fluid 40:60 distilled water (DW) and Ethylene Glycol (EG) at different concentrations using the two-step method. The heat transfer rate increase with increasing the concentration of the nanoparticles in the base fluid; the heat transfer rate (Q) has improved from 5.59% to 29.83% at concentrations of 0.1 vol % to 0.15 vol % respectively, and the heat transfer rate also increases with the increase in fluid flow rate.

Chougule 2013 [37] investigated the performance of the functional nanofluid (carbon nanotube + water) at different volumetric concentrations ((0.15%, 0.45%, 0.60%, and 1%) and a different pH of the base fluid. The results showed that the maximum improvement in heat transfer was 90.7% at a volume concentration of 1% compared to distilled water, as well as, the thermal performance of the nanofluid at PH (5.5) is better than that of nanofluid with PH (6.5 and 9). **Ramaraju et al.** 2014 [38] found a significant enhancement in heat transfer when adding nanoparticles of MWCNT to the base fluid (water + Ethylene glycol). The results showed an increase in the automotive radiator performance by 30% compared to the base fluid. **Rashmi et al.** 2014 [39] study the effect of corrosion and heat transfer when adding carbon nanotubes with (water and Ethylene glycol) as a base fluid with adding surfactants such as Gum Arabic (C₁₅H₂₀NNaO₄). It was found that the addition of Gum Arabic enhances the stability of the nanofluid and its

corrosion resistance. Using carbon nanotubes improved the automotive radiator's performance, which led to a reduction in fuel consumption and reduced radiator volume. **Moorthy and Srinivas** 2016 [40] studied the heat transfer in the carbon nanotubes with 20–40 nm in outer diameter, 1–25 μm in length and 80 % purity and found that the average heat transfer rate at a concentration of 0.1 vol % was 87.3%. **M'hamed et al.** 2016 [41] used a 1000 cc Perodua Kelisa engine to study the effect of adding MWCNT nanoparticles with (water + Ethylene glycol at a mixing ratio of 50: 50) with Diameter 20–30 nm , Length 3–8 μm and at a flow rate of (2-6) L/min. It was found that the heat transfer coefficient increased by 19.63% at a concentration of 0.5% compared to the base fluid.



Figure 2.3 Photograph of test set up for **M'hamed et al.** 2016 [41]

Ebrahimi et al. 2014 [42] used silicon oxide nanofluids to increase the heat transfer rate. They found that the Nusselt number has increased by increasing the fluid inlet temperature and the nanofluid concentration, with Reynolds number ($8000 < \text{Re} < 24000$). **Hussein et al.** 2014 [43] found that the addition of silicon oxide nanoparticles at

volume concentrations 1-2 % with to the base fluid (water + Ethylene glycol) has increased the Nusselt number by 17.85%. Also, the increase in titanium oxide particles has increased the Nusselt number by 16.4% at a concentration of 2.5%. **Hussein et al.** 2014 [44] studied the effect of silicon oxide nanofluids at volume concentrations 1-1.25% on the distilled water as a base fluid of the automotive radiator using a low concentration. found that the heat transfer rate (Q) has improved by 50%.

Ali et al. 2015 [45] investigated the heat transfer efficiency of the automotive radiator using (zinc oxide and water) as a nanofluid with a concentration of nanoparticles (0.01-0.3) vol%. found that the heat transfer coefficient has increased by 46% at a concentration of 0.2 vol%. **Qasim et al.** 2020 [46] studied the heat transfer with a laminar flow rate of (2-12) L/min. The maximum increase in the heat transfer rate was found to increase by 41% at a concentration of 0.2 vol % when using zinc oxide nanoparticles. The Nusselt numbers and the total heat transfer coefficient was 31% and 50%, respectively, and the average pressure drop and the friction factor were 47% and 46%, at 0.2% volumetric concentration. **Kurhe et al.** 2016 [47] used titanium oxide nanoparticles with water as a base fluid in the automotive radiator. The added nanoparticles have reduced the radiator volume by 15% and saved 5% of the fuel. **Salamon et al.** 2017 [48] carried out an experimental study on titanium oxide nanoparticles added to water and Ethylene glycol with a concentration of (0.1-0.3) vol%. It was found that the Nusselt number was dependent on the flow rate, and the highest Nusselt number was 14.4 at a flow rate of 6 L/sec and a temperature of 80 degrees.

2.2 Numerical Study of Flow and Heat Transfer mechanism of nanofluids in automobile radiators

Many numerical studies have been conducted using the CFD technique to simulate and analyze automobile radiators' fluid flow and heat transfer. **He et al.** 2009 [49]. It was found that the data obtained from the simulation was 25-30% higher than the experimental data; they attributed the reason for this significant difference to many factors, including the aggregation and the random movement of the particles. It was also shown that the heat transfer coefficient increases with the increase in Reynolds number and the concentration of particles. **Gunnasegaran et al.** 2012 [50] conducting a numerical simulation process for nanofluid flow and heat transfer properties in a heat exchanger for nanoparticles (diamond, copper, silicon oxide) at Reynolds number 4000-6000. The results showed that the heat transfer coefficient is 9.1% higher than that of the base fluid, and 18% of the pumping power must be added when using the silicon oxide nanofluid at Reynolds 7000 compared to the base fluid. **Bozorgan et al.** 2012 [51] used water as a base fluid and copper oxide as nanoparticles to make a nanofluid in a Chevrolet Suburban diesel engine. A numerical study under conditions of turbulent flow was performed. The results indicated that the total heat transfer coefficient (h) of the nanofluid is higher by 10% than the total heat transfer coefficient of the base fluid. These findings lead to the possibility of reducing the radiator's size in the automotive and increasing the pumping power. **Duangthongsuk and Wongwises** 2012 [52] suggest a model for predicting the heat transfer coefficient of nanofluids at laminar flow. TiO₂ nanoparticles were dispersed in water at different concentrations to calculate nanofluids' dispersal coefficient; compared the obtained results with work of **Sheikhzadeh** 2014 [53] investigated the thermal performance of

nanofluids on the automotive radiator numerically. An increase in the heat transfer coefficient was increased by 4.5% for Ethylene glycol and 12.4% for the nanofluid. (Copper nanoparticles + water base fluid). **Huminic.** 2013 [54] applied a numerical study using the ANSYS Fluent software to study the effect of copper oxide (CuO) nanoparticles added to (Water + EG). determined the volume concentration of nanoparticles and Reynolds number on the heat transfer coefficient is higher than that of the base fluid at 1 vol % and 4 vol % concentration. Under the same conditions, the flat tube showed a better thermal performance than the circular and elliptic tube. **Delavari and Hashemabadi** 2014 [55] applied a numerical study on water and Ethylene glycol behaviour as a base fluid with aluminium oxide nanoparticles using laminar and turbulent flow boundary conditions; the data indicated that increasing the volume concentration of nanoparticles in the fluid has increased the Nusselt number and the heat transfer coefficient and that the single-phase flow predicted less of the Nusselt number for the experimental data than the two-phase flow that gave a better result. **Che Sidik et al.** 2014 [56] Used a numerical analysis to study the effect of aluminium oxide nanoparticles with a concentration of 0.5-5% added to (water + Ethylene glycol 50:50) as base fluid. Results showed that the heat transfer has improved with the increasing concentration of the nanofluids.

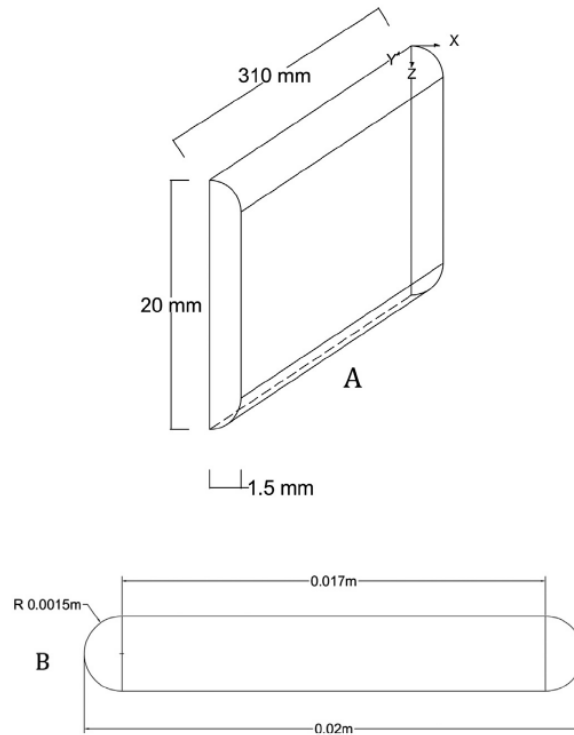


Figure 2.4 Dimensions of flat tube for **Delavari and Hashemabadi** 2014 [55] (A) side view, (B) top view.

2.3 Summary of Literature Review

After reviewing the previous studies above, the type of nano, the size of the nanoparticles, the volumetric concentration and the percentage of improvement can be summarized in Tables 2.1 to 2.10. It can be concluded that the most common nanofluids used in the automotive cooling system are aluminium oxide, copper oxide, as well as, multi-walled carbon nanotubes; more than the rest of the nanomaterials where the thermal performance improvement rate for the mentioned materials was (50%)[57]. As a result, it was noted that the multi-walled carbon nanotubes could give the best performance than the rest of the other types of nanofluids. Thus, the focus in this study will be on the use of mentioned nanomaterials in order to test the performance of these materials numerically and experimentally. It's Noted that the

effect of nanomaterials on the effect of the radiator size has not been practically studied using two radiators of different sizes. The following table (2.1) to the table (2.10) shows the previous researchers' use of different nanoparticles with different base fluids such as water or water with ethylene glycol with different volumetric concentrations.

2.4 Scope of study

We study the effect of nanofluids on the thermal performance of radiators numerically and experimentally by calculating the Nusselt number, the rate of heat transfer and the possibility of reducing the size and weight of the radiator, thus saving space under the hood, as well as studying the economic analysis of nanofluids as coolant in the cooling system of automotive.

Table 2.1 Summary of experimental study for Alumina or Aluminum Oxide (Al_2O_3) Nanoparticles

Researcher's name	Nano type	Base fluid	Particle volume fraction (%)	Particle size (nm)	Maximum enhancement (%)	Remarks
Chidambaram et al. 2014,[58]	Al_2O_3	water	(0.25-0.5) vol %	45 nm	49 %	total of heat transfers (Q) the flow rate was 4-12 L/min
Goudarzi and Jamali 2017,[13]	Al_2O_3	ethylene glycol (EG)	(0.08-1) vol %	-	9 %	Increasing Heat transfer rate (Q) at $18,500 < \text{Re} < 22,700$
Sundari et al. 2017,[59]	Al_2O_3	mixtures of ethylene glycol, Water and 20% glycerin)	(0.05-0.15) vol %	<50 nm	52.50 %	Enhancement in thermal conductivity (K)
Subhedar, Ramani, and Gupta 2018,[24]	Al_2O_3	(Water-EG) (50:50)	(0 - 0.8) vol %	20 nm	30 % 28.47 %	Heat transfer coefficient (h) Nusselt number (Nu) at flow rate 4-9 L/min

Tijani and Sudirman 2018,[60]	Al ₂ O ₃ CuO	water and ethylene glycol (50:50)	(0.05-0.3) vol%	20 nm 60 nm	5.4 % 27 %	Nusselt number with flow rate 3-6 L/min and 20000 < Re < 85000
Chaurasia et al. 2019 [61]	Al ₂ O ₃	Water	(0.1-0.2) vol %	50–200 nm	44.29 % 40 %	Enhance of Heat transfer rate (Q) and Efficiency of the radiator at 0.66-1.66 L/min flow rate
Said et al. 2019,[26]	Al ₂ O ₃ TiO ₂	Distilled Water (DW) and ethylene glycol (EG) (50:50)	(0.05-0.3) vol%	10 nm 5 nm	24.21 % 14.99 %	Enhance Nusselt number at 50 < Re < 3000 and flow rate 0.5-4 L/min
Elsaid 2019,[25]	Co ₃ O ₄ Al ₂ O ₃	water and ethylene glycol	(0.02– 0.1) vol % (0.05– 0.2) vol %	8–21nm 11–25 nm	31.8 %	Nusselt number at Reynold number was 15000 < Re < 75000 and flow rate 4 -16 L/min
Topuz et al. 2020,[62]	Al ₂ O ₃	water and ethylene glycol (50:50)	0.5 vol %	13 nm	15 %	cooling performance (Q) of the radiator with flow rate 10-25 L/min

Table 2.2 Summary of experimental study for Copper (Cu) Nanoparticles

Researcher's name	Nano type	Base fluid	Particle volume fraction (%)	Particle size (nm)	Maximum enhancement (%)	Remarks
Anuar 2016[63]	Cu	water	(2-10) vol %	10-100 nm	92 %	Heat transfer coefficient (h)
M. Gajendiran, E. Saravanakumar 2016[27]	Cu	Thermic fluid	0.1-0.3) vol%	60 nm	66 %	Heat transfer rate (Q) more than base transformer oil with a flow rate of 10-20 L/min
Ravisankar et al. 2018 [28]	Cu	water	(0.025-0.075) vol%	40 nm	88 %	Heat transfer coefficient (h) when the $8000 < Re < 25000$

Table 2.3 Summary of experimental study for Copper Oxide (CuO) Nanoparticles

Researcher's name	Nano type	Base fluid	Particle volume fraction (%)	Particle size (nm)	Maximum enhancement (%)	Remarks
Peyghambarzadeh et al. 2013[64]	CuO Fe ₂ O ₃	Water	(0.15-0.65) vol%	60 nm 40 nm	9 %	overall heat transfer coefficient (U) for both nanofluid at a flow rate (3-8.4) L/min and 50<Re<1000
Naraki et al. 2013[29]	CuO	Water distilled	(0-0.4) vol%	60 nm	6-8 %	Heat transfer coefficient (h) with laminar flow 100 <Re<1000 and flow rate 0.2-0.5 m ³ /hr.
Heris et al. 2014[30]	CuO	water (DW) and ethylene glycol (EG) (50:50)	(0.05-0.8) vol%	60 nm	55 %	Improving Nusselt number and the flow rate was (4-8) L/min with 2000
Heris et al. 2014[31]	CuO	water and ethylene glycol (60-40) %	(0.05-0.8) %	60 nm	13.17 %	Pressure drops at flow rate 4-6.5 and Reynolds number 1500-7800
Senthilraja, Vijayakumar, and Gangadevi 2015[65]	CuO Al ₂ O ₃	Water	(0.05-0.15) vol%	27 nm 50 nm	55.53 % 40.08 %	The maximum heat transfer (Q) enhancement at 5 L/min

Ravisankar, Venkatachalapathy, and Alagumurthy 2017[66]	CuO	distilled Water	(0.025-0.05) vol%	40 nm	2-4 %	Heat transfer coefficient (h) with turbulent flow 8000 $<Re<2800$
Pambhar et al. 2019[67]	CuO	water and ethylene glycol	(0.05-0.3) vol%	10 nm	20-30 %	Enhancement in the heat transfer (Q) at 0.3% volume fraction

Table 2.4 Summary of experimental study for Iron Oxide (Fe_2O_3) Nanoparticles

Researcher's name	Nano type	Base fluid	Particle volume fraction (%)	Particle size (nm)	Maximum enhancement (%)	Remarks
Vermahmoudi et al. 2014[33]	Fe_2O_3	Water	(0.15-0.65) vol%	40 nm	13 % 11.5 %	the overall heat transfer coefficient (U) and heat transfer rate (Q) at flow rate (0.2-0.25) m ³ /h
Tafakhori et al. 2020[34]	Fe_3O_4	distillated Water	(0-0.9) vol%	28 nm	21 %	Improve performance of the radiator

Table 2.5 Summary of experimental study for magnesium Oxide (MgO) Nanoparticles

Researcher's name	Nano type	Base fluid	Particle volume fraction (%)	Particle size (nm)	Maximum enhancement (%)	Remarks
Ali et al. 2015 [68]	MgO	Pure Water	(0.06-0.12) vol%	20 nm	31 %	Heat transfer rate (Q) at 0.12vol% and flow rate (8-16) L/min
Hamzah and Al-amir 2017 [35]	MgO	Pure Water	(0.125-2) vol%	-	40 %	heat transfer rate (Q) at flow rate 1-10 L/min and $4500 < Re < 19000$

Table 2.6 Summary of experimental study for Multi Welded Carbon Nanotube (MWCNT) Nanoparticles

Researcher's name	Nano type	Base fluid	Particle volume fraction (%)	Particle size (nm)	Maximum enhancement (%)	Remarks
Teng and Yu 2013[69]	MWCNT	water and ethylene glycol	(0.1-0.4) vol%	20-30 nm	12.8 %	The maximum enhanced heat exchange (Q)
Chougule 2013[37]	MWCNT	Water	(0.15-1) vol%	20-30nm	90.76 %	Increasing Nusselt number at a flow rate (2-5) L/min and $9000 < Re < 27000$
Rashmi et al. 2014[39]	CNT	water and ethylene glycol	(0.02-0.1) vol%	20-30 nm	19.69 %	Heat transfer rate (Q)

Chougule & Sahu, 2014 [70]	CNT Al ₂ O ₃	Water	(0.15-1) vol%	20-30 nm 100 nm	90.76 % 52.03 %	The maximum heat transfer performance (Q) at a flow rate (2-5) L/min
Ramaraju et al. 2014 [38]	MWCNT	water and ethylene glycol 40:60	0.02 vol%	-	30 %	the performance of an automobile radiator
Moorthy & Srinivas, 2016 [40]	MWCNT	Water	(0.025-0.1) vol%	20-40 nm	94.9 %	maximum heat transfer rate (Q) at 2500<Re<6000
M'hamed et al. 2016 [41]	MWCNT	water and ethylene glycol 50:50	(0.1-0.5) vol%	20-30 nm	19.63 %	maximum average heat transfer coefficient (h) enhancement
Jadar et al. 2019[71]	A- MWCNT	Pure Water	0.1 vol%	20 nm	45 %	heat transfer (Q) of nanofluid
Muruganandam & Mukesh Kumar 2020 [72]	MWCNT	Water	(0.1-0.3) vol%	50-80 nm	18 %	Increasing mechanical efficiency and total fuel consumption at 0.3%
Kılınç et al. 2020 [73]	GO GNR	Water	(0.01-0.02) vol%	-	33.9 %	The enhancements of the overall heat transfer coefficient (U)

Table 2.7 Summary of experimental study for Silica (SiO₂) Nanoparticles

Researcher's name	Nano type	Base fluid	Particle volume fraction (%)	Particle size (nm)	Maximum enhancement (%)	Remarks
Ebrahimi et al. 2014[42]	SiO ₂	Water	(0.1-0.4) vol %	-	13 %	Nusselt number increases with increasing Reynolds number
Hussein, Bakar, & Kadirgama, 2014 [44]	SiO ₂	Water	(1-2.5) vol%		22 % 40 %	friction factor Nusselt number
Hussein et al., 2014 [43]	SiO ₂ TiO ₂	water and ethylene glycol	(0.1-2.5) vol%	22 nm 50 nm	32 % 24 and 29.5 %	energy rate enhancement effectiveness for TiO ₂ , SiO ₂ nanofluids respectively
Kannan & Sivakumar, 2015 [74]	SiO ₂ CuO ZnO	Water	(0.5-3) vol%	22.91nm 19.29 nm 70 nm		The nanofluids can improve heat transfer; the automotive coolant can achieve fuel consumption and size reduction.

Table 2.8 Summary of experimental study for Zinc oxide (ZnO) Nanoparticles

Researcher's name	Nano type	Base fluid	Particle volume fraction (%)	Particle size (nm)	Maximum enhancement (%)	Remarks
Ali et al., 2015 [45]	ZnO	Water	(0.01-0.3) vol %	20 nm	46 %	Enhancement of heat transfer rate (Q) at a flow rate (7-11) L/min
Ahmad et al., 2019 [75]	ZnO Al ₂ O ₃	Water	(0.1-0.4) vol%	140 nm	70 %	heat transfer (Q) increases by using ZnO
Qasim et al., 2020 [46]	ZnO	Water	(0.1-0.3) vol%	20 nm	41 % 50 % 31 % 47 % 46 %	heat transfer rate (Q) overall heat transfer coefficient (U) Nusselt number (Nu) pressure drops friction factor

Table 2.9 Summary of experimental study for Titanium Oxide (TiO₂) Nanoparticles

Researcher's name	Nano type	Base fluid	Particle volume fraction (%)	Particle size (nm)	Maximum enhancement (%)	Remarks
Salamon et al. 2017 [48]	TiO ₂	water and ethylene glycol (70-30) %	(0.1-0.3) vol%	-	8.3 % 8.5 %	Nusselt number enhancement heat transfer (Q) enhancement
Bhimani et al., 2013 [76]	TiO ₂	Water	(0.2-1) vol%	15 nm	45 %	enhance heat transfer efficiency
Kurhe et al., 2016 [47]	TiO ₂	Water	-	10-100 nm	10 % 5%	Reducing in the area of the radiator Fuel-saving
Ahmed et al., 2018 [77]	TiO ₂	Pure Water	(0.1-0.3) vol%	44nm	47%	heat transfer rate (Q)
Devireddy et al., 2016 [78]	TiO ₂	water and ethylene glycol (60-40) %	(0.1-0.5) vol%	21 nm	35%	heat transfer rate (Q)
Nieh et al., 2014 [79]	TiO ₂ Al ₂ O ₃	water and ethylene glycol	(0.5-2) wet %	50 nm	2.5% 25.6% 6.1%	pumping power heat dissipation capacity (Q) pressure drops

Table 2.10 Summary of experimental study for Hybrid Nanoparticles

Researcher's name	Nano type	Base fluid	Particle volume fraction (%)	Particle size (nm)	Maximum enhancement (%)	Remarks
Ramadhan et al., 2020 [80]	$Al_2O_3+TiO_2+SiO$	water/ethylene glycol	(0.05 to 0.3) vol %	13 nm 50 nm 23 nm	39.7 %	heat transfer coefficient (h)
Prasanna Shankara et al., 2020 [81]	MWCNT+CuO+ Graphene	deionized Water	(0.05 to 0.15) vol %.	50-100 nm	295 %	heat transfer coefficient (h)

CHAPTER THREE

THEORETICAL ANALYSIS AND NUMERICAL SIMULATION

CHAPTER THREE

THEORETICAL ANALYSIS AND NUMERICAL SIMULATION

3.1 Introduction

In this chapter, a three-dimensional numerical analysis of a flat tube with fins, such as in an automotive radiator, was performed to simulate the effect of nanofluids of aluminium oxide (Al_2O_3), copper oxide (CuO), and multi-walled carbon nanotubes (MWCNT) on the thermal performance of automotive engine radiator. Fluid flow and heat transfer were solved by using the COMSOL Multiphysics software V.5.4.

3.2 Mathematical Modelling

3.2.1 Assumption for Numerical Simulation

1. 3-Dimensional Cartesian coordinate.
2. Steady-state.
3. The fluid flow velocity inside the tubes is constant as shown in Figure 3.1.
4. Incompressible fluid flow
5. Single-phase flow
6. Constant inlet temperature of fluid flow
7. Forced convection
8. radiations
9. Constant fluid thermal properties
10. Newtonian fluid as assumed for nanofluid
11. Laminar flow
12. Fully developed flow
13. Symmetry was applied, including the radiator tube with fins on each side.

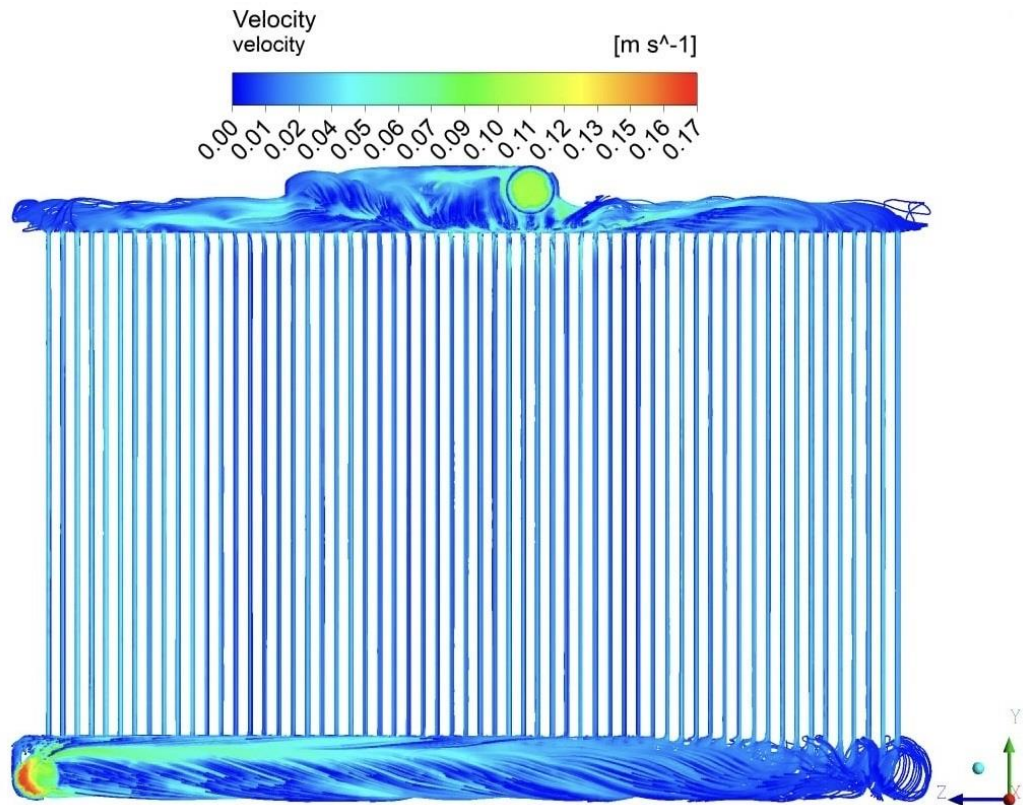


Figure 3.1 Variation of flow velocity in all tubes

3.2.2 Geometry

The effect of heat transfer was studied numerically on automotive radiators, especially on flat tubes with fins. As shown in Figure 3.2, a coolant fluid flows inside the tube, and air flows through the tubes and fins to dissipate heat by forced convection. Figure 3.3 show the flat tube with dimensions. The length of the entry region of the tube for laminar flow was calculated to ensure that the flow is fully developed after crossing this area. It will be calculate by the following equation [82] .

$$L_{laminar} = 0.05 * Re * D_h \quad (3.1)$$

The study was conducted using COMSOL Multiphysics 5.4. The flat Tube geometry is found in most automotive radiators made of aluminium, as it works effectively in heat exchangers compared to tubes

with a circular section [54]. The tube and fins dimensions are shown in Table 3.1.

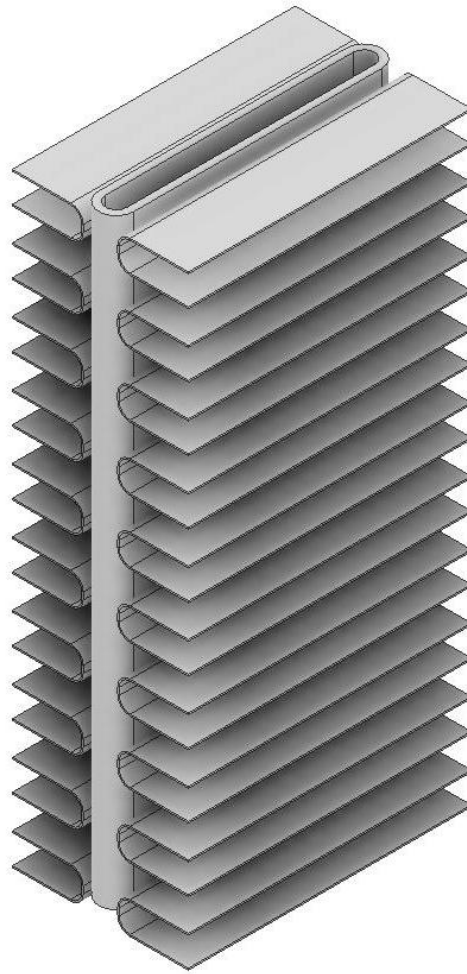


Figure 3.2 The 3-D geometry of the flat tube with fins

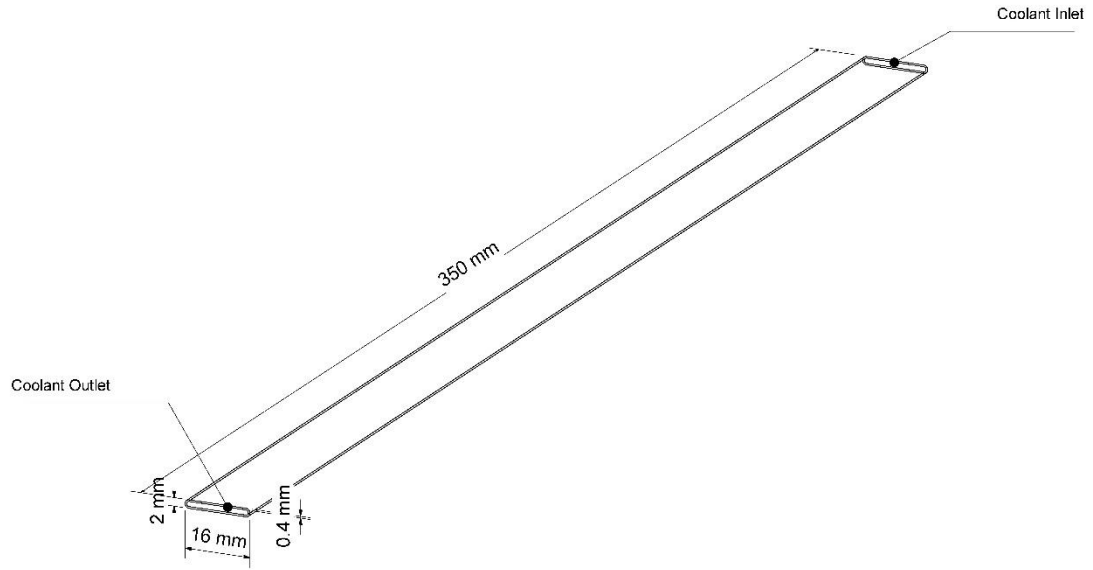


Figure 3.3 Flat tube with dimensions

Table 3.1 show the dimension of geometry in this study measured experimentally

Description	Specification
Length of tube	350 mm
Height of tube	16 mm
Width of tube	2 mm
Thickness of tube	0.4 mm
Height of fins	16 mm
Width of fins	8 mm
Thickness of fins	0.09 mm

3.2.3 Governing Equations

The computational fluid dynamics (CFD) Navier-stokes equation and the following conservation equations were used to simulate the nanofluid thermal performance [83].

Continuity Equation:

$$\rho \left(\frac{\partial u}{\partial x} + \frac{\partial u}{\partial y} + \frac{\partial u}{\partial z} \right) = 0 \quad (3.2)$$

Momentum Equation in 3D:

$$\begin{aligned} \rho \left(u \frac{\partial u}{\partial x} + v \frac{\partial u}{\partial y} + w \frac{\partial u}{\partial z} \right) &= -\frac{\partial p}{\partial x} + \mu \left(\frac{\partial^2 u}{\partial x^2} + \frac{\partial^2 u}{\partial y^2} + \frac{\partial^2 u}{\partial z^2} \right) \\ \rho \left(u \frac{\partial v}{\partial x} + v \frac{\partial v}{\partial y} + w \frac{\partial v}{\partial z} \right) &= -\frac{\partial p}{\partial y} + \mu \left(\frac{\partial^2 v}{\partial x^2} + \frac{\partial^2 v}{\partial y^2} + \frac{\partial^2 v}{\partial z^2} \right) \\ \rho \left(u \frac{\partial w}{\partial x} + v \frac{\partial w}{\partial y} + w \frac{\partial w}{\partial z} \right) &= -\frac{\partial p}{\partial z} + \mu \left(\frac{\partial^2 w}{\partial x^2} + \frac{\partial^2 w}{\partial y^2} + \frac{\partial^2 w}{\partial z^2} \right) - \rho g \end{aligned} \quad (3.3)$$

Energy Equation:

$$\rho \cdot C_p \cdot \left(u \frac{\partial T}{\partial x} + v \frac{\partial T}{\partial y} + w \frac{\partial T}{\partial z} \right) = k \cdot \left(\frac{\partial^2 T}{\partial x^2} + \frac{\partial^2 T}{\partial y^2} + \frac{\partial^2 T}{\partial z^2} \right) \quad (3.4)$$

Where (u) is the velocity vector (m/s), (ρ) the nanofluid density (kg/m^3), (P) is the static pressure (Pa), (Cp) the nanofluid specific heat at constant pressure (J/kg. K), (T) temperature of flow (K), and (k) is the nanofluid thermal conductivity (W/m. K).

3.2.4 Initial and Boundary Conditions

The above equations with couple systems are represented by the equations of conservation of mass and momentum. The equation for energy was solved by defining the boundary conditions where the inlet of the fluid was uniform along the tube from (4-8) L/min, and the used inlet temperature was 60, 70, 80 ° C. The thermal boundary conditions on the outside of the automotive radiator are subjected to convective heat transfer with an air velocity of 3 m/s on the tube walls and fins, and the ambient temperature was 30 ° C for all the distilled water and nanofluids.

Initial Conditions I.C.

$$u(x, y, z) = 0 \quad (3.5)$$

$$v(x, y, z) = 0 \quad (3.6)$$

$$w(x, y, z) = 0 \quad (3.7)$$

$$P(x, y, z) = 0 \quad (3.8)$$

Boundary Conditions B.C.

I - Inlet boundary conditions

$$U_{in}(x, y, z) = (0.0619 - 0.123) \text{ m/s} \quad (3.9)$$

$$T_{in}(x, y, z) = 60, 70, 80 \text{ °C} \quad (3.10)$$

II - Outlet boundary conditions

$$P(x, y, z) = 0 \quad (3.11)$$

III - Wall boundary conditions

$$u(x, y, z) = 0 \quad (3.12)$$

$$v(x, y, z) = 0 \quad (3.13)$$

$$w(x, y, z) = 0 \quad (3.14)$$

$$q'' = h_{out} * (T_{wall\ avg.} - T_{amb.}) \quad (3.15)$$

Heat transfer coefficient is taken from Heat-Transmission by McAdams [84] can be calculated from the following equation which is valid for wind speed ranging from 0 to 10 m/s [85]

$$h_{out} = 5.7 + 3.8 * U_{air} \quad (3.16)$$

$$T_{amb}(x, y, z) = 30 \text{ } ^\circ\text{C} \quad (3.17)$$

$$U_{air} = 3 \text{ m/s} \quad (3.18)$$

3.2.5 COMSOL Multiphysics

COMSOL Multiphysics is a finite element analysis solver and Multiphysics simulation software. It is used to perform many thermal analysis cases. It supports standard physics-based, as well as coupled systems of partial differential equations (PDEs). COMSOL offers an integrated development environment (IDE) and a single workflow for electrical, mechanical, fluid, acoustics, and chemical applications. Using COMSOL Multiphysics as a simulator software can reduce prototyping costs and time.

3.2.6 Mesh Independency

A tetrahedral mesh in this model was used, as shown in Figure 3.4. Several numerical attempts were carried out to obtain and verify results for five different mesh sizes. The chosen mesh and the solution approved contained 3,358,956 elements with a minimum quality of 0.5637 and an average of 0.8865. Figure 3.5 showing mesh independence with outlet temperature. The solution time took about 8 hours for each case.

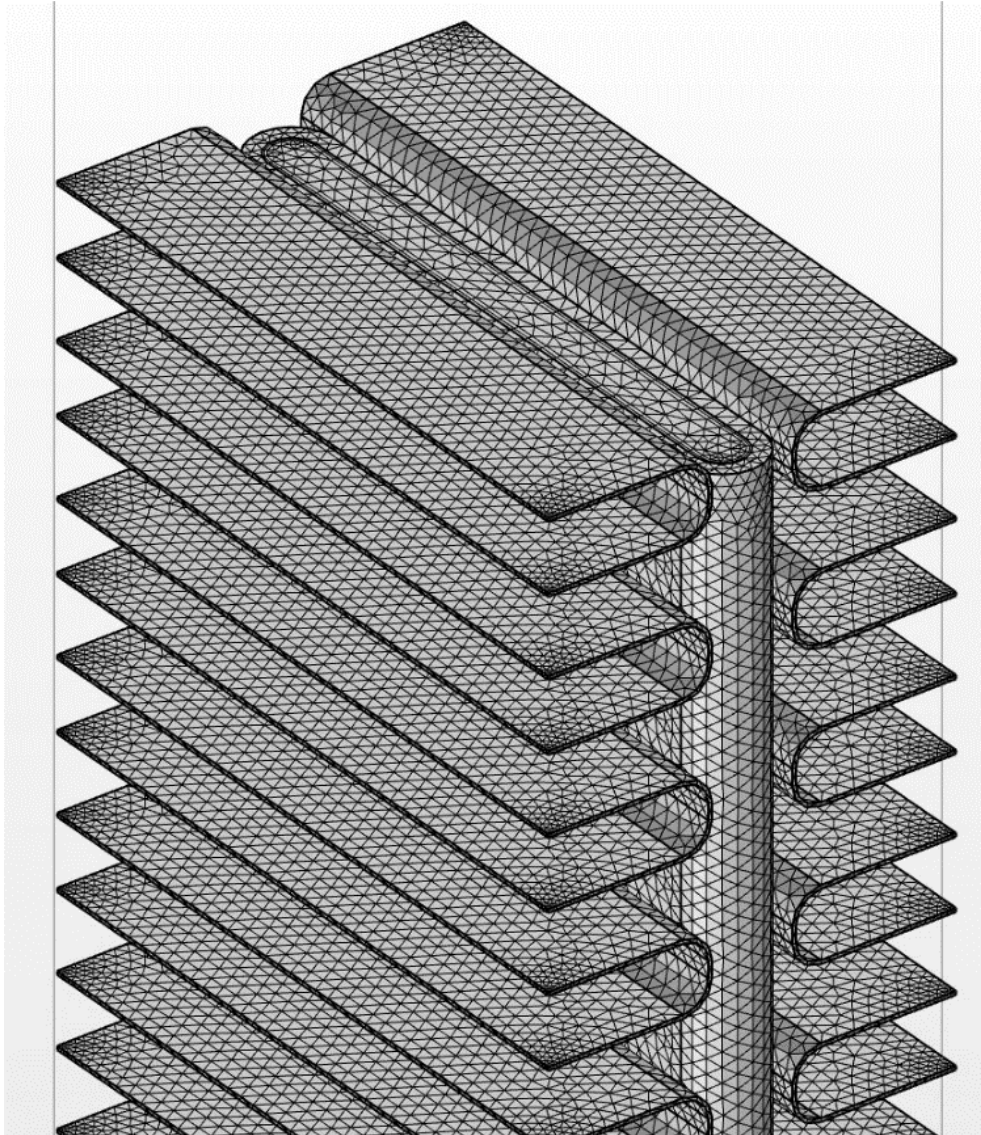


Figure 3.4 The 3D mesh model tetrahedra type used for numerical simulations

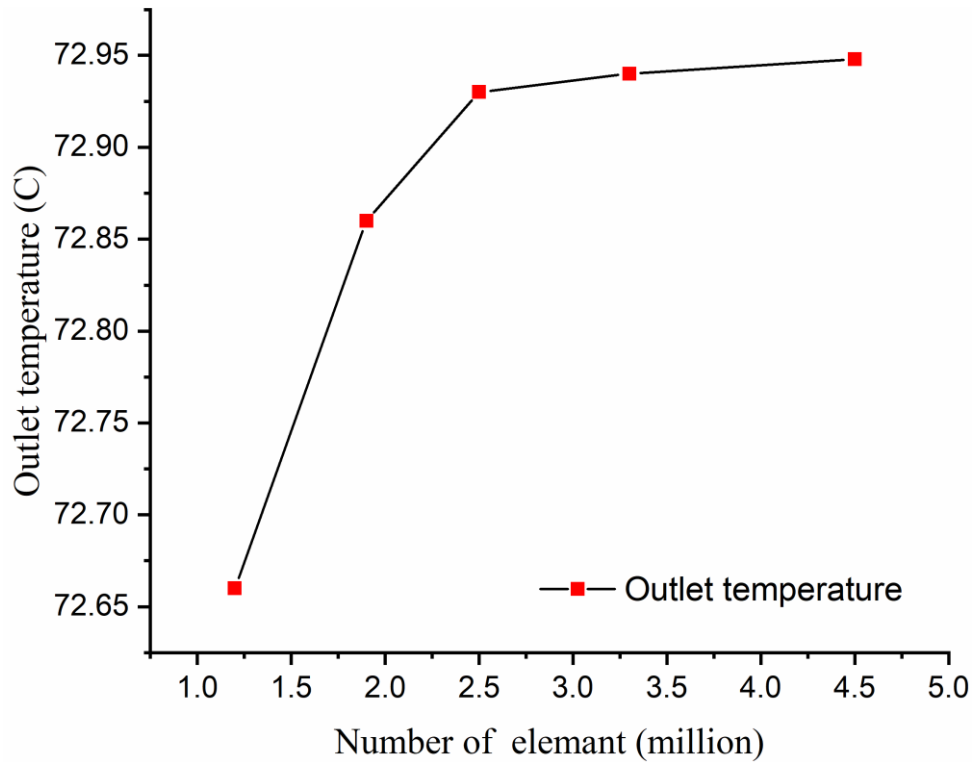


Figure 3.5 Mesh independency curve with outlet temperature

3.2.7 Thermophysical Properties of Nanofluid

The thermal properties of the base fluid (distilled water) were taken at a temperature of 60, 70, 80 °C from a thermodynamic chart [86]. The nanofluids thermal properties were calculated by equations to predict the values of thermal conductivity (K), viscosity (μ), density (ρ), and specific heat (C_p). Maxwell's model Eq. 3.1 [87] was used to calculate the thermal conductivity of spherical nanoparticles such as aluminium oxide (Al_2O_3) and Copper Oxide (CuO). The Hamilton and crosser model Eq. 3.2 was used to calculate the effective thermal conductivity for cylindrical nanoparticles (MWCNT) [88]. Einstein's equation Eq. 3.3 [89] used for calculating the viscosity of nanofluids and Eq. 3.4 and Eq. 3.5 was used to calculate the specific heat and density [79].

$$K_{nf} = \frac{K_p + 2K_{bf}(K_p + K_{bf})\varphi}{K_p + 2K_{bf} - (K_p - K_{bf})\varphi} * K_{bf} \quad (3.19)$$

$$K_{nf} = \frac{K_p + (n-1)K_{bf} + (n-1)(K_p + K_{bf})\varphi}{K_p + (n-1)K_{bf} - (K_p - K_{bf})\varphi} * K_{bf} \quad (3.20)$$

$$\mu_{nf} = (1 - 2.5\varphi_p)\mu_{bf} \quad (3.21)$$

$$\rho_{nf} = (1 - \varphi)\rho_{bf} + \varphi\rho_p \quad (3.22)$$

$$Cp_{nf} = (1 - \varphi)Cp_{bf} + \varphi Cp_p \quad (3.23)$$

Where (φ) is the volume concentration of nanoparticles [78] which can be calculated using Eq. 3.6, other abbreviations such as (bf, nf, p) denote to base fluid, nanofluid and particles, respectively.

$$\varphi = \left[\frac{\frac{W_p}{\rho_p}}{\frac{W_p}{\rho_p} + \frac{W_{bf}}{\rho_{bf}}} \right] \times 100 \quad (3.24)$$

Where W_p , ρ_p , W_{bf} and ρ_{bf} Represents the weight and density of the base fluid and the nanoparticles respectively.

3.2.8 Data Extraction

From the following equation [44], the heat transfer rate can be calculated

$$Q = \dot{m} Cp (T_{in} - T_{out}) \quad (3.25)$$

$$\dot{m} = \rho V A_{in} \quad (3.26)$$

Where (Q) is the heat transfer rate, (Cp) specific heat, (T_{in}) is the inlet temperature and (T_{out}) is the outlet temperature, the (\dot{m}) is the mass flow rate, (ρ) is the density of fluid, (V) velocity of the fluid and (A_{in}) is the inlet area of the flat tube.

The heat transfer coefficient was calculated using the following equation [13].

$$h = \frac{\dot{m} C_p (T_{in} - T_{out})}{A_s (T_b - T_w)} \quad (3.27)$$

Where (A_s) is the surface area of the flat tube, (T_b) is the average temperature of the inlet and outlet, (T_w) is the average wall temperature.

The Nusselt number and Reynold number can be calculated using the following equation:

$$Nu = \frac{h * D_h}{k} \quad (3.28)$$

$$Re = \frac{\rho * u * D_h}{\mu} \quad (3.29)$$

Where (k) is the thermal conductivity of the fluid; (D_h) hydraulic diameter, which can be calculated from the following equation[44]:

$$D_h = \frac{4 * [\pi d^2 (D - d) * d]}{\pi d + 2 * (D - d)} \quad (3.30)$$

The enhancement and error ratio can be calculated from the following equations [41].

$$\text{Enhancement} = \frac{Nu_{nf} - Nu_{bf}}{Nu_{bf}} \quad (3.31)$$

$$\% \text{ Error} = \frac{\text{Approx} - \text{Exact}}{\text{Exact}} * 100 \quad (3.32)$$

the Pumping power of the flat tube for study flow of a coolant is defined as[83]:

$$P = N * u * \Delta p * A_{cs} \quad (3.33)$$

Where the N is the total number of flat tube and A_{cs} is the cross – sectional area of the flow m^2 .

CHAPTER FOUR

EXPERIMENTAL WORK

CHAPTER FOUR

EXPERIMENTAL WORK

4.1 Introduction

In general, the objective of the experimental work is to study the effect of nanofluids on the cooling system's performance in an automotive radiator. The considered experimental parameters are; Nusselt number, heat transfer rate, the volumetric concentration of nanoparticles, fluid outlet temperature and fluid flow rate.

4.2 Experimental Setup

Figure 4.1 shows the schematic diagram of an experimental setup test rig. The diagram shows the parts and equipment used to study the effect of nanofluids on the automotive radiator. An induction consisting of an automotive radiator with a flat tube section, an axial fan with capable to ensure air velocity of 3 m/s, pipes and connections were used with a circular section of 0.5 inches to circulate the fluid within the system. A 25-litre fluid tank and 3000-watt heater with a thermostat were attached with a 0.5-hp centrifugal pump; the system flow rate was controlled with a unit containing an electric frequency converter Ls type to control the speed pump, and a flowmeter ranged from 2 to 18 L/min. Two thermocouples (K-type) were employed to measure the fluid inlet and outlet temperature. Six thermocouples (K-type) were placed on the walls of the automotive radiator tubes at specific locations to measure the temperature of the tube surfaces with accuracy ± 0.1 °C. Temperatures curves were plotted using eight channels Data Logger connected to a PC with a software interface. Fluid pressure gauges were fixed at the inlet and outlet pipe to measure the static pressure. Figure 4.2 show a photograph of the experimental setup .

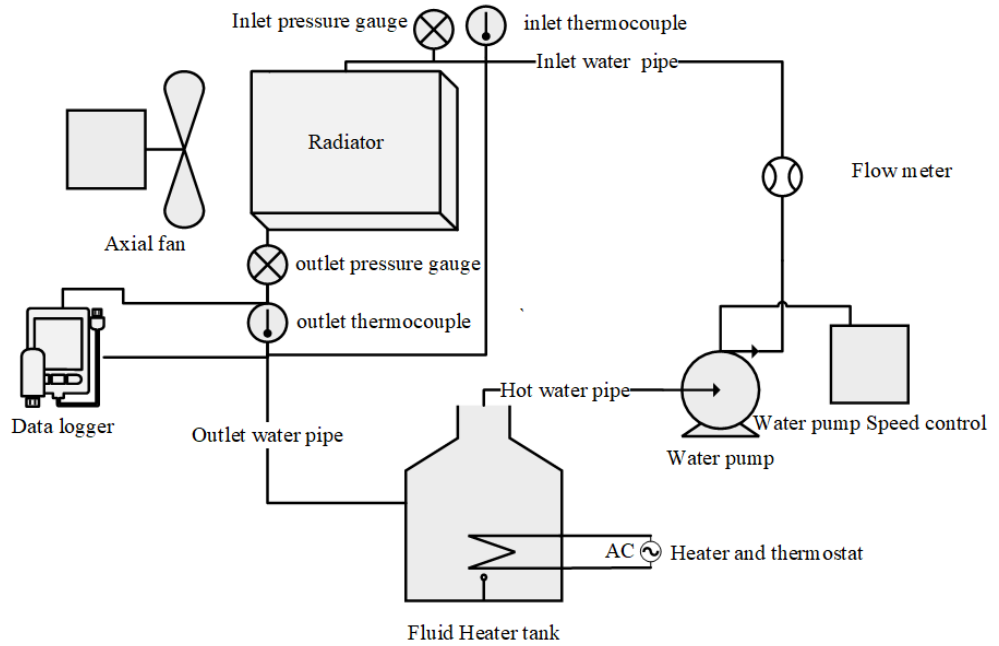


Figure 4.1 the schematic diagram of an experimental setup

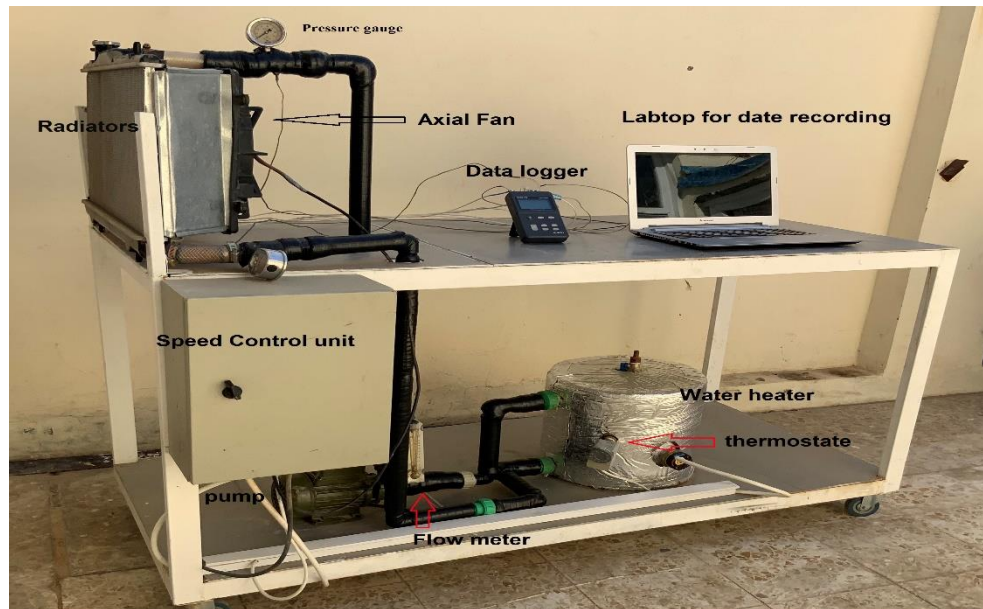


Figure 4.2 photograph of the experimental setup

4.2.1 Radiators

Figure 4.3 shows the radiators used in the current study. Two automotive radiators with different sizes were used, the first one (63 cm x 35 cm) and the second one (38 cm x 34 cm), thickness for both radiators were 16 mm; the tubes are distributed vertically, flat section fins made of aluminium are distributed between the tubes. Table 4.1 shows the dimensions of both radiators.



Figure 4.3 Radiators used in the study

Table 4.1 The specification of radiators

Description	details of the first radiator	details of the second radiator
Number of tubes	60	37
Tube length	350 mm	340 mm
Tube height	16 mm	16 mm
Tube width	2 mm	2 mm
Thickness of tube	0.4 mm	0.4 mm
Height of fins	16 mm	16 mm
Width of fins	8 mm	8 mm
Thickness of fins	0.09 mm	0.09 mm
Material	Aluminium	Aluminium

4.2.2 Cooling Fan

Figure 4.4 shows the cooling fan used in the study; this fan is used to dissipate the heat from the outside surfaces of the radiator by increasing the heat transfer coefficient. Anemometer (AM- 4206) with Resolution (0.1 m/s) and range (0.4 - 25.0 m/s) as shown in Figure 4.5 were used to measure the fan speed (3 m/s).



Figure 4.4 the cooling fan used in the study



Figure 4.5 Anemometer to measure airflow velocity

4.2.3 Water Pump

A Centrifugal pump with a capacity of 0.5 HP and a speed of 2850 RPM, as shown in Fig 4.6, continuously circulates the fluid from the water tank to the automotive radiator. The speed is controlled by an Ls frequency converter shown in Figure 4.7.



Figure 4.6 Centrifugal pump



Figure 4.7 Ls frequency converter

4.2.4 Water Tank

Figure 4.8 shows a cylindrical water tank with a capacity of 25 liters, dimensions of 30 cm in height and a base diameter of 30 cm, insulated by a thermal insulator (Thermobreak) which has low thermal conductivity ($k = 0.032 \text{ W / m.K}$). The tank contains two holes with a diameter of 1 inch for the inlet and outlet of the fluid and another hole to fill the reservoir with fluid.



Figure 4.8 cylindrical water tank

4.2.5 Water Heater

Figure 4.9 shows the water heater with a capacity of 3000 watts, placed inside the water tank to heat the fluid. The temperature, which ranges from (40-80) Celsius, is controlled by a thermostat set inside.



Figure 4.9 water heater and thermostat

4.2.6 Rotameter

Figure 4.10 shows the flowmeter (LZM-15J) to measure the amount of fluid flow through the system. The scale ranges from (2-18) L/min with accuracy $\pm 3\%$. The study was at a flow rate ranging from (4-8) L/min, and the flowmeter was calibrated with a 2 L graduated cylinder.



Figure 4.10 Flowmeter and beaker

4.6.7 Thermocouples

Eight thermocouples were used in the study; two of them are at the inlet and outlet of the fluid, and the other six are placed on the wall of the tube to measure the surface temperature, as shown in (Figure 4.11). Eight-channel data logger (Huato) model (S220-T8) with accuracy ± 0.1 °C were used to record temperatures during the test. The thermocouples were calibrated using a cold and hot bath using an alcohol thermometer with 0-100 °C gradient as shown in Appendix - A.



Figure 4.11 Distribution of thermocouples on the radiator

4.3 Nanofluid Preparation

A stable nanofluid gives more efficient results and is important in heat transfer applications nanofluids. The three types of nanofluids used in this study were prepared at different volume concentrations (0.5%, 1%) by using the two-step method, in which the nanoparticles of each of (aluminium oxide, copper oxide, and multi-walled carbon nanotubes) were mixed with the distilled water as a base fluid by Ultrasonic device (Elmasonic-P180H) for 3 hours with a frequency of 37 kHz and power 100 Watts as shown in the Figure 4.13. Surfactant (Gum Arabic) was added to increase the stability, and fluid samples were taken after adding the

surfactant; the difference between the fluid without the surfactant was observed compared with those that did not contain it. As shown in Figure 4.14, even after three months had passed, it was not noticed any sedimentation or accumulation on the nanoparticles in which the Gum Arabic ($C_{15}H_{20}NNaO_4$) was used. The weights of the nanoparticles were calculated using an accurate scale shown in Figure 4.15. The specifications of nanoparticles are shown in Appendix - B.



Figure 4.13 Ultrasonic device

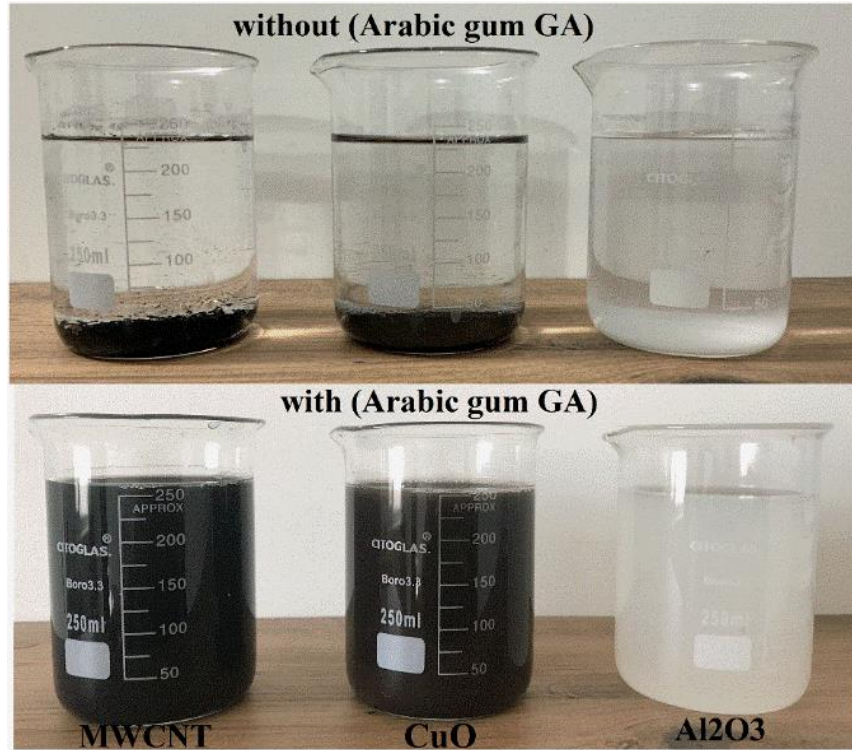


Figure 4.14 Nanofluids stability with surfactant Gum Arabic (C₁₅H₂₀NNaO₄)



Figure 4.15 Sensitive scale

4.3 Nanofluid Properties Measurement

Figure 4.16 shows the device (Decagon KD2 Pro) with Accuracy (± 5 to $\pm 10\%$) used to measure the thermal conductivity of the nanofluids used in this study; the thermal conductivity was calculated at room temperature and a concentration of 1%. The experimental results were compared with the results of the equations in Chapter 5. Figure 4.17 shows the device (Brookfield DV-111 ultra-viscometer) used to measure the viscosity of nanofluids at room temperature.



Figure 4.16 Thermal conductivity measurement device



Figure 4.17 viscosity measurement device

4.4 Experiment Procedures

- 1- Connecting and assembling the parts of the model, such as measuring devices, heater, radiator and pump, and connecting them to tubes covered with thermal insulation, and then equipping the device with electrical power for the heater and pump. Installing two thermocouples on the inlet and outlet of the fluid tubes, as well as installing six thermocouples on the outside of the radiator tubes to know the surface temperature of the tube. The experiment took place in the fourth month (April) of the year 2021
- 2- Testing the system using distilled water. The heater tank was filled with 25 liters of distilled water and the heater was turned on at a

certain temperature for the purpose of reaching the required temperature after a period of approximately 30 minutes to reach the state study temperature. Then the pump was turned on to circulate the liquid from the heater to the radiator and vice versa, making sure that there was no leakage in the pipes. The experiment was carried out in stages, where the readings are taken at different temperatures. The temperature is controlled by a thermostat at temperatures of 60, 70 and 80 degrees Celsius. As well as at different flow rates of 4, 6 and 8 liters per minute, the flow is controlled by a flowmeter that controls the pump speed, which is the frequency converter.

- 3-** Preparation of the nanofluid: The preparation was made using the two-step method, where the nanoparticles are extracted with the base fluid using an ultrasonic device. The aim of this is to obtain an optimal dispersion of the particles within the fluid for the longest possible period by using a surfactant (Gum Arabic).
- 4-** Fill the heater tank with the nanofluid and operate the heater to reach the required temperature, then the pump is turned on to rotate the fluid and the speed of the pump is controlled by the frequency converter device, The readings of the thermocouples are taken by connecting them to the eight-channel data logger. The experiment was repeated more than once for the purpose of verifying the validity of the recorded data. An error rate was analyzed according to the equations used and the accuracy of the devices used in the experimental results as shown in the Appendix - C.

CHAPTER FIVE

RESULT AND DISCUSSION

CHAPTER FIVE

RESULTS AND DISCUSSION

5.1 Introduction

In this chapter. The numerical and experimental results are presented and discussed. In the experimental results, the Nusselt number and heat transfer rate were calculated for two different radiator sizes using three different nanofluids (Al_2O_3 , CuO, MWCNT) at different volume concentrations and different flow rates. A numerical model was developed using the COMOSL Multiphysics V.5.4 simulation software to reduce the cost of experiments and obtain results at the appropriate volumetric concentration and inlet temperatures as reported in Appendix - D.

5.2 Numerical Results

To understand the effect of Al_2O_3 , CuO, MWCNT nanofluids in the automotive radiator and reduce the experimental side's cost, the CFD model has been used by employing COMOSL Multiphysics 5.4 simulation software. The boundary conditions were used for numerical results at inlet temperatures of 60, 70, 80 °C with flow rates of (4,6,8) L/min and volume concentrations of (0.5, 1, 2) %.

5.1.1 CFD Model's Verification

The numerical result conducted using COMSOL 5.4 software is compared with other researchers to validate the Programmed model.

A comparison with previous work was carried out to verify the model used to study the flat tubes of the radiator using distilled water. **Hussein et al.**[90] used an automotive radiator containing 32 flat copper

tubes and an inlet temperature 80 °C fluid flow rate of 2-8 L/min. Figure 5.1 shows a variation between the Nusselt number and Reynolds number for the present study compared with the previous studies of the researcher. After comparing the present results with Hussein et al., It has been conducted the percentage error is 6.2%, which is reliable.

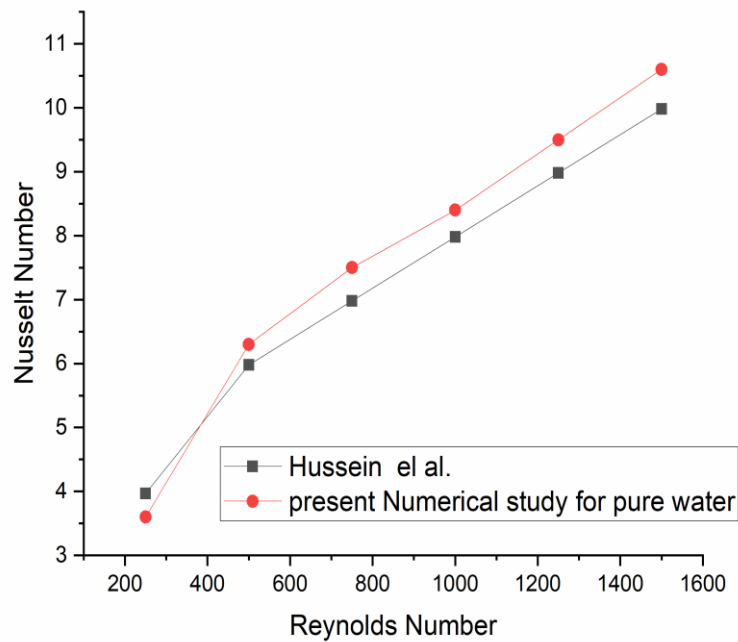


Figure 5.1 Comparison of the numerical results of the current study with the experimental results of Hussein et al.[90]

Elsebay et al. [91] presented numerical results using ANSYS Fluent software to study the heat transfer coefficient of flat tube used in the automotive radiator with Reynolds number ranging from 250 to 1750, inlet temperatures 80 °C and air temperatures were 30 °C with tube dimensions of height (3mm), width (9mm) and length (345mm). Figure 5.2 shows a variation between the Nusselt number and the heat transfer coefficient for the present study compared with the previous studies of

the researcher. After comparing the present results with Elsebay et al., It has been conducted the percentage error is 6.2%, which is reliable.

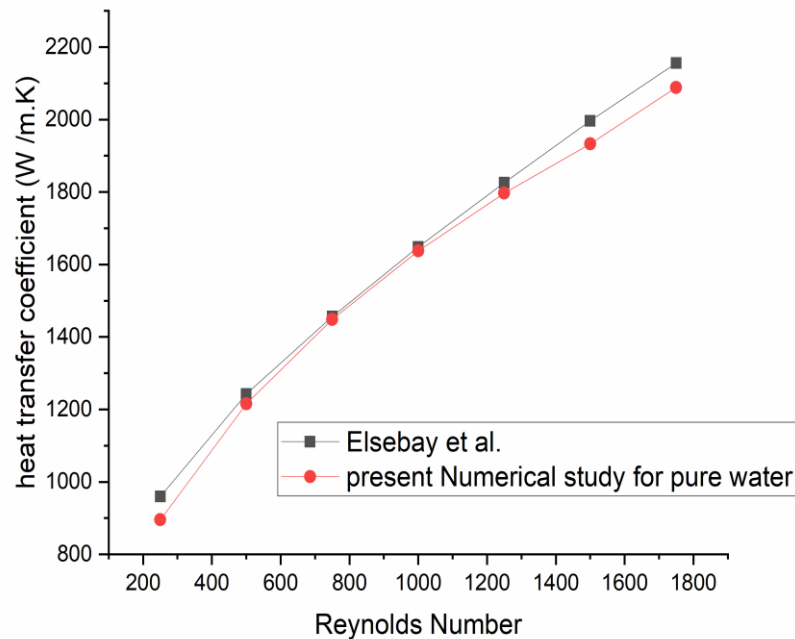


Figure 5.2 Comparison of the numerical results of the current study with the Elsebay et al. [91]

5.1.2 Effect of Distilled Water Flow Rate in Radiators With Different Inlet Temperatures

Initially, the effect of inlet temperature on distilled water at different flow rates has been studied.

Figure 5.3 shows the variation of the Nusselt number with flow rates for different inlet temperatures, where we notice that the flow rate increases, the Nusselt number increases. The Nusselt number is directly proportional to the convective heat transfer coefficient, which depends on the mass flow of the fluid. Increasing the flow velocity leads to an

increase in the Nusselt number. When the inlet temperature of the water increases, the Nusselt number increases because of the change of thermal properties of the fluid, such as increases the thermal conductivity of the fluids and decreases of the specific heat.

Figure 5.4 shows CFD results of the surface temperature distribution on three dimensional a flat tube with fins using distilled water for three cases, the first case 4 L/min, the second case 6 L/min, the third case for 8 L/min. We note the temperature distribution along the length of the tube, where there is a rectangle at the top of the tube, represents the inlet temperature 80 °C, and the other at the bottom of the tube represents the outlet temperature. The outlet temperature varies when the flow rate is different, as it is clear that at a flow rate of 4 L/min, the outlet temperature was approximately 71.5 °C and at 6 L/min was approximately 74 °C. Finally, at 8 L/min, it was approximately 76.4 °C. The temperature difference decreases when the flow rate increases. As it is clear at a flow rate of 4 L/min, we got the lowest temperature from the outlet, and the outlet temperature increased by increasing this flow rate due to the speed of flow inside the pipes and the time it takes for heat to transfer from the fluid to the outside environment by convection.

Figure 5.5 shows the surface temperature distribution of the fins and tube at the inlet, middle and end of the tube.

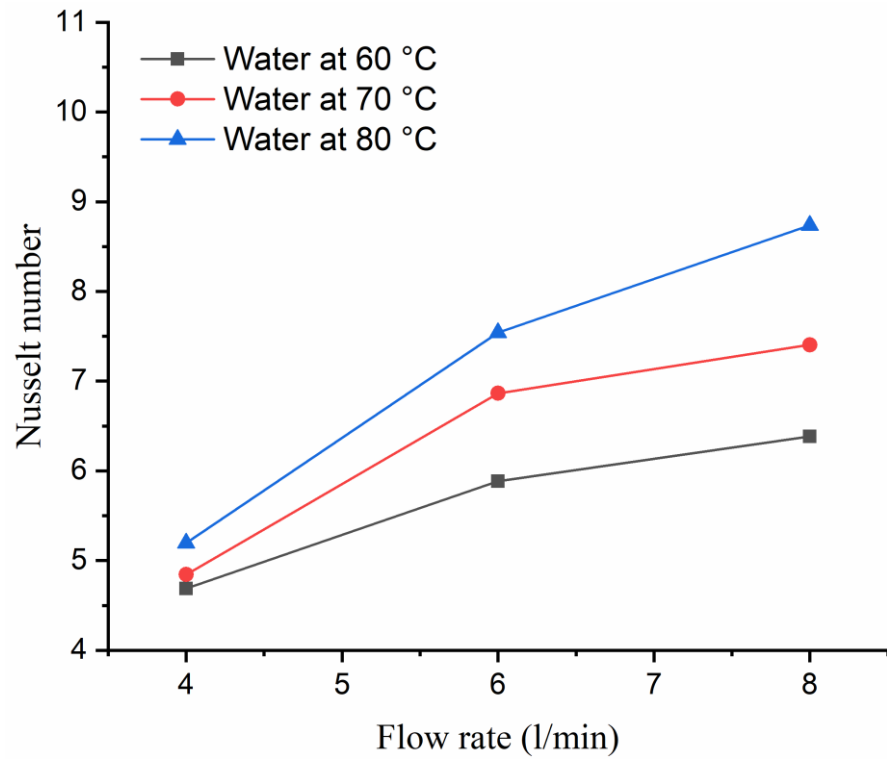


Figure 5.3 variation of the Nusselt number for distilled water

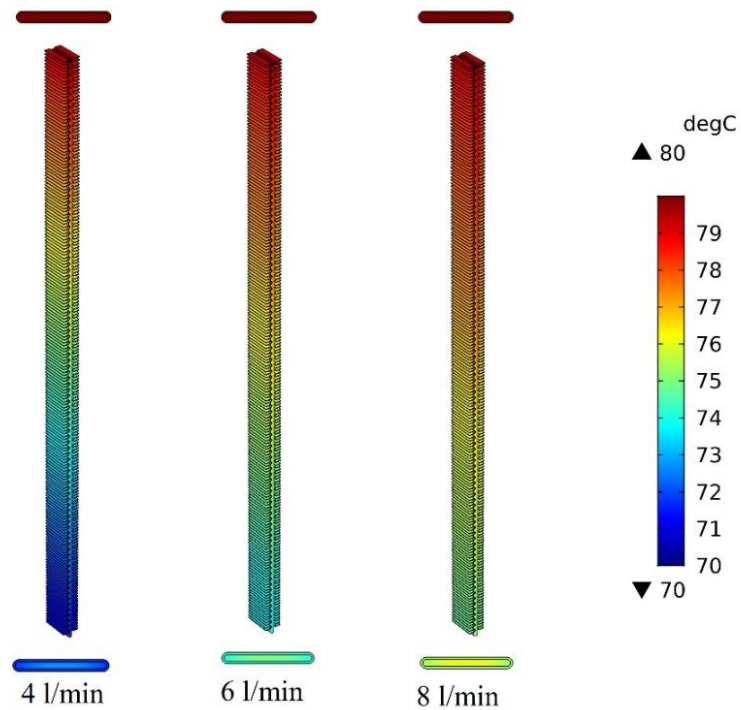


Figure 5.4 Temperature variation of distilled water with a different flow

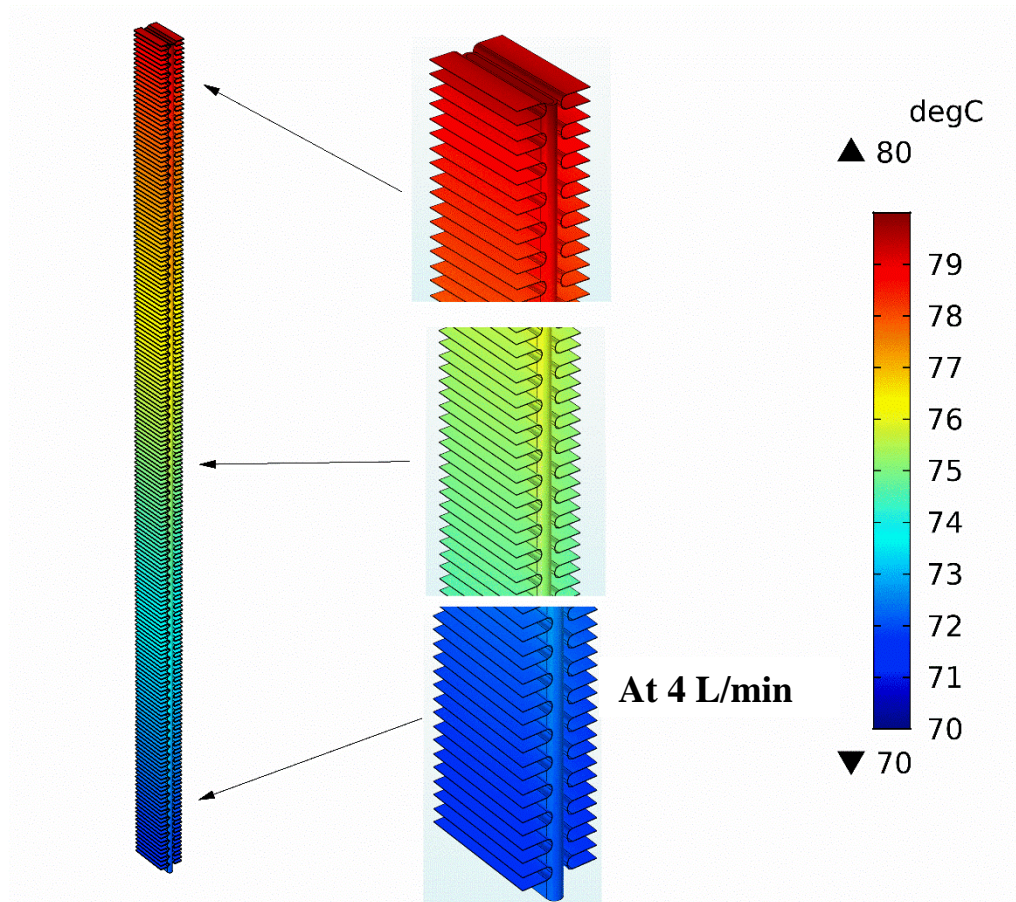


Figure 5.5 fins and the tube with the temperature variation flow rate and temp

The increase in Nusselt number due to fluid temperature increase has been explained in previous studies. It is attributed to the increase in thermal conductivity and the decrease in specific heat [92].

Table 5.1 shows a comparison of the experimental results of the thermal properties test with the results of the equations in chapter 3, where the error rate was 1%.

Table 5.1 Comparison of the thermal properties obtained using of experimental test with the recommended correlations

Nanofluid	Thermal properties	Experimental test	Value by Equation
MWCNT 1%	Conductivity	0.71	0.707
	Viscosity	0.00037	0.0003625
CuO 1%	Conductivity	0.691	0.687
	Viscosity	0.000368	0.0003625
Al ₂ O ₃ 1%	Conductivity	0.688	0.685
	Viscosity	0.000365	0.0003692

5.1.3 Effect of Nanofluid Flow Rate in Radiators with Different Inlet Temperatures

Figures (5.6, 5.7, 5.8) show the variation of the Nusselt number with flow rates (4, 6, 8) L/min at different volume concentrations (0.5, 1, 2) % at different inlet temperatures (60,70,80) °C. for the three nanofluids (Al₂O₃, CuO, MWCNT) The results indicated that the increase in the volume concentration of nanoparticles had increased the Nusselt number. Al₂O₃ nanofluid at 2 % volume concentration showed an increase in Nu number of 29%, 32.7% and 32.9% at 60, 70, 80 °C respectively, whereas, for CuO at 2% volume concentration was 38.9%, 43.7%, 48.6% at 60, 70, 80 °C respectively. MWCNT at 2% volume concentration showed an increase of 45%, 52.8%, 59.7 % for each input temperature 60, 70 and 80 °C, respectively. Since it is clear that the increase in the Nusselt number increases with the increase in the inlet

temperature of the nanofluid as well as the increase in the flow rate, it is directly proportional to the convective heat transfer coefficient and thus leads to the enhancement of the Nusselt number, the increase obtained at 2% volume concentration differs from another nanofluid is due to the thermal properties of nanofluids. Figure 5.9 shows the Nusselt enhancement when using nanofluids at different volume concentrations. It's proved that the nanofluids have significantly enhanced the Nusselt number of the automotive radiator compared to distilled water. Adding a small amount of nanoparticles in the base fluid, such as distilled water, can change the fluid's thermal properties by increasing the thermal conductivity, density and viscosity, and decreasing the specific heat. This change in the thermal properties has led to a significant increase in the heat transfer coefficient of the nanofluid [55]. In addition, the collision between the nanoparticles and the tube's surface has resulted in the dispersion and oscillation of the particles near the wall leading to an increase in the rate of heat transfer [93].

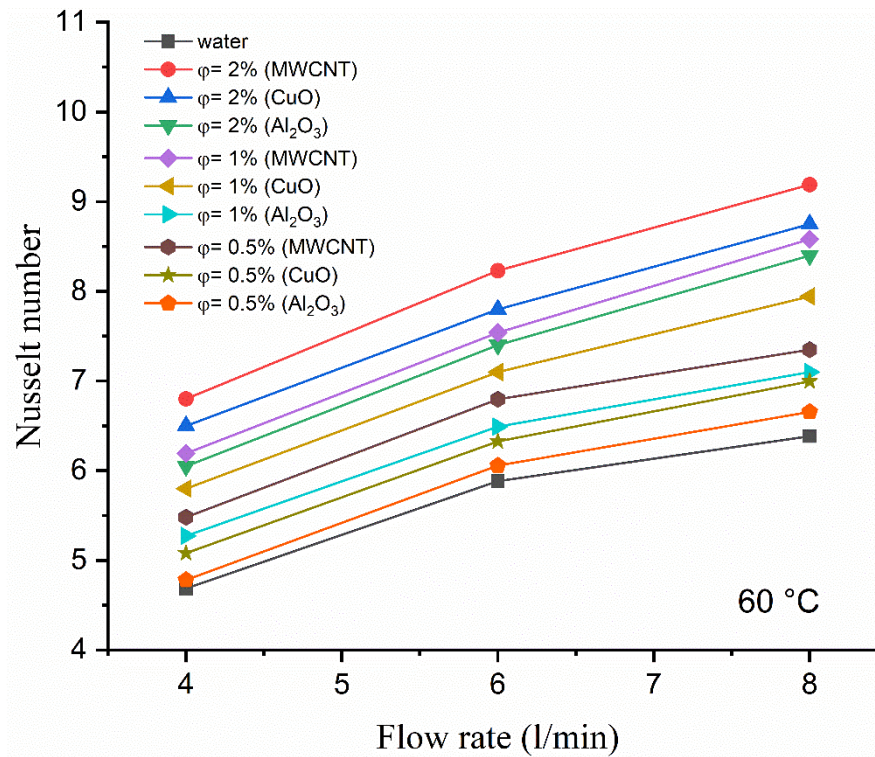


Figure 5.6 Nusselt number varied with different flow rates at 60 ° C

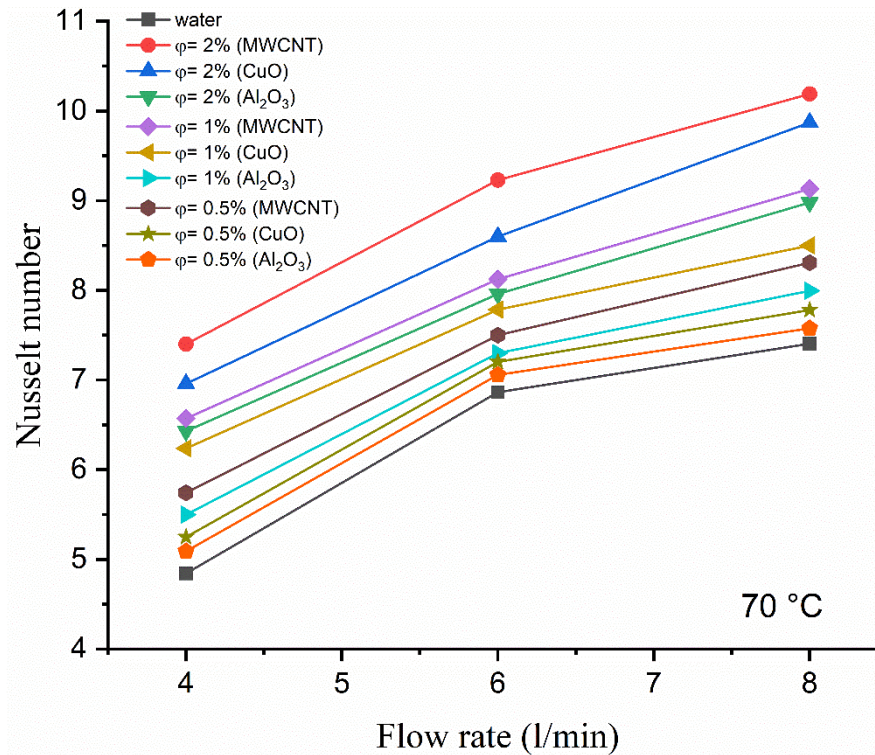


Figure 5.7 Nusselt number varied with different flow rates at 70 ° C

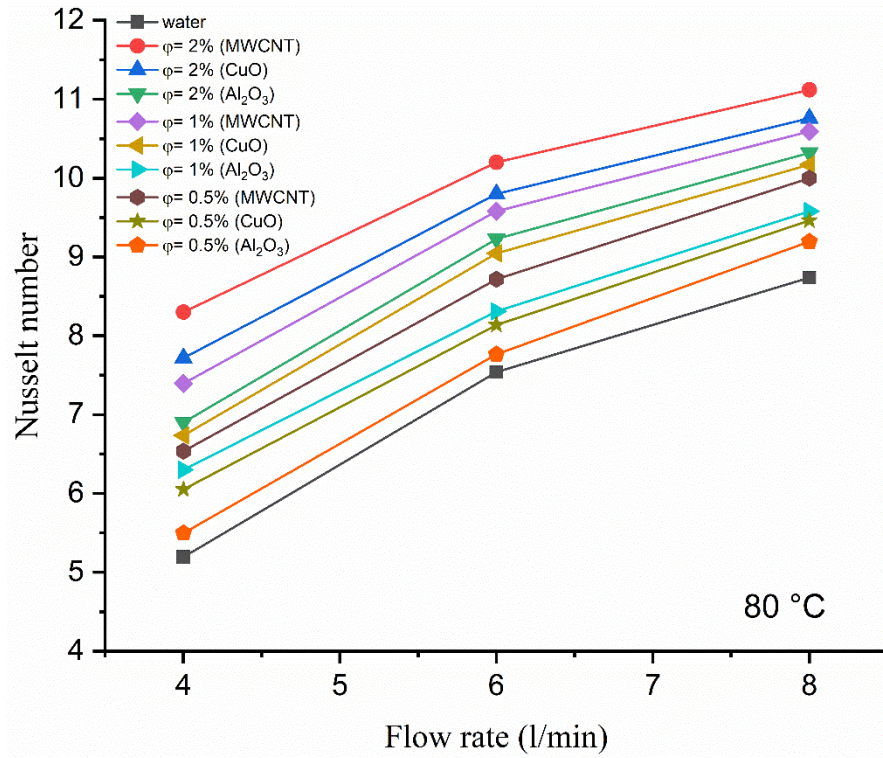


Figure 5.8 Nusselt number varied with different flow rates at 80 ° C

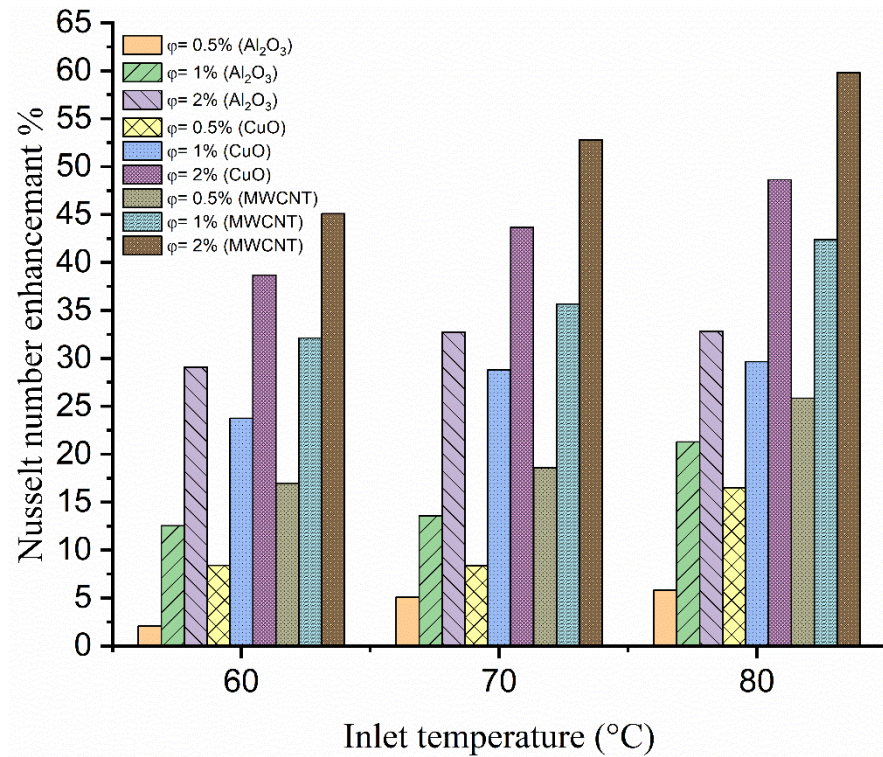


Figure 5.9 Enhancement of Nusselt number for Numerical result

Figures 5.10, 5.11, 5.12. show the variation of the heat transfer rate with flow rates (4, 6, 8) L/min at different volume concentrations (0.5, 1, 2) % at different inlet temperatures (60,70,80) °C. for the three nanofluids (Al₂O₃, CuO, MWCNT). The highest percentage was obtained at a volume concentration of 2%, the heat transfer rate enhancement for Al₂O₃ was 15.6%, 19%, 34%, and for CuO was 23.6%, 40.9%, 51.3%, whereas for MWCNT was 32%, 52.8%, 65.2% at the inlet temperatures of 60, 70, 80 ° C respectively. This increase is due to the amount of heat transfer rate, which is calculated by $(T_i - T_o) * \dot{m}$. The heat transfer rate increases with the increase in the flow rate and the temperature difference between the inlet and outlet. Then the engine will run with better heat transfer rate. Moreover, at a high flow rate, nanoparticles are more affected by dispersion and chaotic movement, which causes an increase in heat transfer rates and reduces the amount of accumulation and aggregation of particles in the nanofluid [93]. Figure 5.13 shows the heat transfer rate enhancement for nanofluids at different volume concentrations. It shows that the best improvement in the heat transfer rate is for the MWCNT nanofluid at a concentration of 2% compared with other nanofluids and the base fluid.

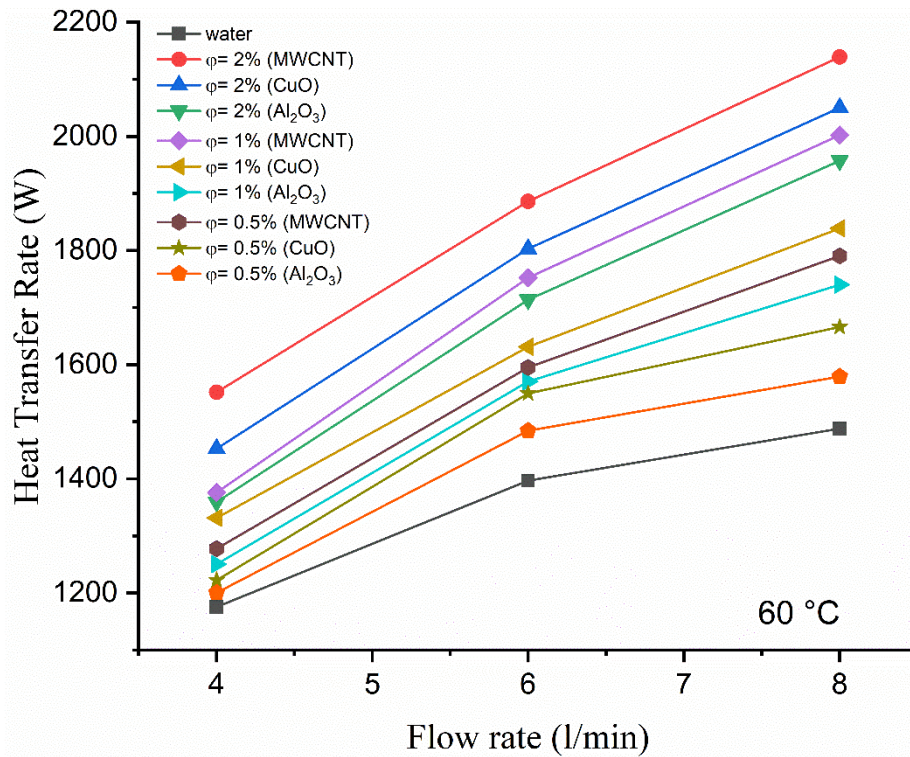


Figure 5.10 Heat transfer rate varied with different flow rates at 60 ° C

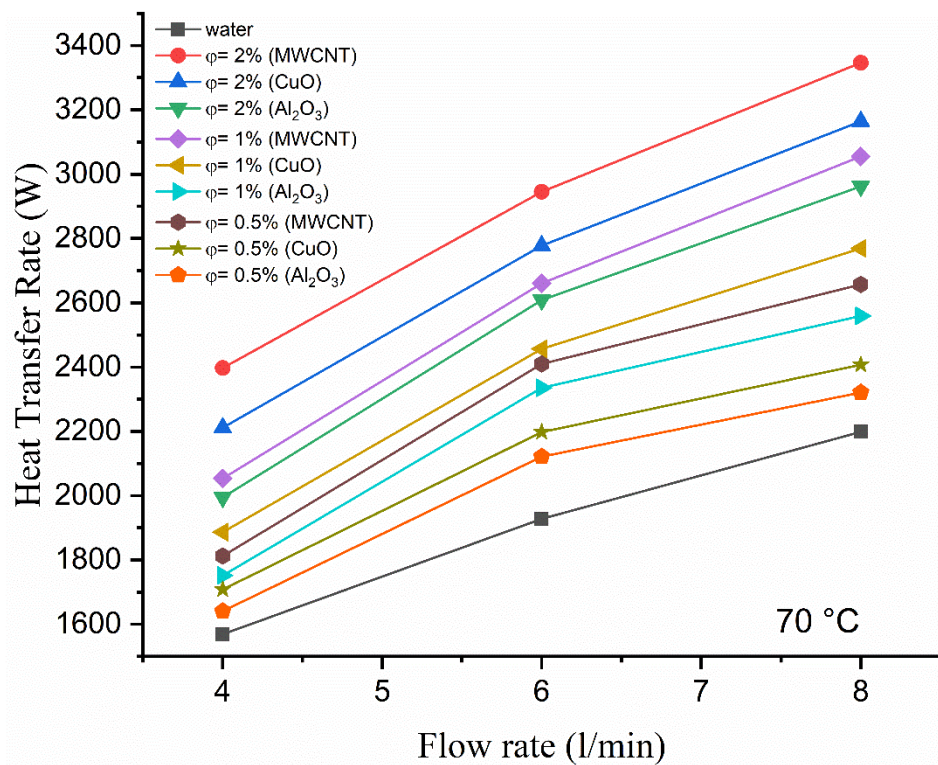


Figure 5.11 Heat transfer rate varied with different flow rates at 70 ° C

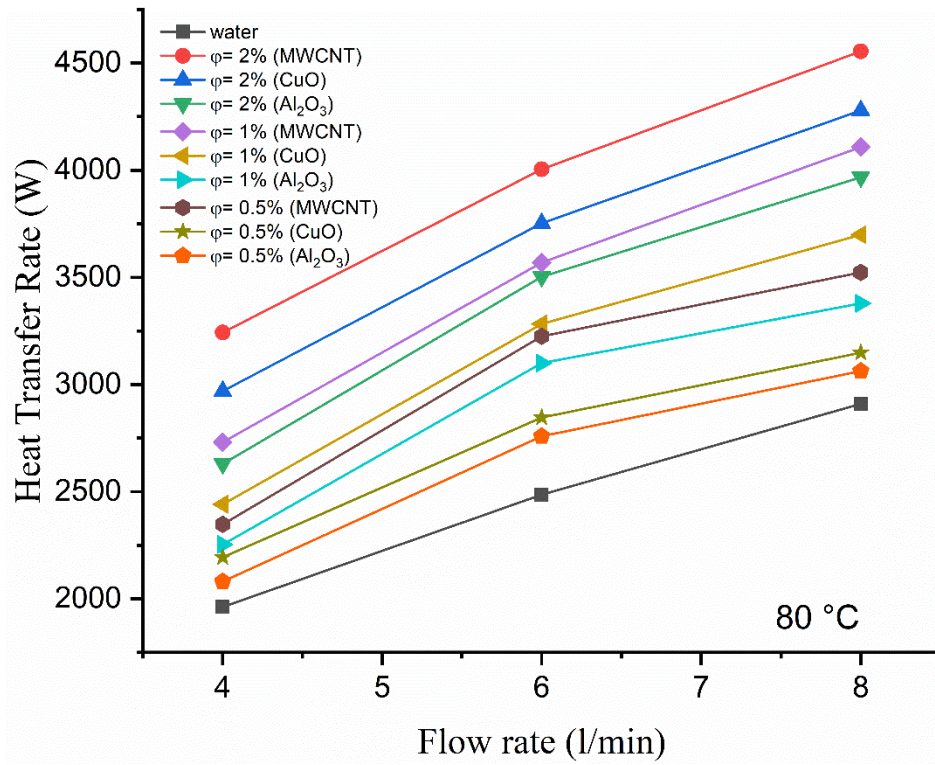


Figure 5.12 Heat transfer rate varied with different flow rates at 80 ° C

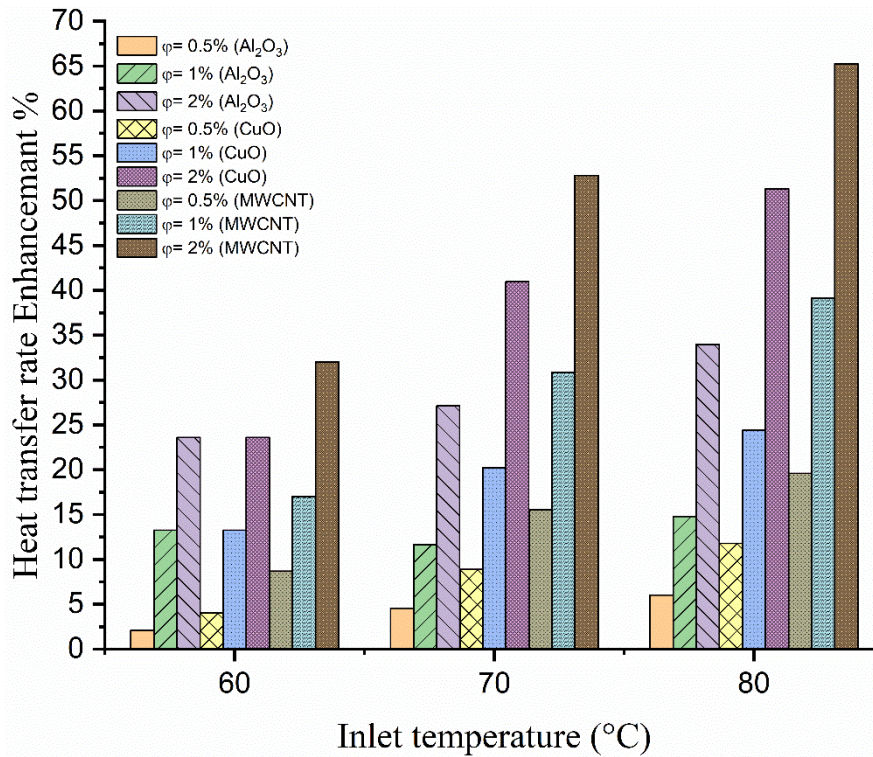


Figure 5.13 Enhancement of heat transfer rate for Numerical result

Figures (5.14, 5.15, 5.16) shows CFD results of the surface temperature distribution on three dimensional a flat tube with fins using the three nanofluids for three cases, the first case at 0.5% volume concentration, the second case at 1% volume concentration, the third case for at volume concentration 2%. The figures show the temperature distribution of the flat tube and fins, and the rectangle at the bottom represents the outlet temperature of the nanofluid. The outlet temperature decreases with the increasing volumetric concentration of nanoparticles and varies with the nanofluid. The lowest temperature at a volume concentration of 2% using MWCNTs nanofluid has given better thermal performance than Al_2O_3 and CuO nanofluids at the same volume concentration. This improvement in nanofluids can be attributed to the high heat transfer officiation of the nanofluid, which leads to a more significant heat transfer and, as the interaction between the dynamic particles and the molecules in fluids leads to an improvement in the thermal conductivity. Likewise, the random movement of particles through the fluid has enhanced the fluid convection, and thus the heat transfer rate will increase [94].

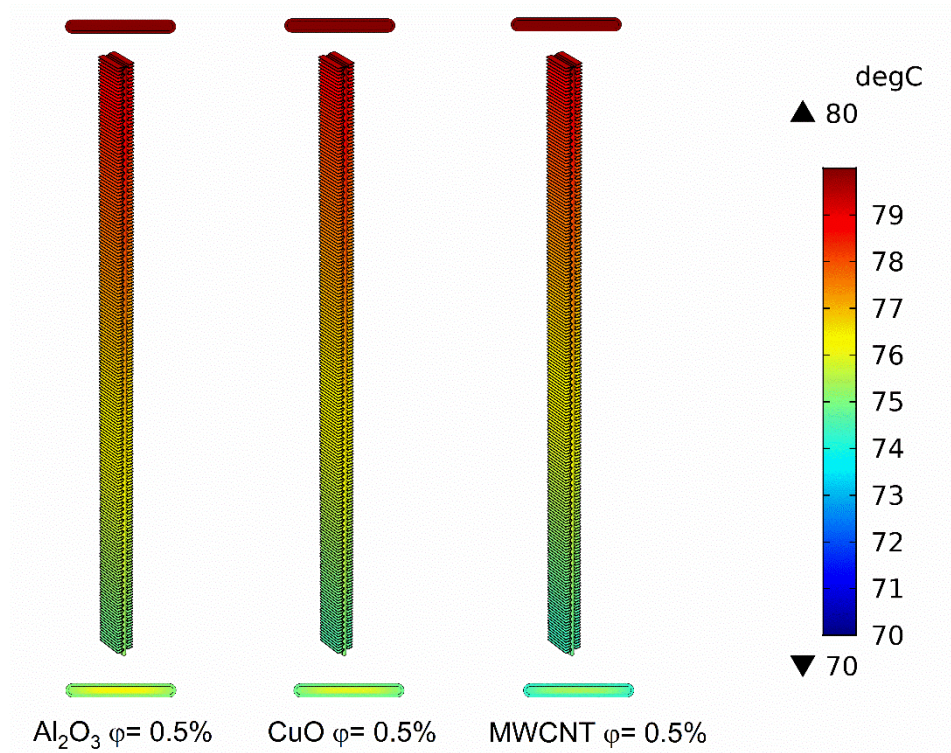


Figure 5.14 Temperature variation of the flat tube with fins at 0.5 vol%

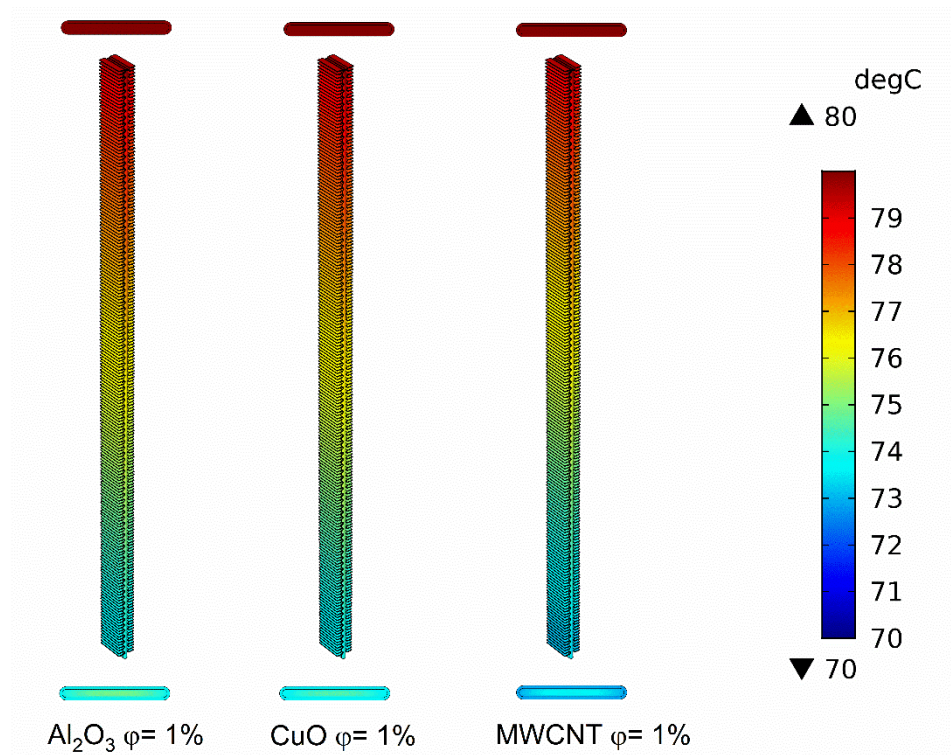


Figure 5.15 Temperature variation of the flat tube with fins 1 vol%

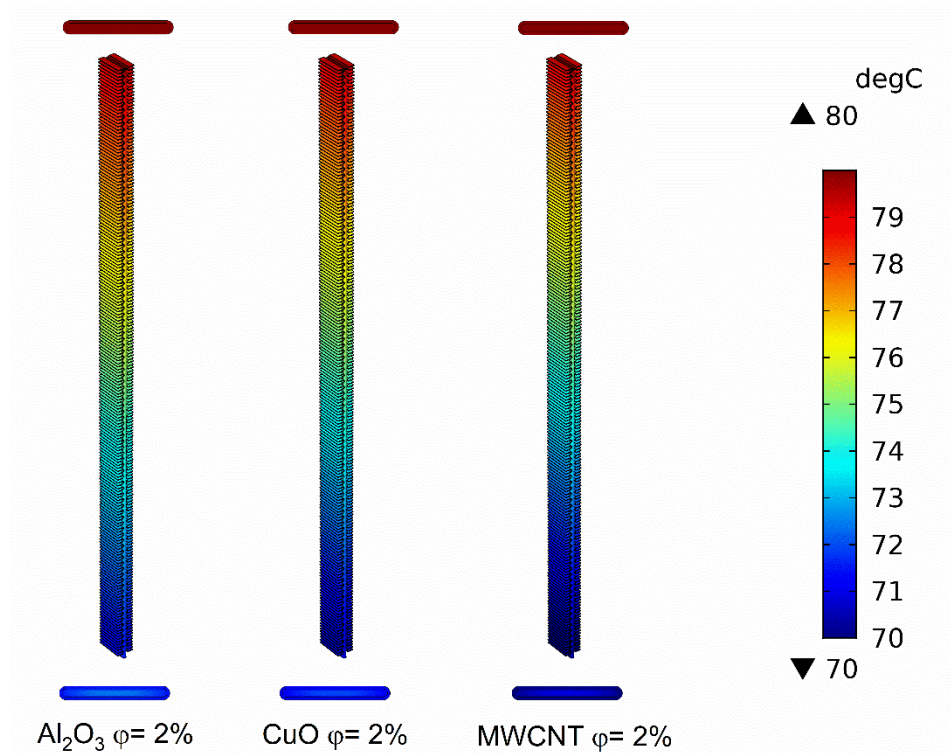


Figure 5.16 Temperature variation of the flat tube with fins at 2 vol%

Figures (5.17, 5.18, 5.19, 5.20) show the variation of the outlet temperature of the fluid along the radiator flat tube length. A decrease in the outlet temperature for the three flow rates (4,6,8) L/min of each nanofluid (Al_2O_3 , CuO , MWCNT) as well as the distilled water at the inlet temperature of $80\text{ }^\circ\text{C}$ is achieved. The difference between the inlet and outlet temperatures was $6.8\text{ }^\circ\text{C}$ for distilled water, $7.8\text{ }^\circ\text{C}$ for Al_2O_3 , $8\text{ }^\circ\text{C}$ for CuO and $9.2\text{ }^\circ\text{C}$ for MWCNT . The decrease in the outlet temperature depends on the fluid flow velocity and the volume flow rate. The increase in heat transfer rate is caused by the increase in the temperature difference between the inlet and outlet. Table 5.2 summarizes the results of the Nusselt number at different inlet temperatures and different volume concentrations of nanofluids under the current study.

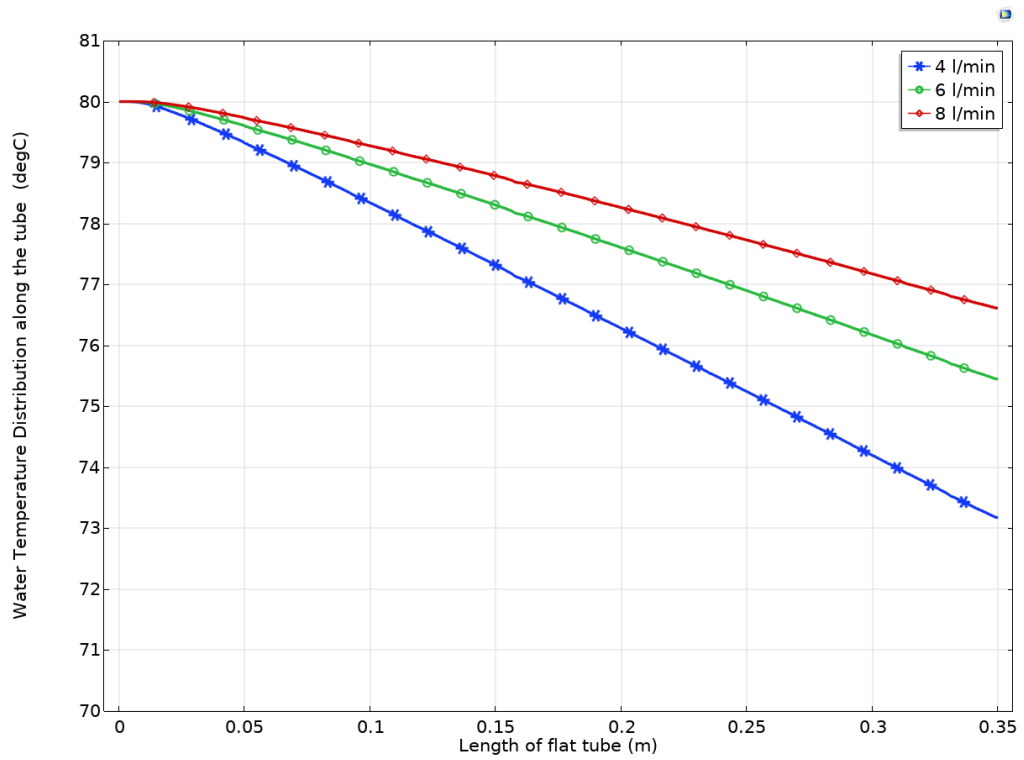


Figure 5.17 Temperature variation of distilled water flow along the flat tube

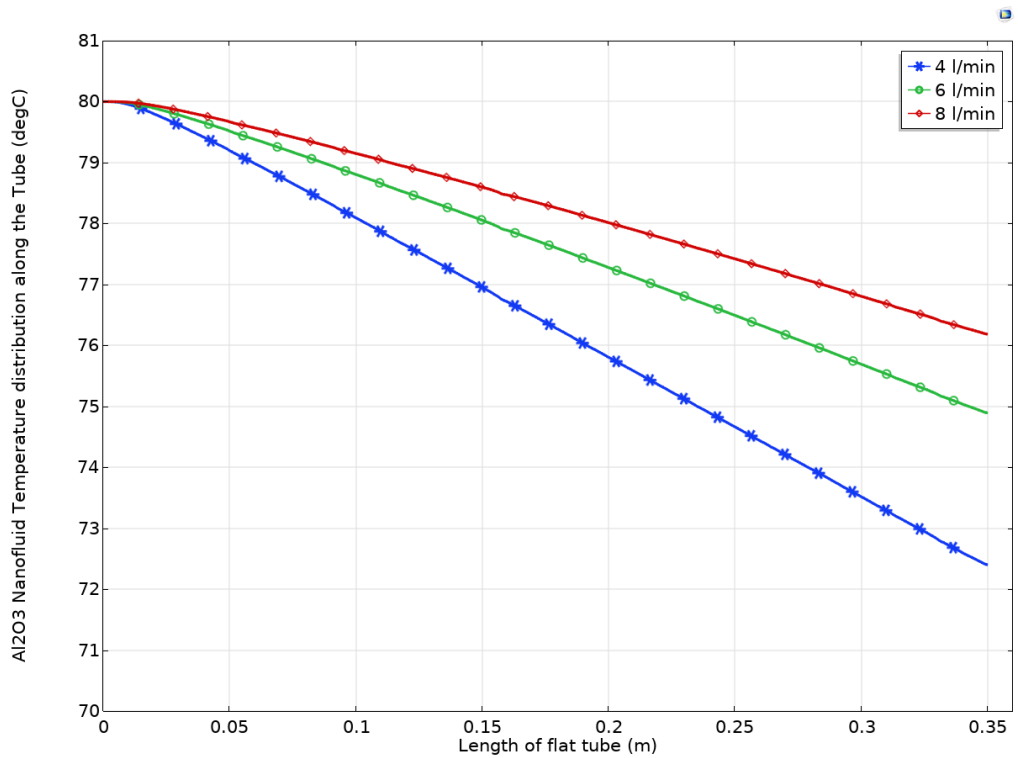


Figure 5.18 Temperature variation Al₂O₃ flow along the flat tube

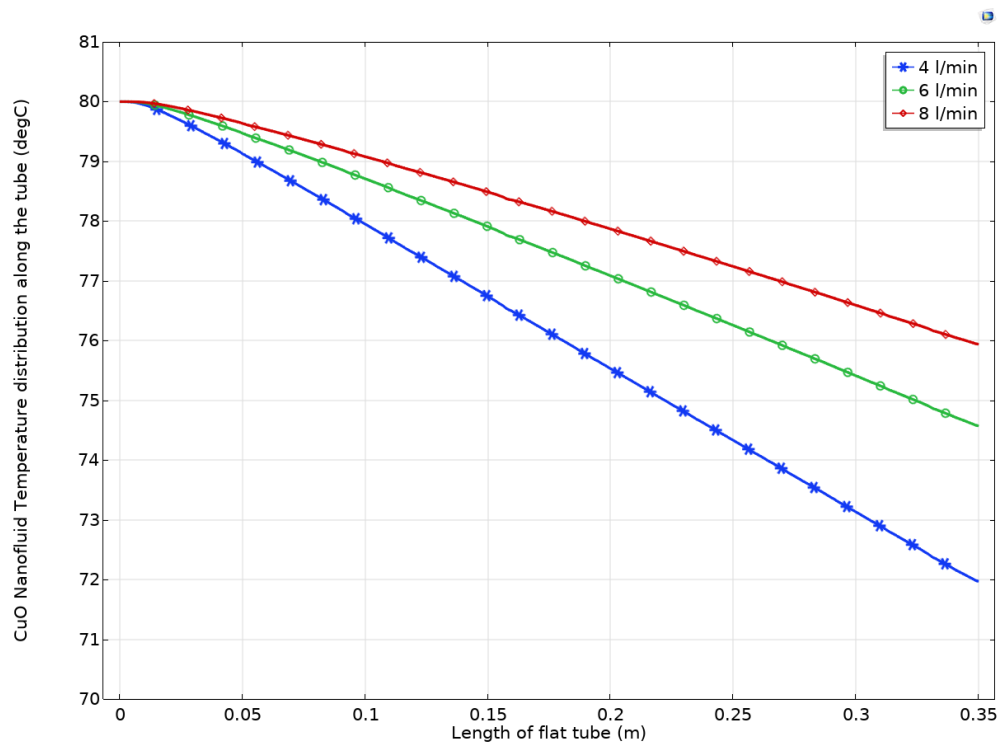


Figure 5.19 Temperature variation of CuO flow along the flat tube

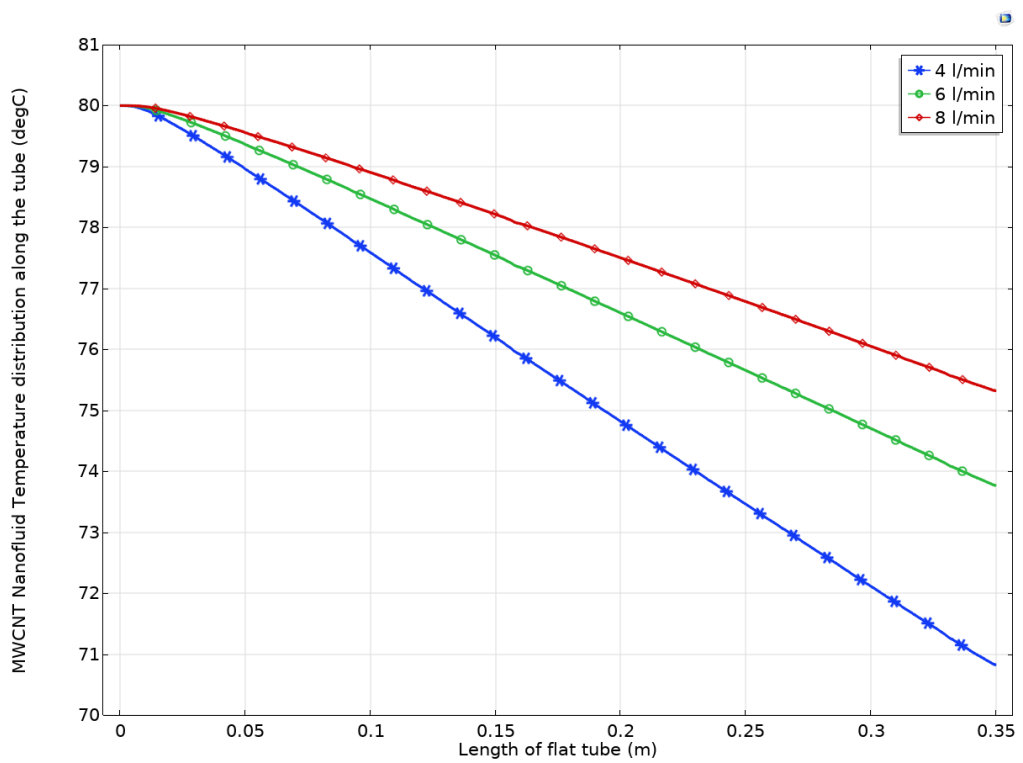


Figure 5.20 Temperature variation of MWCNT flow along the flat tube

Figure (5.21) shows the pumping power required for each of the distilled water and nanofluids previously studied numerically at a volume concentration (1%), where the percentage increase in the pumping power of the nanofluids is (1.7%, 1.46%, 0.73%) for each of CuO, Al₂O₃, and MWCNT, respectively compared with distilled water, as it is clear that the result of the lower pumping power was for MWCNT nanofluid, and therefore because it has a lower density and viscosity compared to other nanofluids such as Al₂O₃ and CuO nanofluid, where these properties affect the flow significantly as it increases. Therefore, its need a greater pumping power. This increase in the pumping power is slight and can be neglected as the thermal performance increase significantly. Figures (5.22, 5.23) show the velocity and temperature profile at different flow rates (4,6 and 8) L/min for distilled water. It shows that the flow has become fully developed after crossing the entry region that was previously determined from the by Eq. 3.1. Where the velocity at the walls is equal to zero m/s whereas in the middle is at the highest value; this behavior is also found in the temperature profile, as the temperature at the wall is less valuable than that in the middle of the pipe. Figures (5.24, 5.25) show the flow in full development in the form of arrows along the pipe, as well as the streamlines of the flow. The velocity at the walls is at the lowest value with blue color and at the middle is the highest value with red color. This phenomenon of velocity distribution (if the flow is fully developed or not) cannot be observed on the experimental side, but only in the numerical simulation at the flow rate (4-8) L/min.

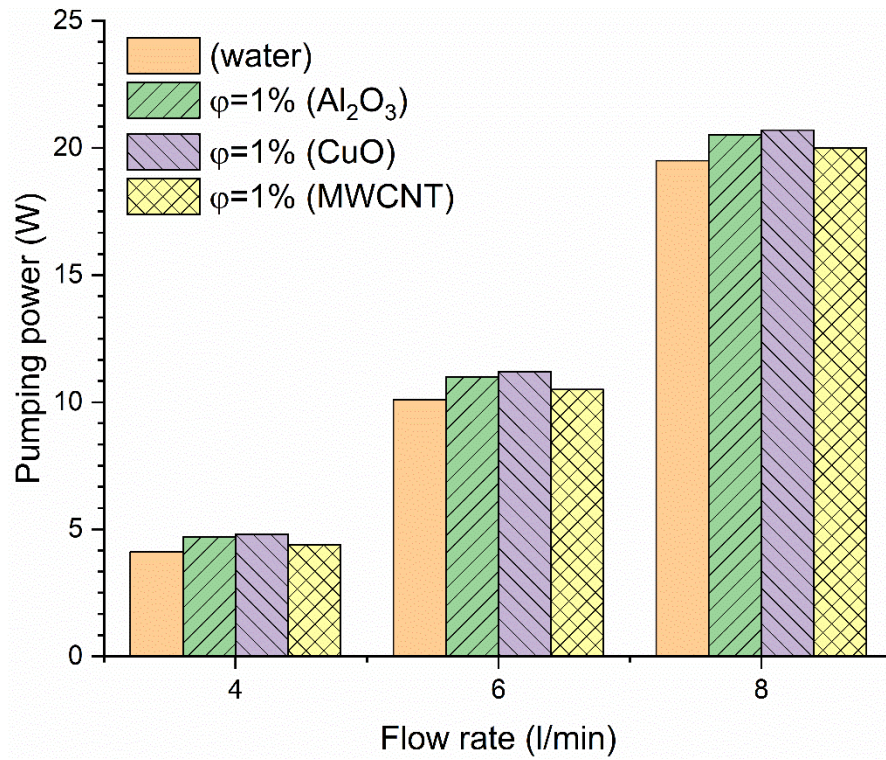


Figure 5.21 the pumping power of the water and nanofluid

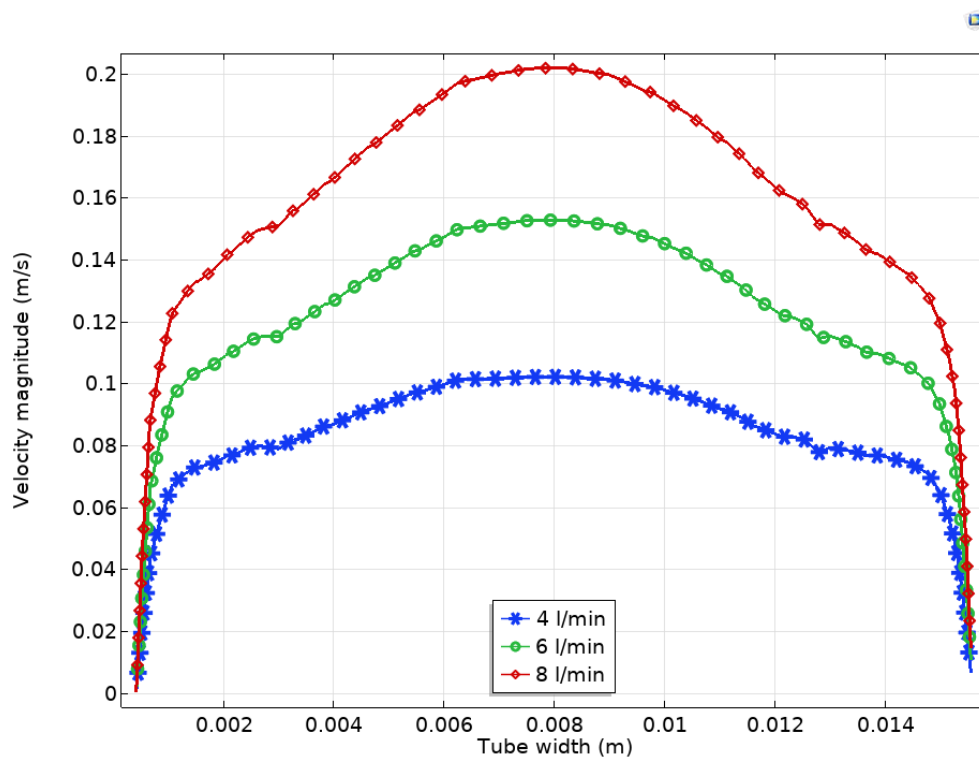


Figure 5.22 Fluid Velocity profile for the tube with the different flow rate

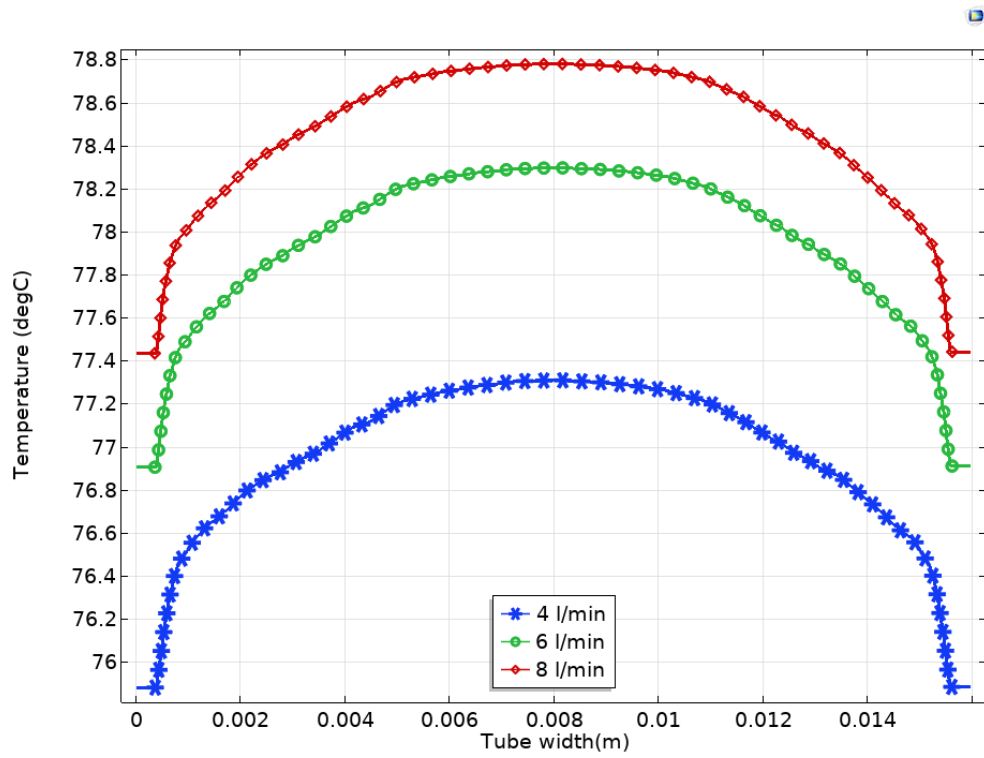


Figure 5.23 Fluid temperature profile for the tube with the different flow rate

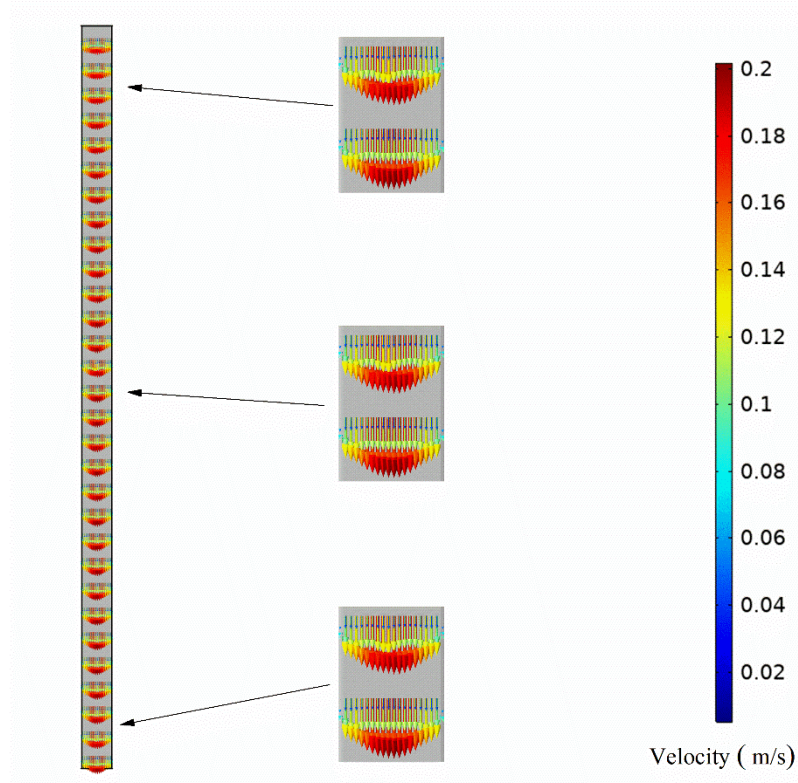


Figure 5.24 Velocity profile as an arrow along the tube

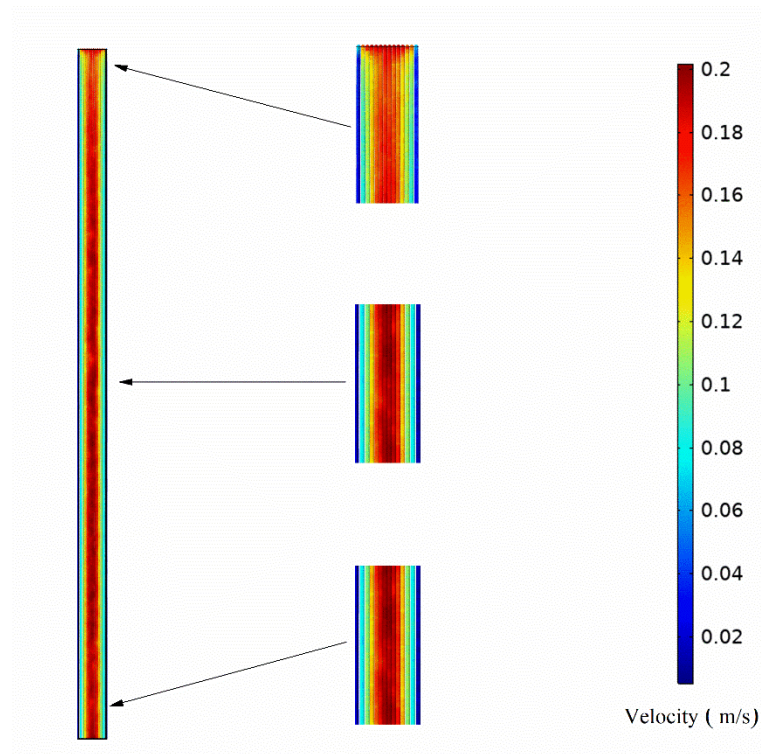


Figure 5.25 Streamline of the fluid along the tube

Table 5.2 Table for summarizing the results of improvement in the Nusselt number at 4 L/min

Temp.	60 ° C			70 ° C			80 ° C		
	0.5%	1%	2%	0.5%	1%	2%	0.5%	1%	2%
Al₂O₃	2.05	12.53	29.08	5.10	13.55	32.75	5.814	21.29	32.84
CuO	8.41	23.75	38.69	8.39	28.81	43.70	16.51	29.66	48.63
MWCNT	16.97	32.13	45.09	18.59	35.67	52.78	25.83	42.37	59.79

5.2 Experimental Result

5.2.1 Verification of The Experimental Setup

Before starting experiments on nanofluids, and for the reliability and accuracy of the measurement by conducting test runs of distilled water in the Automotive radiator, the results obtained experimentally were compared with the experimental correlation below. Figure (5.26) Show the variation of the Nusselt number with the Reynolds number. The test data showed excellent agreement with an equation of Sieder and Tate [95] (Eq 5.1) with a percentage error was 6.7% at Fully developed laminar flow and fluid inlet temperature of 80 ° C.

$$Nu = 1.86 * \left(\frac{Re * Pr}{L/D_h} \right)^{0.3} * \left(\frac{\mu}{\mu_s} \right)^{0.14} \quad (5.1)$$

$$Re * Pr * \frac{D_h}{L} > 10 \quad (5.2)$$

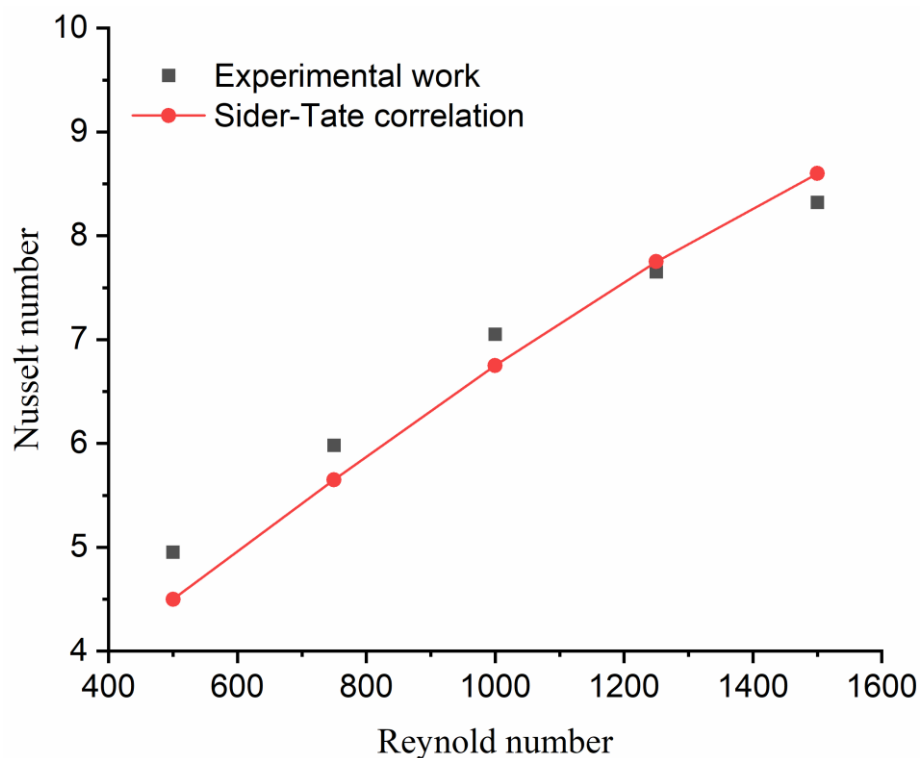


Figure 5.26 Verification of the experimental setup

5.2.2 The Effect of The Nanofluid on The Performance of Regular Size Radiator

The numerical results showed that the higher the inlet temperature of nanofluid, the higher the system's thermal performance. Thus, the current study was carried out at an inlet temperature of 80 °C. At the same time, the highest thermal performance of the nanofluid was at the highest volume concentration of 2%. However, the experiments were carried out at lower concentrations to overcome the issues in the experimental study in terms of the accumulation of nanoparticles in the tubes, as well as the economic cost coming from the price of nanoparticles and preparation of the nanofluid.

Experiments were conducted with Al₂O₃, CuO, MWCNT nanofluids at different flow rates (4, 6, and 8) L/min and volume concentration (0.5%, 1%) with a constant fluid inlet temperature of 80 °C. The Nusselt number, heat transfer rate, and the outlet temperature variation with a fluid flow rate of the aluminium oxide Al₂O₃ nanofluid shown in Figures (5.27, 5.28, 5.29) respectively was at volume concentrations 0.5, 1% and compared to the distilled water as the base fluid. The maximum achieved enhancement of the Nusselt number was 21 %, the heat transfer rate 10 % and decreased outlet temperatures by 1.3 % at a concentration of 1%, and the flow rate of 4 L/min. This increase is due to the thermal properties of the nanoparticles, which in turn led to an increase in the system thermal performance. The Nusselt number increases with an increase in the fluid flow rate as the fluid velocity inside the tube increases, thus improving heat transfer from the fluid to the wall and then the outside environment [78]. Many researchers [22], [96] suggested that the physical explanation for enhancing heat transfer and the thermal performance of the system using nanofluids is affected by many factors, including the high thermal

conductivity of the nanofluid compared to the base fluid, as well as, Brownian motion, chaotic movement of nanoparticles inside the liquid [97], the collision of nanoparticles with the wall of the tube can reduce the boundary layer. Other factors such as fluid temperature, density, viscosity, flow rate, and suspension performance of nanoparticles can also play an important role in thermal performance [79].

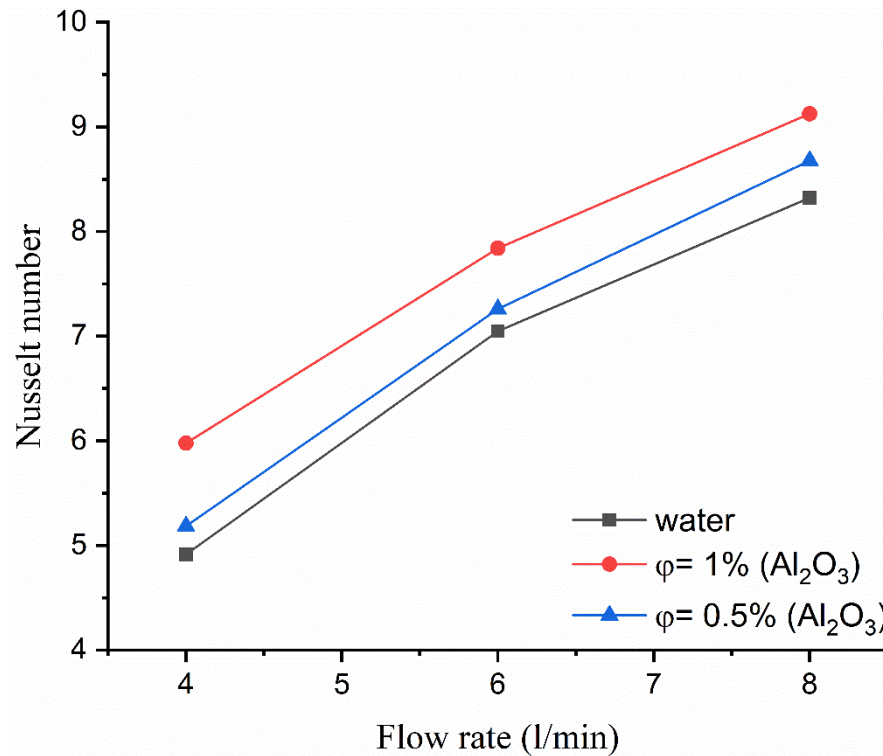


Figure 5.27 Variation of the Nusselt number of Al_2O_3 nanofluid at 80 °C

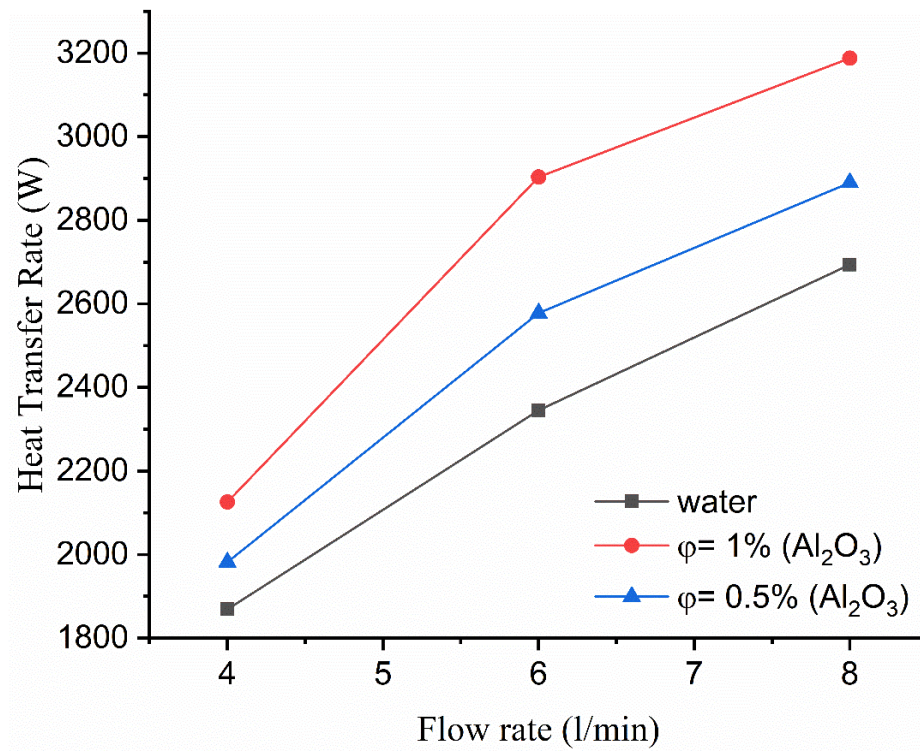


Figure 5.28 Variation of the heat transfer rate of Al₂O₃ nanofluid at 80 °C

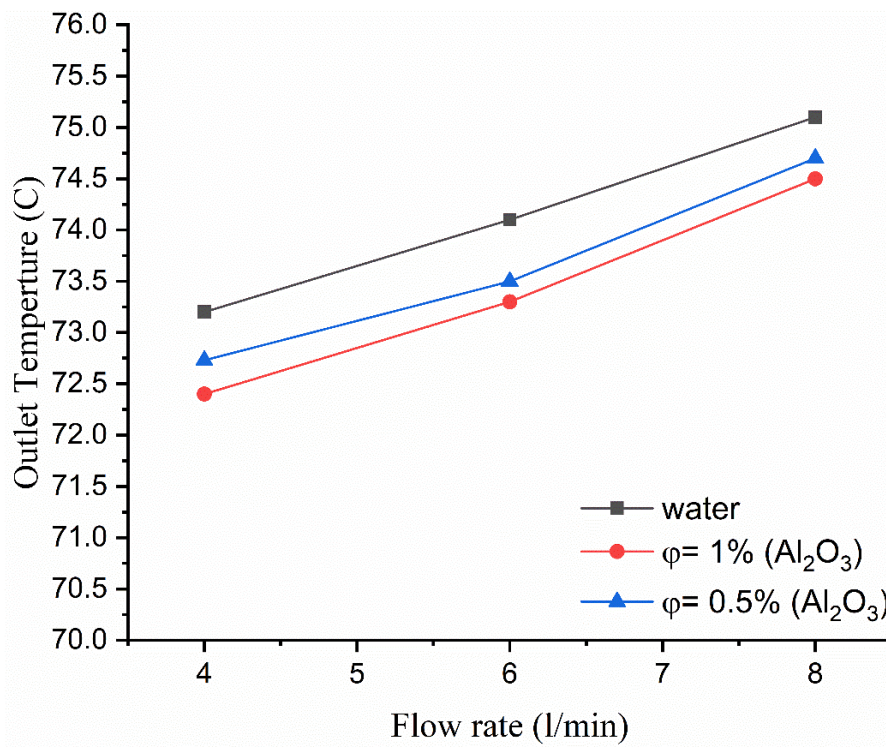


Figure 5.29 Variation of the outlet temperature of Al₂O₃ nanofluid at 80 °C

The nanofluid results of copper oxide CuO, Nusselt number and heat transfer rate, and the outlet temperature variation with a fluid flow rate are shown in Figures (5.30, 5.31, 5.32), respectively. The experiments were at volume concentrations of 0.5, 1% and flow rates 4,6 and 8 L/min with inlet temperature 80 °C. The maximum enhancement of the Nusselt number was 26.6% and the heat transfer rate 24.3% and decreased outlet temperatures by 2.4 % compared to distilled water as the base fluid. This improvement was due to the change in the thermal properties of the nanofluids, where copper oxide has a high thermal conductivity coefficient compared to distilled water as a base fluid. In addition, the thermal performance increases with increasing the volume concentration of nanoparticles in the base fluid, which improves the nanofluid's thermal properties. The heat transfer rate is increased by using CuO nanofluid because it contains a specific heat less than the specific heat of the base fluid, as it acquires heat more slowly than the base fluid. So, the heat transfer rate increases with the increase in the flow rate because it is directly proportional to the mass flow of the fluid and temperature difference.

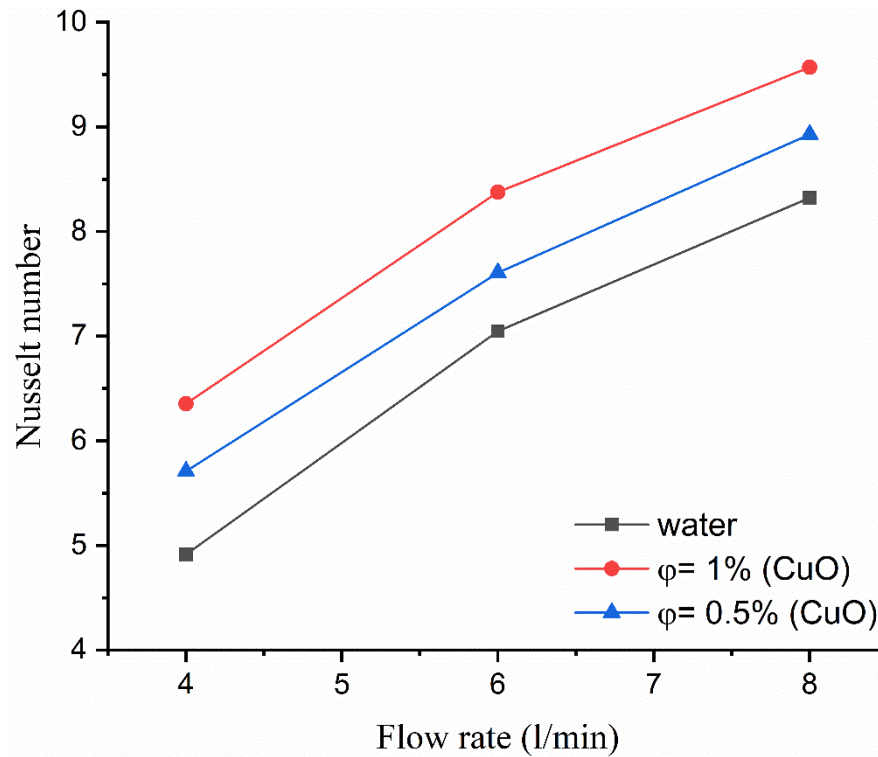


Figure 5.30 Variation of the Nusselt number of CuO nanofluid at 80 °C

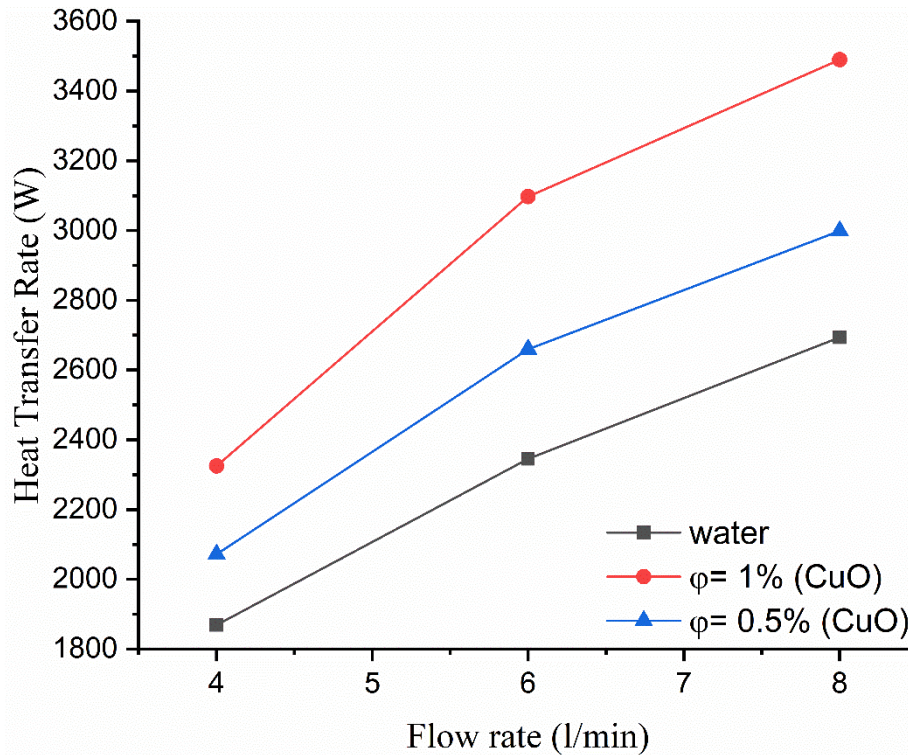


Figure 5.31 Variation of the heat transfer rate of CuO nanofluid at 80 °C

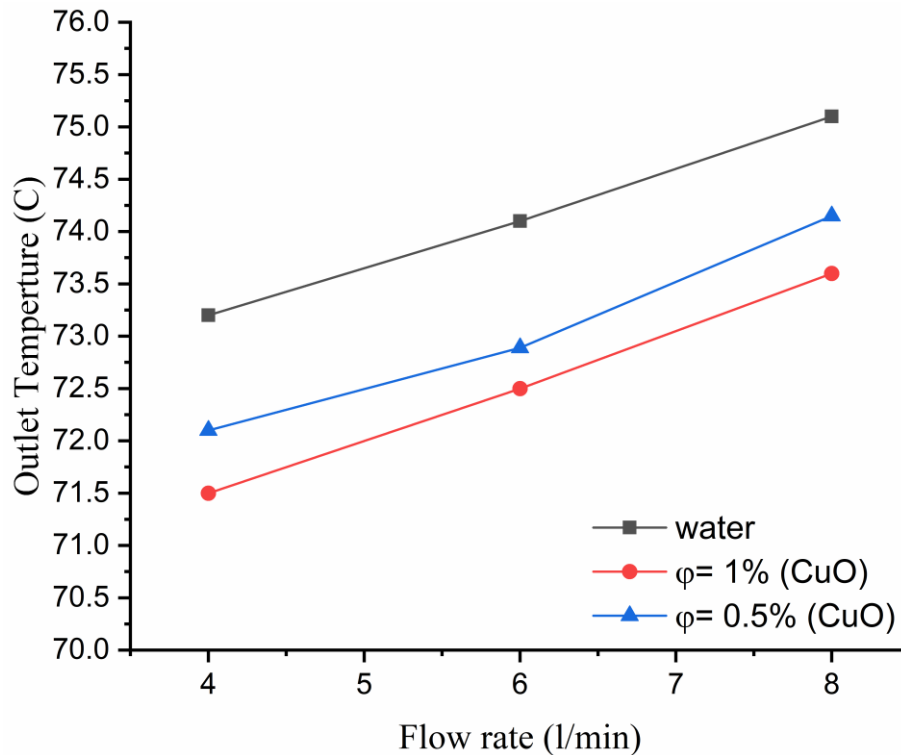


Figure 5.32 Variation of the outlet temperature of CuO nanofluid at 80 °C

The results of multi-walled carbon nanotubes MWCNT nanofluid, including the Nusselt number, heat transfer rate, and outlet temperature variation with a fluid flow rate, are shown in Figures (5.33, 5.34, 5.35). The experiments were at volume concentrations of 0.5, 1% and flow rates 4, 6, and 8 L/min with an inlet temperature of 80 °C. The maximum enhancement of the Nusselt number was 42 % and the heat transfer rate 32.7 %, and decreased outlet temperatures by 3.4 % compared to distilled water as the base fluid. The thermal performance of the nanofluid is increased by increasing the flow rates and the volume concentration of nanoparticles, which leads to enhancing the thermal properties of the nanofluid compared to distilled water as a base fluid. The highest thermal performance enhancement was obtained by using MWCNT nanofluid due to the high thermal conductivity of the fluid; at the same time, it contains the lowest specific heat compared to other

nanofluids, thus losing the heat it acquires more slowly than the rest of the fluids. That led to a decrease in outlet temperatures by 3.3% compared to distilled water.

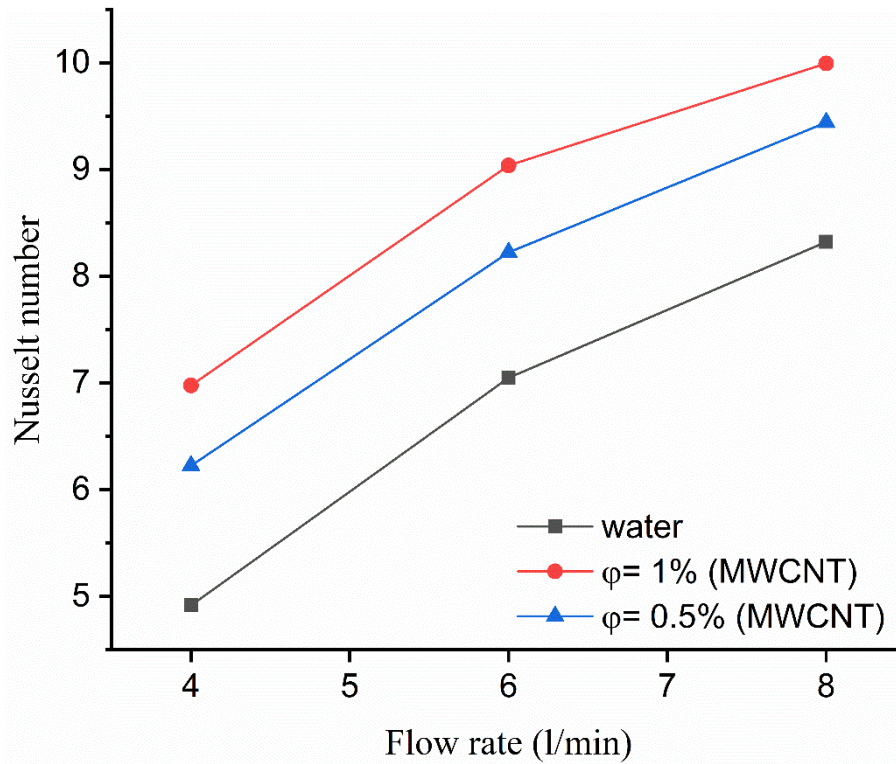


Figure 5.33 Variation of the Nusselt number of MWCNT nanofluid at 80 °C

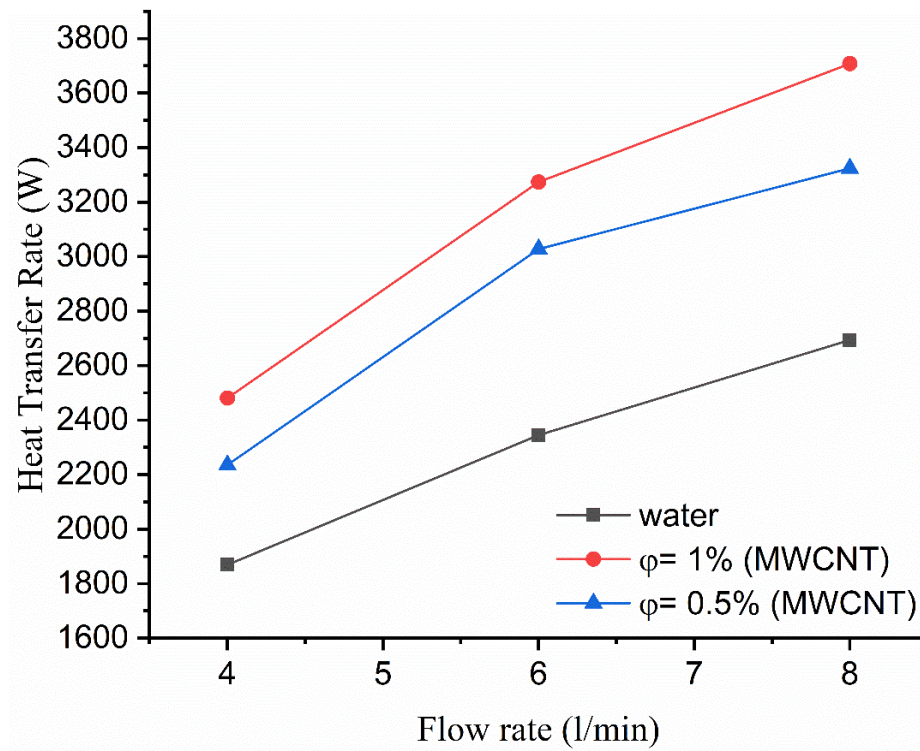


Figure 5.34 Variation of the heat transfer rate of MWCNT nanofluid at 80 °C

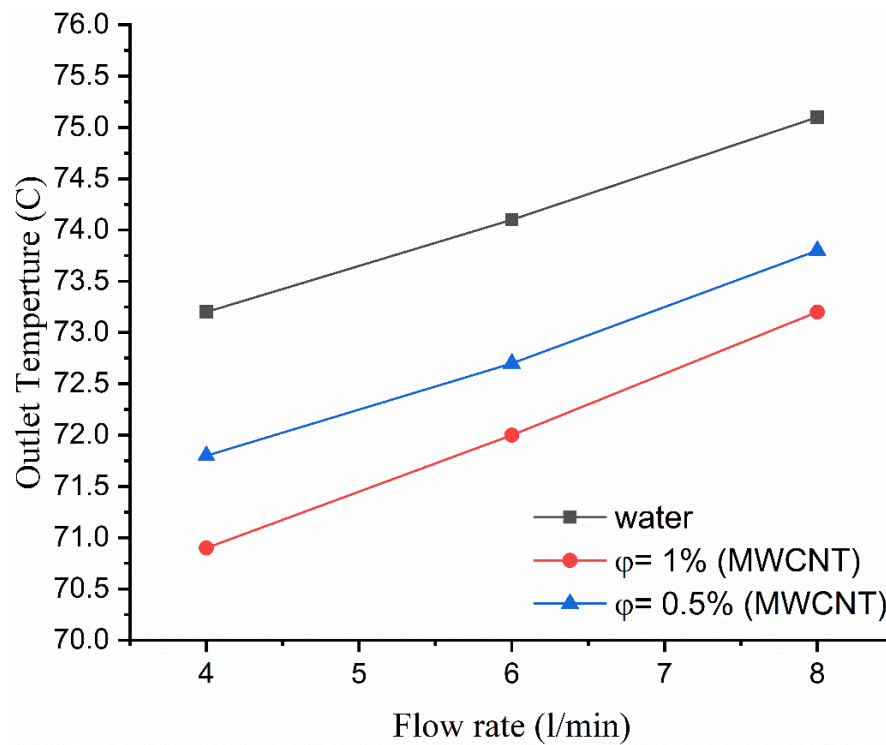


Figure 5.35 Variation of the outlet temperature of MWCNT nanofluid at 80 °C

Figures (5.36, 5.37, 5.38) compared the thermal performance in terms of the Nusselt number, heat transfer rate and the outlet temperature variation with fluid flow rate of the system using the three different nanofluids (Al_2O_3 , CuO, MWCNT) at volume concentrations (0.5%, 1%) and flow rates of (4, 6, and 8) L/min and an inlet temperature of 80 °C using the regular size automotive radiator. The most effective thermal performance was found when using the MWCNT nanofluid at 42% and 32.7% regarding the Nusselt number and the heat transfer rate, respectively, at a volume concentration of 1% and a flow rate of 4 L/min. This is because it has distinctive thermal properties such as a very high thermal conductivity compared to the other nanoparticles up to 3000 W/m. K. The nanofluid enhances the heat transfer in the radiators. Thus, it can reduce the radiator's volume, which reduces fuel consumption due to reducing the cooling system's weight and more spacious area for the engine[24]. The concentration of nanoparticles results in an increase in effective thermal conductivity. Besides, the enhancement of heat transfer is related to the collision between the nanoparticles and the automotive radiator tube wall. This leads to an increase in Brownian motion and the rate of energy exchange of the nanoparticles. The particle migration increases with the increase in the nanoparticle concentration, which leads to an increase in heat transfer.

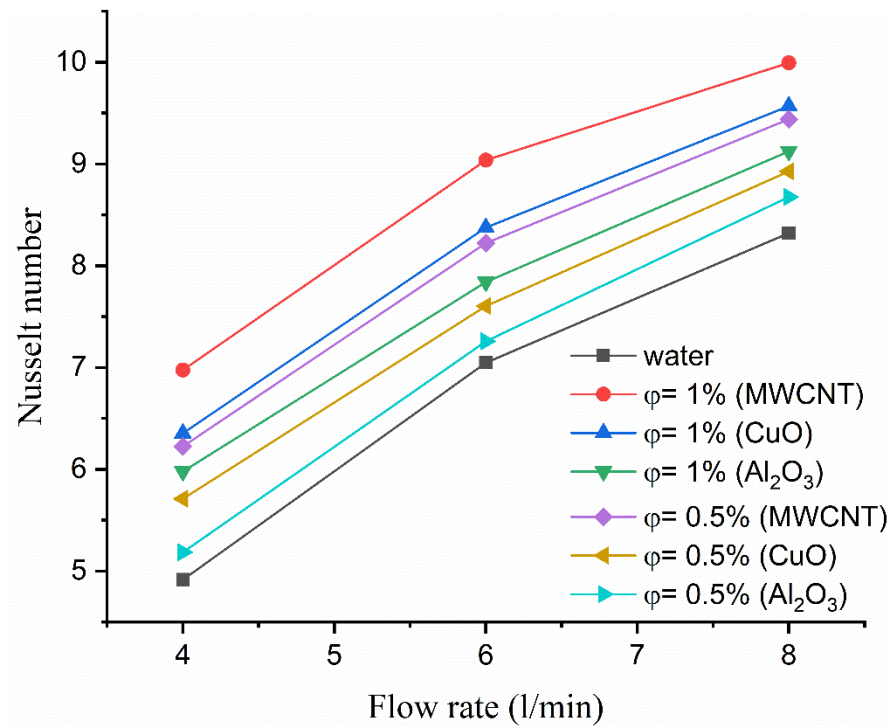


Figure 5.36 Variation of the Nusselt number of Al₂O₃, CuO, and MWCNT nanofluid at 80 °C

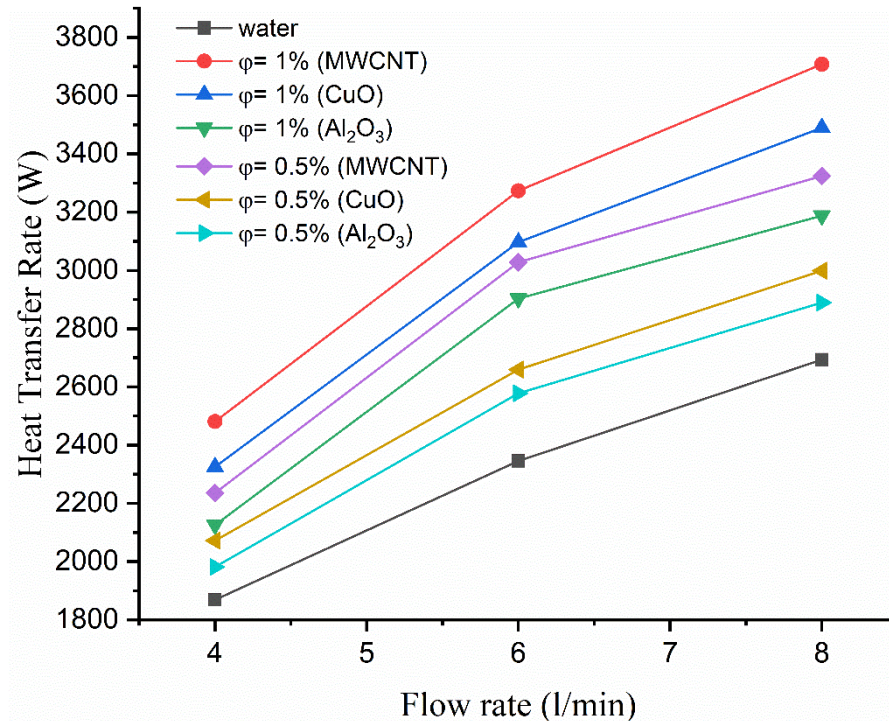


Figure 5.37 Variation of the heat transfer rate of Al₂O₃, CuO, and MWCNT nanofluid at 80 °C

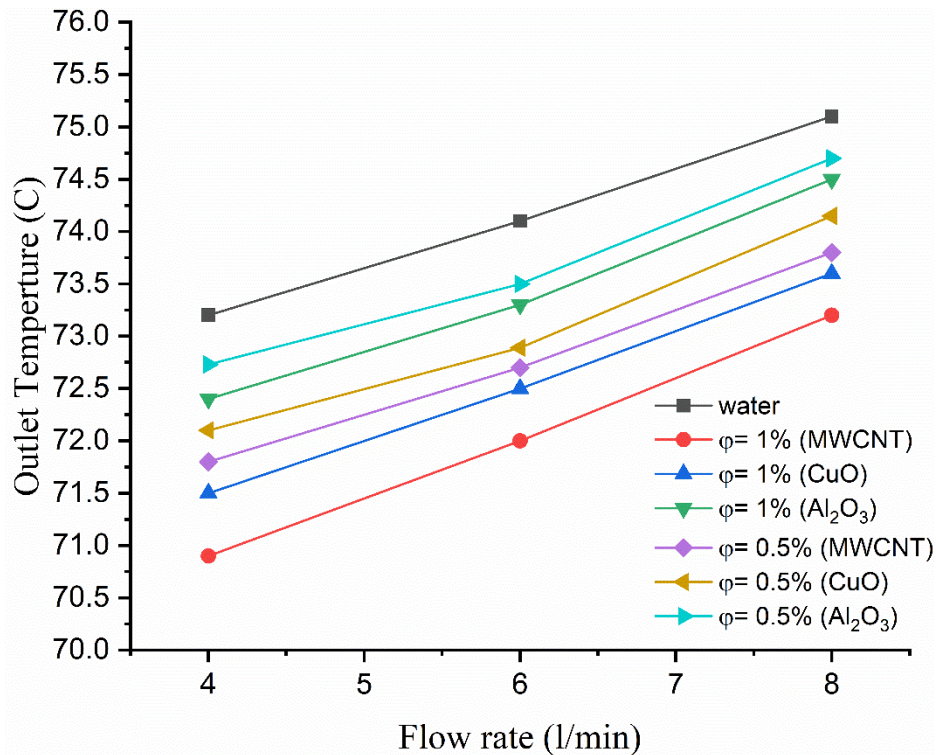


Figure 5.38 Variation of the outlet temperature of Al₂O₃, CuO, and MWCNT nanofluid at 80 °C

5.2.3 Effect The Nanofluid Performance on Smaller Size Radiator With MWCNT

The previous results on the regular size radiator showed that the best thermal enhancement was found when using MWCNT nanofluid compared to other nanofluids. Accordingly, the same nanofluid was used on an automotive radiator, 35% smaller than the regular size, in order to show the effect of thermal performance and to compare this effect of nanofluid, at the same working conditions, with the distilled water in regular size radiator.

The nanofluid results of Nusselt number, heat transfer rate and the outlet temperature are shown in Figures (5.39, 5.40, 5.41) using MWCNT nanofluid. The experiments were at volume concentrations of 0.5, 1, 1.25%. The enhancement of Nusselt number was 20%, 31.7%, and 57.1%, at volume concentrations of respectively. The heat transfer

rate was 19.8%, 29% and 40.7%, at concentrations of (0.5, 1, 1.25 %) respectively. In contrast, the decrease in the outlet temperature, compared with distilled water as the base fluid in small size radiator was (1.5, 2.1, 3.89 %) at concentrations of (0.5, 1, 1.25 %) respectively compared with distilled water in a smaller radiator. The maximum thermal performance was 10.8% for the Nusselt number, 9.7% for heat transfer rate at 1.25% volume concentration of MWCNT nanofluid used in the small size radiator compared to the distilled water regular size radiator. Additionally, the concentration of nanoparticles plays an important role in heat transfer efficiency. It can be shown that whenever the concentration becomes greater, the heat transfer coefficient becomes larger. This leads to the fact that it is possible to reduce the volume of the car radiator to a certain percentage when adding nanoparticles to the base fluid, taking into account the sedimentation and agglomeration of the particles, for example, they can be disposed of by adding surfactants such as gum Arabic.

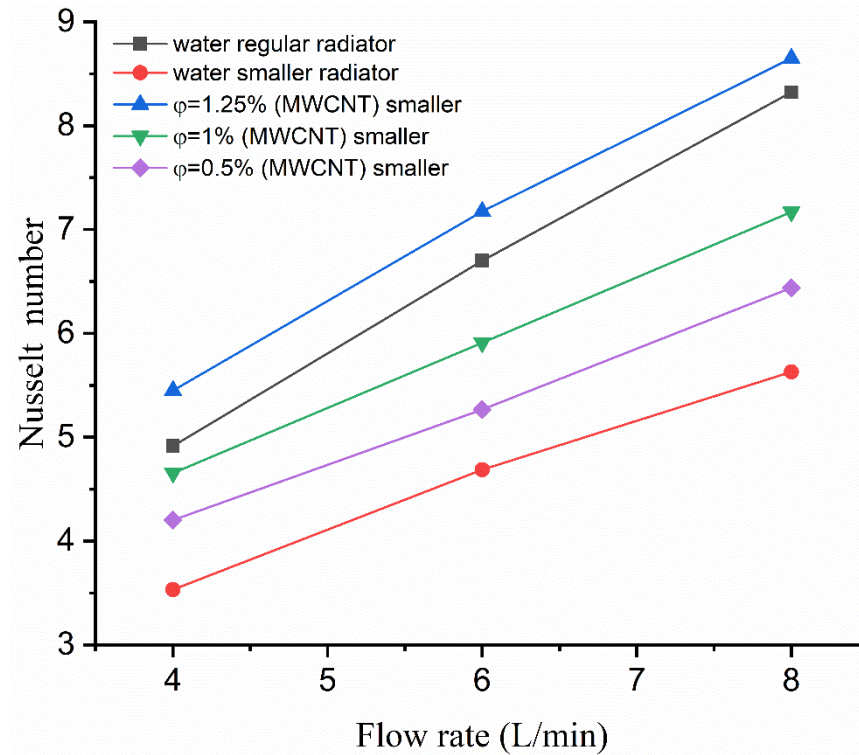


Figure 5.39 Variation of the Nusselt number of MWCNT nanofluid for a small radiator at 80 °C

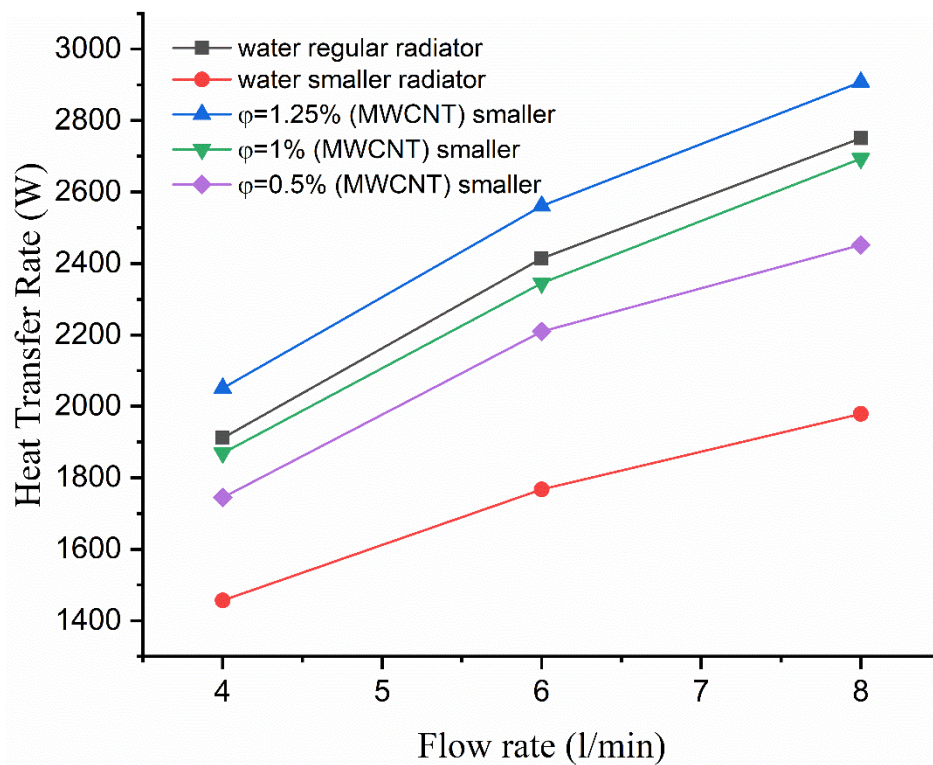


Figure 5.40 Variation of the heat transfer rate of MWCNT nanofluid for a small radiator at 80 °C

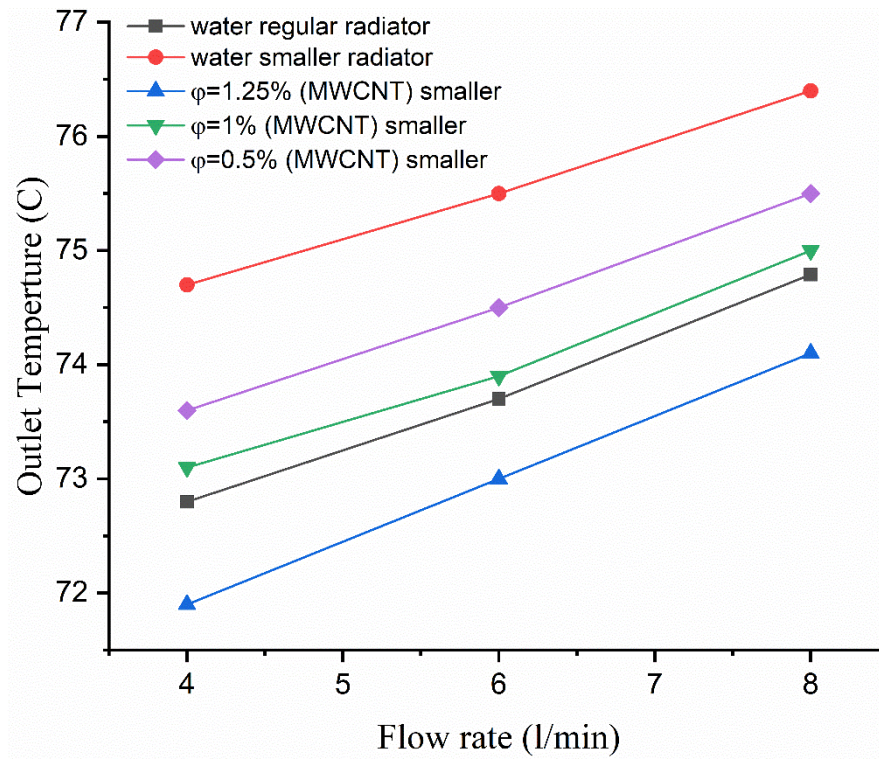


Figure 5.41 Variation of the outlet temperature of MWCNT nanofluid for a small radiator at 80 °C

5.3 Comparing The Numerical Results with The Experimental Results of Nanofluids

The experimental results were compared with the numerical results obtained from the COSOL model of the three nanofluids at a volume concentration of 1% and a temperature of 80°C. The results of the comparison showed convergence of values by not more than 3.5% between the numerical and experimental results. Figure 5.42 shows the values of Nusselt number with the flow rate for comparison between the results.

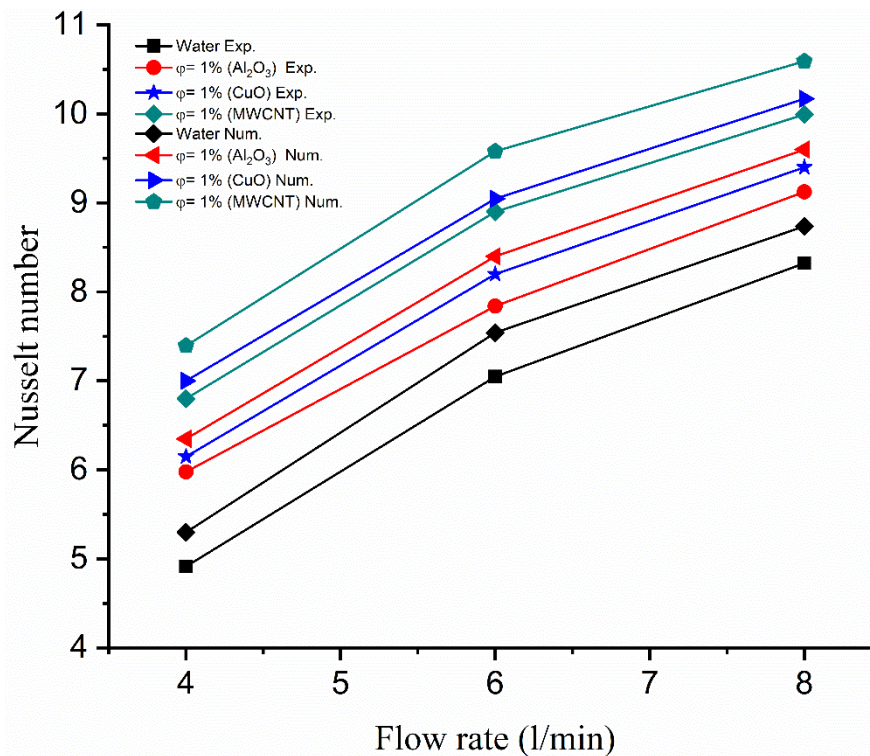


Figure 5.42 Comparison of Numerical Results with The Experimental Results at 1% and a temperature of 80°C

5.4 Economic Analysis Using for Nanofluid in Radiators

Economic analysis is a scientific method of research and giving a logical method of study. It aims to achieve the product's efficiency to satisfy the customer through the best use of materials. The current study was about the use of nanofluids in automobile radiators. The results were studied and analyzed on the thermal performance in heat transfer and heat dissipation using three nanofluids aluminum oxide Al_2O_3 , copper oxide CuO , multi-walled carbon nanotubes MWCNT, with different volume concentrations (0.5%, 1%, 2 %) and different temperatures (60, 70, 80) °C as well as different flow rates (4, 6, 8) L/min, where their results were compared with distilled water as the base fluid. The best fluid used is MWCNT nanofluid, which achieved the highest thermal performance compared with other nanofluids because of the high thermal properties of this fluid, as well as with distilled water. At the same time, this nanofluid was used in an automotive radiator that was 35% smaller than the regular radiator. The results found that using MWCNT nanofluid in small radiator is better than using distilled water in the regular radiator at the same operating conditions, such as ambient temperature, flow rate, and inlet fluid temperature. The costs of each of the small and the regular size of radiator were calculated, the costs of purchasing the three nanoparticles and surfactants, the costs of preparing the nanofluid that includes the ultrasound device, and calculating the duration of the nanofluid remaining stable without sedimentation for the longest possible period inside the radiator. Table (5.2, 5.3) shows the costs of using nanofluids in this study. Thus, it was possible to reduce the volume of the radiator and thus reduce the cost of purchasing the radiator and reduce the amount of fluid inside the radiator. In addition, providing additional space under the hood. A recent Massachusetts Institute of

Technology study estimates that vehicle weight that for every 100-kg reduction, the combined city/highway fuel consumption could decrease by about 0.4 L/100 km for car [98].

Table 5.2 Cost of radiators and nanofluid

	Regular radiator	Smaller radiator
Radiator's weight	2.275 kg	1.575 kg
Volume of radiator	0.0358 m ³	0.0135 m ³
Fluid capacity	1.2 liter	0.75 liter
Radiator price	37.5 \$	17 \$
Cost of the nanofluid	5\$	3.2 \$
fuel Cost for 200,000 km	16.64 \$	10.4 \$
Comparison	More weight, more cost for automotive radiator and Nanofluid more space under the hood	Less weight, lower price for automotive radiator and nanofluid than the regular size. less space under the hood

Table 5.3 Cost of nanoparticles

Nanoparticles	Volume Concentration	Wight of Particles	Price by Gram	Total Price
MWCNT	0.5 %	1.08 g	10.3 \$	11.12 \$
	1 %	2.16 g		22.2 \$
	1.25 %	2.7 g		27.8 \$
CuO	0.5 %	8.23 g	8.6 \$	70.7 \$
	1 %	16.46 g		141.5 \$
Al ₂ O ₃	0.5 %	0.98 g	5.5 \$	5.39 \$
	1 %	2 g		11 \$

CHAPTER SIX

CONCLUSIONS AND RECOMMENDATIONS

CHAPTER SIX

CONCLUSIONS AND RECOMMENDATIONS

6.1 Conclusions

In this study. The effect of nanofluids (Al_2O_3 , CuO and MWCNT) on convective heat transfer by laminar flow in automotive radiators has been numerically and experimentally investigated. The numerical results were validated by comparing with experimental and numerical results of previous researchers, comparing the results of the present study with the results of previous researchers, the comparison with the experimental research was an error rate of 6.2%, and with the numerical analysis, the error rate was 7.2%. These results are good agreement for comparison and verifying the validity of the experimental results by comparing the results with correlations and changing Reynolds number from 250 to 1750 (4-8) L/min was an error rate of 6.7%.

1. The heat transfer of the three nanofluids was studied numerically at volume concentrations 0.5, 1, 2 % and inlet temperature 60,70,80 °C, and flow rate (4,6,8) L//min. The results showed the maximum enhancement of the Nusselt number by 25.8%, 42.3% and 59.7 % at a volume concentration of 0.5%, 1 % and 2%, respectively, when using MWCNT nanofluid with a flow rate of 4 L/min compared with distilled water as a base fluid.
2. Experimental results were carried out on two automotive radiators of different sizes. The small size was 35% smaller than the regular size, using the three nanofluids, with a volume concentration of 0.5, 1%, inlet temperature at 80 °C and a 4, 6, and 8 L/min flow

rate. The experimental results showed that the maximum enhancement of the Nusselt number was 42 % when using MWCNT nanofluid with a volume concentration of 1% and a flow rate of 4 L/min compared with distilled water a regular size radiator.

3. Experimental results on a smaller automotive radiator with MWCNT nanofluid at volume concentration (0.5, 1, 1.25%) and 80 °C. The maximum enhancement of the Nusselt number was 10.8 % and heat transfer rate was 9.7 % at volume concentration 1.25 % of the experiment for the smaller size radiator compared to the with the distilled water of the regular size radiator.
4. The numerical and experimental results showed that the best nanofluid is MWCNT at a flow rate of 4 L/min compared with the results of other nanofluids (aluminium oxide Al₂O₃, copper oxide CuO).
5. It is possible to reduce the volume of the car radiator by 35% when using MWCNT nanofluid with a volume concentration of 1.25%. Thus, providing additional space under the hood, saving the amount of fluid inside the tubes of the radiator.
6. The economic analysis was conducted on the radiators in automotive, where it was found that it was possible to reduce the size of the radiator when using the MWCNT nanofluid, as well as an economy in the price of the radiator, with a difference of \$ 20 for the smaller radiator, as well as the cost of the cooling fluid by 1.8% compared to the regular size radiator.

6.2 Recommendations

Based on the previous conclusions, we suggest the following recommendations.

- 1- Experimental study of the thermal properties of nanofluids and observing the change in the properties by increasing the temperature at different volume concentrations.
- 2- Experimental study of the effect of nanofluids on pressure drop and friction factor at laminar and turbulent flow.
- 3- Study of the thermal performance of hybrid nanofluids in heat exchangers.

References

- [1] C. Rica, “Kyoto Protocol to the United Nations Framework Convention on Climate Change,” *Int. Law Doc.*, no. December 1997, pp. 491–508, 2018, doi: 10.1017/9781316577226.067.
- [2] I. K. Yoo, K. Simpson, M. Bell, and S. Majkowski, “An engine coolant temperature model and application for cooling system diagnosis,” *SAE Tech. Pap.*, no. 724, 2000, doi: 10.4271/2000-01-0939.
- [3] J. Sarkar, P. Ghosh, and A. Adil, “A review on hybrid nanofluids: Recent research, development and applications,” *Renew. Sustain. Energy Rev.*, vol. 43, pp. 164–177, 2015, doi: 10.1016/j.rser.2014.11.023.
- [4] N. A. C. Sidik, M. N. A. W. M. Yazid, and R. Mamat, “A review on the application of nanofluids in vehicle engine cooling system,” *Int. Commun. Heat Mass Transf.*, vol. 68, pp. 85–90, 2015, doi: 10.1016/j.icheatmasstransfer.2015.08.017.
- [5] M. Holik, M. Živić, Z. Virag, and A. Barac, “Optimization of an organic Rankine cycle constrained by the application of compact heat exchangers,” *Energy Convers. Manag.*, vol. 188, pp. 333–345, 2019, doi: 10.1016/j.enconman.2019.03.039.
- [6] M. Bayareh, A. H. Pordanjani, A. A. Nadooshan, and K. S. Dehkordi, “Numerical study of the effects of stator boundary conditions and blade geometry on the efficiency of a scraped surface heat exchanger,” *Appl. Therm. Eng.*, vol. 113, pp. 1426–1436, 2017, doi: 10.1016/j.applthermaleng.2016.11.166.
- [7] S. Javed, H. M. Ali, H. Babar, M. S. Khan, M. M. Janjua, and M. A. Bashir, “Internal convective heat transfer of nanofluids in different flow regimes: A comprehensive review,” *Phys. A Stat. Mech. its Appl.*, vol. 538, no. October, p. 122783, 2020, doi: 10.1016/j.physa.2019.122783.
- [8] M. A. Al-Nimr and A. A. Alajlouni, “Internal combustion engine waste heat recovery by a thermoelectric generator inserted at combustion chamber walls,” *Int. J. Energy Res.*, vol. 42, no. 15, pp. 4853–4865, 2018, doi: 10.1002/er.4241.
- [9] J. P. Yadav and B. R. Singh, “Study on Performance Evaluation of Automotive Radiator,” *SAMRIDDHI A J. Phys. Sci. Eng. Technol.*, vol. 2, no. 2, pp. 47–56, 2015, doi:

10.18090/samriddhi.v2i2.1604.

- [10] S. U. S. Choi, "Enhancing thermal conductivity of fluids with nanoparticles," *Am. Soc. Mech. Eng. Fluids Eng. Div. FED*, vol. 231, no. March, pp. 99–105, 1995.
- [11] J. Sarkar, "A critical review on convective heat transfer correlations of nanofluids," *Renew. Sustain. Energy Rev.*, vol. 15, no. 6, pp. 3271–3277, 2011, doi: 10.1016/j.rser.2011.04.025.
- [12] M. B. Bigdeli, M. Fasano, A. Cardellini, E. Chiavazzo, and P. Asinari, "A review on the heat and mass transfer phenomena in nanofluid coolants with special focus on automotive applications," *Renew. Sustain. Energy Rev.*, vol. 60, pp. 1615–1633, 2016, doi: 10.1016/j.rser.2016.03.027.
- [13] K. Goudarzi and H. Jamali, "Heat transfer enhancement of Al₂O₃-EG nanofluid in a car radiator with wire coil inserts," *Appl. Therm. Eng.*, vol. 118, pp. 510–517, 2017, doi: 10.1016/j.applthermaleng.2017.03.016.
- [14] A. M. Azad, "Fabrication of transparent alumina (Al₂O₃) nanofibers by electrospinning," *Mater. Sci. Eng. A*, vol. 435–436, pp. 468–473, 2006, doi: 10.1016/j.msea.2006.07.075.
- [15] V. E. Bondybey and J. H. English, "Structure of CuO₂ and its photochemistry in rare gas matrices," *J. Phys. Chem.*, vol. 88, no. 11, pp. 2247–2250, 1984, doi: 10.1021/j150655a014.
- [16] Brian O'Regan & Michael Grätzel, "Helical microtubules of graphitic carbon," *Nature*, vol. 354, pp. 737–740, 1991.
- [17] S. Das, "A review on Carbon nano-tubes - A new era of nanotechnology," *Int. J. Emerg. Technol. Adv. Eng.*, vol. 3, no. 3, pp. 774–783, 2013,. Available: www.ijetae.com.
- [18] A. O. Borode, N. A. Ahmed, and P. A. Olubambi, "Surfactant-aided dispersion of carbon nanomaterials in aqueous solution," *Phys. Fluids*, vol. 31, no. 7, 2019, doi: 10.1063/1.5105380.
- [19] M. K. and N. M. M. W. Rashmi, A.F. Ismail, I. Sopyan, A.T. Jameel, F. Yusof, "Stability and thermal conductivity enhancement of carbon nanotube nanofluid using gum arabic," *J. Exp. Nanosci.*, vol.6,no.6,pp.567–579,2011,doi: 10.1080/1536383X.2017.1283615.
- [20] J. A. Eastman, S. U. S. Choi, S. Li, W. Yu, and L. J. Thompson, "Anomalously increased effective thermal conductivities of

- ethylene glycol-based nanofluids containing copper nanoparticles,” *Appl. Phys. Lett.*, vol. 78, no. 6, pp. 718–720, 2001, doi: 10.1063/1.1341218.
- [21] C. H. Lo, T. T. Tsung, L. C. Chen, C. H. Su, and H. M. Lin, “Fabrication of copper oxide nanofluid using submerged arc nanoparticle synthesis system (SANSS),” *J. Nanoparticle Res.*, vol. 7, no. 2–3, pp. 313–320, 2005, doi: 10.1007/s11051-004-7770-x.
- [22] M. S. Liu, M. C. C. Lin, I. Te Huang, and C. C. Wang, “Enhancement of thermal conductivity with CuO for nanofluids,” *Chem. Eng. Technol.*, vol. 29, no. 1, pp. 72–77, 2006, doi: 10.1002/ceat.200500184.
- [23] S. Shimpi, S. Temburne, A. S. Tumane, “Review on Enhancement of Radiator Efficiency using Nanotechnology,” *Int. J. Res. Appl. Sci. Eng. Technol.*, vol. 8, no. 5, pp. 1543–1548, 2020, doi: 10.22214/ijraset.2020.5250.
- [24] D. G. Subhedar, B. M. Ramani, and A. Gupta, “Experimental investigation of heat transfer potential of Al₂O₃/Water-Mono Ethylene Glycol nanofluids as a car radiator coolant,” *Case Stud. Therm. Eng.*, vol. 11, pp. 26–34, 2018, doi: 10.1016/j.csite.2017.11.009.
- [25] A. M. Elsaid, “Experimental study on the heat transfer performance and friction factor characteristics of Co₃O₄ and Al₂O₃ based H₂O/(CH₂OH)₂ nanofluids in a vehicle engine radiator,” *Int. Commun. Heat Mass Transf.*, vol. 108, p. 104263, 2019, doi: 10.1016/j.icheatmasstransfer.2019.05.009.
- [26] Z. Said, Ahmed Amine Hachicha, Duha Zeyad Alazaizeh., “Enhancing the performance of automotive radiators using nanofluids,” *Renew. Sustain. Energy Rev.*, vol. 112, no. m, pp. 183–194, 2019, doi: 10.1016/j.rser.2019.05.052.
- [27] N. M. R. and N. N. M. Gajendiran, E. Saravanakumar, “Research Article Heat transfer enhancement of thermic fluid by using nanofluids in radiator,” vol. 8, no. 3, pp. 686–692, 2016.
- [28] R. Ravisankar, V. S. K. Venkatachalapathy, and N. Alagumurthi, “Application of nanotechnology to improve the performance of tractor radiator using Cu-water nanofluid,” *J. Therm. Eng.*, vol. 4, no. 4, pp. 2188–2200, 2018, doi: 10.18186/journal-of-thermal-engineering.434036.
- [29] M. Naraki, S. M. Peyghambarzadeh, S. H. Hashemabadi, and Y.

- Vermahmoudi, “Parametric study of overall heat transfer coefficient of CuO/water nanofluids in a car radiator,” *Int. J. Therm. Sci.*, vol. 66, pp. 82–90, 2013, doi: 10.1016/j.ijthermalsci.2012.11.013.
- [30] S. Z. Heris, M. Shokrgozar, S. Poorpharhang, M. Shanbedi, and S. H. Noie, “Experimental Study of Heat Transfer of a Car Radiator with CuO/Ethylene Glycol-Water as a Coolant,” *J. Dispers. Sci. Technol.*, vol. 35, no. 5, pp. 677–684, 2014, doi: 10.1080/01932691.2013.805301.
- [31] P. Samira, Z. H. Saeed, S. Motahare, and K. Mostafa, “Pressure drop and thermal performance of CuO/ethylene glycol (60%)-water (40%) nanofluid in car radiator,” *Korean J. Chem. Eng.*, vol. 32, no. 4, pp. 609–616, 2015, doi: 10.1007/s11814-014-0244-7.
- [32] karema assi Hamad, “experimental investigation of heat transfer in automobile radiator by using alternative working fluids and nanoparticles,” vol. 16, pp. 446–462, 2016.
- [33] Y. Vermahmoudi, S. M. Peyghambarzadeh, S. H. Hashemabadi, and M. Naraki, “Experimental investigation on heat transfer performance of Fe₂O₃/water nanofluid in an air-finned heat exchanger,” *Eur. J. Mech. B/Fluids*, vol. 44, pp. 32–41, 2014, doi: 10.1016/j.euromechflu.2013.10.002.
- [34] M. Tafakhori, D. Kalantari, P. Biparva, and S. M. Peyghambarzadeh, “Assessment of Fe₃O₄-water nanofluid for enhancing laminar convective heat transfer in a car radiator,” *J. Therm. Anal. Calorim.*, 2020, doi: 10.1007/s10973-020-10034-0.
- [35] H. K. Hamzah and Q. R. Al-amir, “Experimental Investigation to Heat Transfer Augmentation in A Car Radiator Worked with (Water - Magnesium Oxide) Nanofluid .,” no. 4, pp. 1179–1193, 2017.
- [36] P. Kumar Rai, A. Kumar, and A. Yadav, “Experimental Investigation of Heat Transfer Augmentation in Automobile Radiators using Magnesium Oxide/Distilled Water-Ethylene Glycol based Nanofluid,” *Mater. Today Proc.*, vol. 24, pp. 1525–1532, 2018, doi: 10.1016/j.matpr.2020.04.472.
- [37] S. S. Chougule, S. K. Sahu “experimental investigation of heat transfer augmentation in automobile radiator with cnt/water nanofluid,” pp. 1–7, 2013.
- [38] R. V. Ramaraju, M. Kota, H. Bin Manap, and V. R. Veeredhi,

- “Enhancement of Heat Transfer Coefficient in an Automobile Radiator Using Multi Walled Carbon Nano Tubes (MWCNTS),” vol. c, pp. 1–9, 2014.
- [39] W. Rashmi, A. F. Ismail, M. Khalid, A. Anuar, and T. Yusaf, “Investigating corrosion effects and heat transfer enhancement in smaller size radiators using CNT-nanofluids,” *J. Mater. Sci.*, vol. 49, no. 13, pp. 4544–4551, 2014, doi: 10.1007/s10853-014-8154-y.
- [40] C. V. K. N. S. N. Moorthy and V. Srinivas, “Corrosion and Heat Transfer Characteristics of Water Dispersed with Carboxylate Additives and Multi Walled Carbon Nano Tubes,” *J. Inst. Eng. Ser. C*, vol. 97, no. 4, pp. 569–577, 2016, doi: 10.1007/s40032-016-0223-3.
- [41] B. M’hamed, N. A. Che Sidik, M. F. A. Akhbar, R. Mamat, and G. Najafi, “Experimental study on thermal performance of MWCNT nanocoolant in Perodua Kelisa 1000cc radiator system,” *Int. Commun. Heat Mass Transf.*, vol. 76, pp. 156–161, 2016, doi: 10.1016/j.icheatmasstransfer.2016.05.024.
- [42] M. Ebrahimi, M. Farhadi, K. Sedighi, and S. Akbarzade, “Experimental investigation of force convection heat transfer in a car radiator filled with SiO₂-water nanofluid,” *Int. J. Eng. Trans. B Appl.*, vol. 27, no. 2, pp. 333–340, 2014, doi: 10.5829/idosi.ije.2014.27.02b.17.
- [43] A. M. Hussein, R. A. Bakar, K. Kadirgama, and K. V. Sharma, “Heat transfer augmentation of a car radiator using nanofluids,” *Heat Mass Transf. und Stoffuebertragung*, vol. 50, no. 11, pp. 1553–1561, 2014, doi: 10.1007/s00231-014-1369-2.
- [44] A. M. Hussein, R. A. Bakar, and K. Kadirgama, “Study of forced convection nanofluid heat transfer in the automotive cooling system,” *Case Stud. Therm. Eng.*, vol. 2, pp. 50–61, 2014, doi: 10.1016/j.csite.2013.12.001.
- [45] H. M. Ali, H. Ali, H. Liaquat, H. T. Bin Maqsood, and M. A. Nadir, “Experimental investigation of convective heat transfer augmentation for car radiator using ZnO-water nanofluids,” *Energy*, vol. 84, pp. 317–324, 2015, doi: 10.1016/j.energy.2015.02.103.
- [46] M. Qasim, M. Sajid Kamran, M. Ammar, M. Ali Jamal, and M. Yasar Javaid, “Heat Transfer Enhancement of an Automobile Engine Radiator using ZnO Water Base Nanofluids,” *J. Therm. Sci.*, vol. 29, no. 4, pp. 1010–1024, 2020, doi: 10.1007/s11630-

020-1263-9.

- [47] E. D. Kurhe, S. S. Kale, A. D. Purane, S. S. Kale, and S. R. Ransing, "Heat Enhancement using TiO_2 -Nano fluid in Automotive Cooling System," vol. 6, no. 6, pp. 51–55, 2016.
- [48] V. Salamon, D. Senthil kumar, and S. Thirumalini, " Experimental Investigation of Heat Transfer Characteristics of Automobile Radiator using TiO_2 -Nanofluid Coolant ," IOP Conf. Ser. Mater. Sci. Eng., vol. 225, p. 012101, 2017, doi: 10.1088/1757-899x/225/1/012101.
- [49] Y. He, Y. Men, Y. Zhao, H. Lu, and Y. Ding, "Numerical investigation into the convective heat transfer of TiO_2 nanofluids flowing through a straight tube under the laminar flow conditions," Appl. Therm. Eng., vol. 29, no. 10, pp. 1965–1972, 2009, doi: 10.1016/j.applthermaleng.2008.09.020.
- [50] P. Gunnasegaran, N. H. Shuaib, M. F. Abdul Jalal, and E. Sandhita, "Numerical Study of Fluid Dynamic and Heat Transfer in a Compact Heat Exchanger Using Nanofluids," ISRN Mech. Eng., vol. 2012, no. April, pp. 1–11, 2012, doi: 10.5402/2012/585496.
- [51] N. Bozorgan, K. Krishnakumar, and N. Bozorgan, "Numerical Study on Application of CuO -Water Nanofluid in Automotive Diesel Engine Radiator," Mod. Mech. Eng., vol. 02, no. 04, pp. 130–136, 2012, doi: 10.4236/mme.2012.24017.
- [52] W. Duangthongsuk and S. Wongwises, "A dispersion model for predicting the heat transfer performance of TiO_2 -water nanofluids under a laminar flow regime," Int. J. Heat Mass Transf., vol. 55, no. 11–12, pp. 3138–3146, 2012, doi: 10.1016/j.ijheatmasstransfer.2012.02.016.
- [53] G. Sheikhzadeh, M.Hajilou, H. Jafarian "Analysis of Thermal Performance of a Car Radiator Employing Nanofluid," Int. J. Mech. Eng. Appl., vol. 2, no. 4, p. 47, 2014, doi: 10.11648/j.ijmea.20140204.11.
- [54] G. Huminic and A. Huminic, "Numerical analysis of laminar flow heat transfer of nanofluids in a flattened tube," Int. Commun. Heat Mass Transf., vol. 44, pp. 52–57, 2013, doi: 10.1016/j.icheatmasstransfer.2013.03.003.
- [55] V. Delavari and S. H. Hashemabadi, "CFD simulation of heat transfer enhancement of Al_2O_3 /water and Al_2O_3 /ethylene glycol

- nanofluids in a car radiator,” *Appl. Therm. Eng.*, vol. 73, no. 1, pp. 380–390, 2014, doi: 10.1016/j.applthermaleng.2014.07.061.
- [56] N.A.Che Sidik, N.G.Yen Cheong, and A. Fazeli, “Computational Analysis of Nanofluids in Vehicle Radiator,” *Appl. Mech. Mater.*, vol. 695, pp. 539–543, 2014, doi: 10.4028/www.scientific.net/amm.695.539.
- [57] N. A. Che Sidik, M. N. A. Witri Mohd Yazid, and R. Mamat, “Recent advancement of nanofluids in engine cooling system,” *Renew. Sustain. Energy Rev.*, vol. 75, no. October 2016, pp. 137–144, 2017, doi: 10.1016/j.rser.2016.10.057.
- [58] K. Chidambaram, T. R. Jayasingh, M. Vinoth, and V. Thulasi, “An experimental study on the influence of operating parameters on the heat transfer characteristics of an automotive radiator with nano fluids,” *Int J Recent Trends Mech Eng*, vol. 2, no. May, pp. 7–11, 2014.
- [59] K. G. Sundari, L. G. Asirvatham, T. M. N. Kumar, and N. Ahammed, “Measurement of thermophysical properties of Al_2O_3 /glycerin (G13) nanofluid for automotive radiator cooling applications,” *Res. J. Chem. Environ.*, vol. 21, no. 3, pp. 17–24, 2017.
- [60] A. S. Tijani and A. S. bin Sudirman, “Thermos-physical properties and heat transfer characteristics of water/anti-freezing and Al_2O_3 /CuO based nanofluid as a coolant for car radiator,” *Int. J. Heat Mass Transf.*, vol. 118, pp. 48–57, 2018, doi: 10.1016/j.ijheatmasstransfer.2017.10.083.
- [61] P. Chaurasia, A. Kumar, A. Yadav, P. K. Rai, V. Kumar, and L. Prasad, “Heat transfer augmentation in automobile radiator using Al_2O_3 –water based nanofluid,” *SN Appl. Sci.*, vol. 1, no. 3, 2019, doi: 10.1007/s42452-019-0260-7.
- [62] A. Topuz, T. Engin, B. Erdoğan, S. Mert, and A. Yeter, “Experimental investigation of pressure drop and cooling performance of an automobile radiator using Al_2O_3 -water + ethylene glycol nanofluid,” *Heat Mass Transf. und Stoffuebertragung*, 2020, doi: 10.1007/s00231-020-02916-8.
- [63] F. S. Anuar, “Thermophysical Properties of Copper / Water Nanofluid for Automotive Cooling System – Mathematical Modeling Thermophysical Properties of Copper / Water Nanofluid for Automotive Cooling System – Mathematical Modeling,” no. April, pp. 1–10, 2016, doi: 10.13140/RG.2.1.5069.6083.

- [64] S. M. Peyghambarzadeh, S. H. Hashemabadi, M. Naraki, and Y. Vermahmoudi, "Experimental study of overall heat transfer coefficient in the application of dilute nanofluids in the car radiator," *Appl. Therm. Eng.*, vol. 52, no. 1, pp. 8–16, 2013, doi: 10.1016/j.applthermaleng.2012.11.013.
- [65] S. Senthilraja, K. C. K. Vijayakumar, and R. Gangadevi, "Experimental Investigation of Heat Transfer Performance of Different Nanofluids Using Automobile Radiator," *Appl. Mech. Mater.*, vol. 787, pp. 212–216, 2015, doi: 10.4028/www.scientific.net/amm.787.212.
- [66] R. Ravisankar, V. S. K. Venkatachalapathy, and N. Alagumurthy, "Thermal Performance Improvement of Tractor Radiator Using CuO/Water Nanofluid," *Heat Transf. - Asian Res.*, vol. 46, no. 1, pp. 61–74, 2017, doi: 10.1002/htj.21198.
- [67] R. Pambhar, I. Vasoya, J. Malaviya, and K. Parmar, "Performance Improvement of Automobile Radiator by Use of Nano Fluid," *I. J. R. in Engineering, Science and Management*. no. 11, 2019.
- [68] H. M. Ali, M. D. Azhar, M. Saleem, Q. S. Saeed, and A. Saieed, "Heat transfer enhancement of car radiator using aqua based magnesium oxide nanofluids," *Therm. Sci.*, vol. 19, no. 6, pp. 2039–2048, 2015, doi: 10.2298/TSCI150526130A.
- [69] T. P. Teng and C. C. Yu, "Heat dissipation performance of MWCNTs nano-coolant for vehicle," *Exp. Therm. Fluid Sci.*, vol. 49, pp. 22–30, 2013, doi: 10.1016/j.expthermflusci.2013.03.007.
- [70] S. S. Chougule and S. K. Sahu, "Comparative study of cooling performance of automobile radiator using Al₂O₃-water and carbon nanotube-water nanofluid," *J. Nanotechnol. Eng. Med.*, vol. 5, no. 1, pp. 1–6, 2014, doi: 10.1115/1.4026971.
- [71] R. Jadar, K. S. Shashishekar, and S. R. Manohara, "Performance evaluation of Al-MWCNT based automobile radiator," *Mater. Today Proc.*, vol. 9, pp. 380–388, 2019, doi: 10.1016/j.matpr.2019.02.167.
- [72] M. Muruganandam and P. C. Mukesh Kumar, "Experimental analysis on internal combustion engine using MWCNT/water nanofluid as a coolant," *Mater. Today Proc.*, vol. 21, no. xxxx, pp. 248–252, 2020, doi: 10.1016/j.matpr.2019.05.411.
- [73] F. Kılınç, E. Buyruk, and K. Karabulut, "Experimental investigation of cooling performance with graphene based nano-

fluids in a vehicle radiator,” *Heat Mass Transf. und Stoffuebertragung*, vol. 56, no. 2, pp. 521–530, 2020, doi: 10.1007/s00231-019-02722-x.

- [74] P. Kannan and D. B. Sivakumar, “Experimental Study of Nanofluids in Automobile Radiator,” *J. Chem. Pharm. Sci.*, no. March, pp. 173–176, 2015.
- [75] S. A. Ahmad, M. Abubakar, M. U. Ghani, and M. Abdullah, “Experimental Study of Heat Transfer Enhancement by using ZnO and Al₂O₃ Water Based Nano Fluids in Car Radiator Experimental Study of Heat Transfer Enhancement by using ZnO and Al₂O₃ Water Based Nano Fluids in Car Radiator,” no. November 2017, pp. 2–7, 2019.
- [76] V. L. Bhimani, P. P. Rathod, and A. S. Sorathiya, “Experimental Study of Heat Transfer Enhancement Using Water Based Nanofluids as a New Coolant for Car Radiators,” *Int. J. Emerg. Technol. Adv. Eng.*, vol. 3, no. 6, pp. 295–302, 2013.
- [77] S. A. Ahmed, M. Ozkaymak, A. Sözen, T. Menlik, and A. Fahed, “Improving car radiator performance by using TiO₂-water nanofluid,” *Eng. Sci. Technol. an Int. J.*, vol. 21, no. 5, pp. 996–1005, 2018, doi: 10.1016/j.jestch.2018.07.008.
- [78] S. Devireddy, C. S. R. Mekala, and V. R. Veeredhi, “Improving the cooling performance of automobile radiator with ethylene glycol water based TiO₂ nanofluids,” *Int. Commun. Heat Mass Transf.*, vol. 78, pp. 121–126, 2016, doi: 10.1016/j.icheatmasstransfer.2016.09.002.
- [79] H. M. Nieh, T. P. Teng, and C. C. Yu, “Enhanced heat dissipation of a radiator using oxide nano-coolant,” *Int. J. Therm. Sci.*, vol. 77, pp. 252–261, 2014, doi: 10.1016/j.ijthermalsci.2013.11.008.
- [80] A. I. Ramadhan, W. H. Azmi, and R. Mamat, “Heat transfer characteristics of car radiator using tri-hybrid nanocoolant,” *IOP Conf. Ser. Mater. Sci. Eng.*, vol. 863, no. 1, 2020, doi: 10.1088/1757-899X/863/1/012054.
- [81] R. Prasanna Shankara, N. R. Banapurmath, A. D. Souza, and S. S. Dhaded, “Experimental investigation of enhanced cooling performance with the use of hybrid nanofluid for automotive application,” *IOP Conf. Ser. Mater. Sci. Eng.*, vol. 872, no. 1, pp. 0–14, 2020, doi: 10.1088/1757-899X/872/1/012074.
- [82] Frank P. Incropera, David P. Dewitt, Theodore L. Bergman,

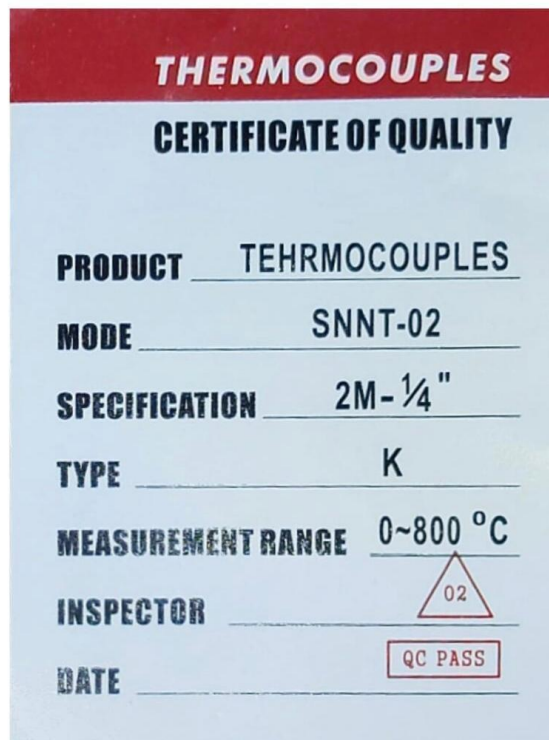
- Adrienne S. Lavine, "Fundamentals of Heat and Mass Transfer", Vol. 112. 2015.
- [83] M. A. R. Sadiq Al-Baghdadi, Z. M. H. Noor, A. Zeiny, A. Burns, and D. Wen, "CFD analysis of a nanofluid-based microchannel heat sink," *Therm. Sci. Eng. Prog.*, vol. 20, no. August, p. 100685, 2020, doi: 10.1016/j.tsep.2020.100685.
- [84] W. H. McAdams and B. Zohuri, "Heat Transmission - Second Edition," Boca Raton, FL. pp. 32742–33487, 1942.
- [85] A. Nahar, M. Hasanuzzaman, and N. A. Rahim, "Numerical and experimental investigation on the performance of a photovoltaic thermal collector with parallel plate flow channel under different operating conditions in Malaysia," *Sol. Energy*, vol. 144, pp. 517–528, 2017, doi: 10.1016/j.solener.2017.01.041.
- [86] M. Çengel, Yunus A. Boles, Michael A. Kanoğlu, *Thermodynamics_ an Engineering Approach*. Ninth Edition. 2019. 2019.
- [87] M. Soltanimehr and M. Afrand, "Thermal conductivity enhancement of COOH-functionalized MWCNTs/ethylene glycol–water nanofluid for application in heating and cooling systems," *Appl. Therm. Eng.*, vol. 105, pp. 716–723, 2016, doi: 10.1016/j.applthermaleng.2016.03.089.
- [88] P. Estellé, S. Halelfadl, and T. Maré, "Thermal conductivity of CNT water based nanofluids: Experimental trends and models overview," *J. Therm. Eng.*, vol. 1, no. 2, pp. 381–390, 2015, doi: 10.18186/jte.92293.
- [89] R. Du, D. Jiang, and Y. Wang, "Numerical investigation of the effect of nanoparticle diameter and sphericity on the thermal performance of geothermal heat exchanger using nanofluid as heat transfer fluid," *Energies*, vol. 13, no. 7, 2020, doi: 10.3390/en13071653.
- [90] A. M. Hussein, R. A. Bakar, K. Kadirgama, and K. V. Sharma, "Heat transfer enhancement using nanofluids in an automotive cooling system," *Int. Commun. Heat Mass Transf.*, vol. 53, pp. 195–202, 2014, doi: 10.1016/j.icheatmasstransfer.2014.01.003.
- [91] M. Elsebay, I. Elbadawy, M. H. Shedid, and M. Fatouh, "Numerical resizing study of Al₂O₃ and CuO nanofluids in the flat tubes of a radiator," *Appl. Math. Model.*, vol. 40, no. 13–14, pp. 6437–6450, 2016, doi: 10.1016/j.apm.2016.01.039.

- [92] M. M. Elias et al., “Experimental investigation on the thermo-physical properties of Al₂O₃ nanoparticles suspended in car radiator coolant,” *Int. Commun. Heat Mass Transf.*, vol. 54, pp. 48–53, 2014, doi: 10.1016/j.icheatmasstransfer.2014.03.005.
- [93] S. Z. Heris, S. H. Noie, E. Talaii, and J. Sargolzaei, “Numerical investigation of al₂o₃/water nanofluid laminar convective heat transfer through triangular ducts,” *Nanoscale Res. Lett.*, vol. 6, no. 1, pp. 1–10, 2011, doi: 10.1186/1556-276X-6-179.
- [94] R. S. Vajjha, D. K. Das, and D. R. Ray, “Development of new correlations for the Nusselt number and the friction factor under turbulent flow of nanofluids in flat tubes,” *Int. J. Heat Mass Transf.*, vol. 80, pp. 353–367, 2015, doi: 10.1016/j.ijheatmasstransfer.2014.09.018.
- [95] E. N. Sieder and G. E. Tate, “Heat Transfer and Pressure Drop of Liquids in Tubes,” *Ind. Eng. Chem.*, vol. 28, no. 12, pp. 1429–1435, 1936, doi: 10.1021/ie50324a027.
- [96] W. Daungthongsuk and S. Wongwises, “A critical review of convective heat transfer of nanofluids,” *Renew. Sustain. Energy Rev.*, vol. 11, no. 5, pp. 797–817, 2007, doi: 10.1016/j.rser.2005.06.005.
- [97] A. F. Chen, Ang Fuk Adzmi, M. Akmal Adam, “Enhancing the performance of automotive radiators using nanofluids,” *Renew. Sustain. Energy Rev.*, vol. 9, no. 2, pp. 183–194, 2019, doi: 10.1016/j.rser.2019.05.052.
- [98] A. E. A. Bandivadekar, Reducing transportation’s petroleum consumption and GHG emissions, no. July. 2008.

APPENDIX - A

THERMOCOUPLE'S CALIBRATION

In this study, eight K-type thermocouples were used to measure the temperature distribution across the flat tube radiator pipe as well as the input and output fluid temperature. The calibration certificate by the manufacturer as shows in Figure A1. For optimum temperature reading, all the thermocouples were calibrated with an alcohol thermometer by using a water bath as shown in Figure A2.



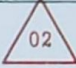
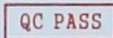
THERMOCOUPLES	
CERTIFICATE OF QUALITY	
PRODUCT	TEHRMOCOUPLES
MODE	SNNT-02
SPECIFICATION	2M- $\frac{1}{4}$ "
TYPE	K
MEASUREMENT RANGE	0~800 °C
INSPECTOR	
DATE	

Figure A1. The calibration certificate by the manufacturer for thermocouples



Figure A2. Thermocouple's calibrations and data logger

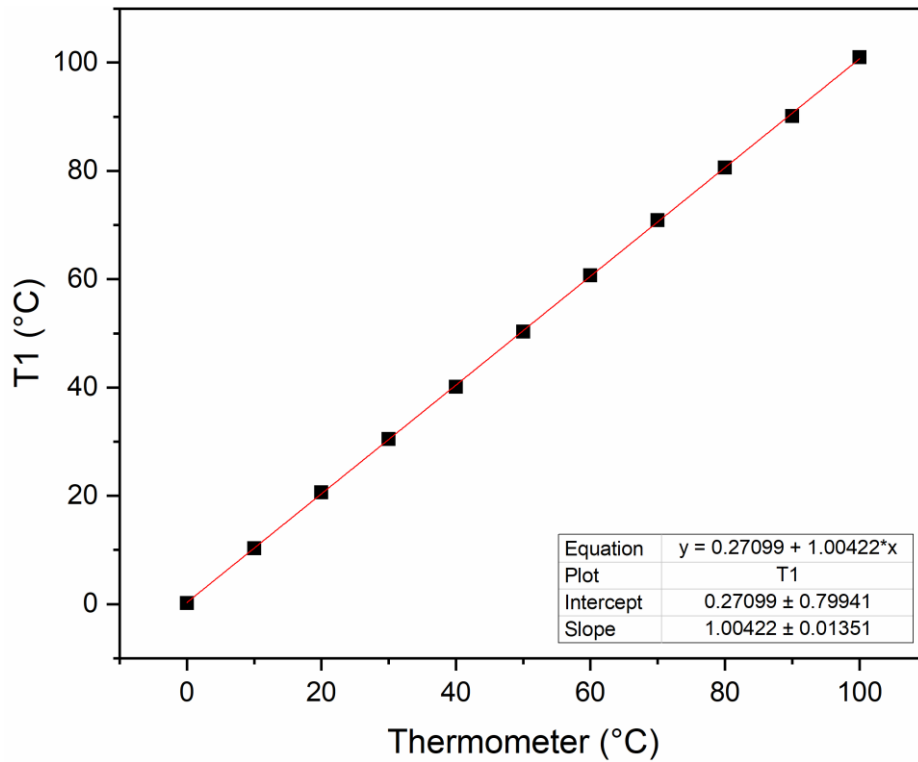


Figure A3. T1 thermocouples calibration

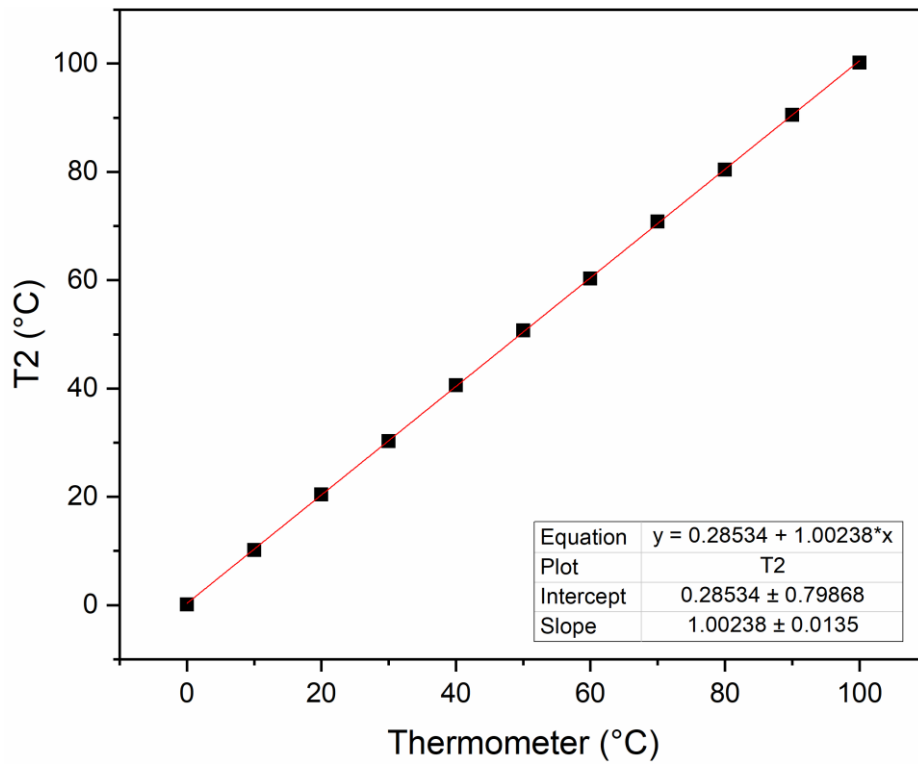


Figure A4. T2 thermocouples calibration

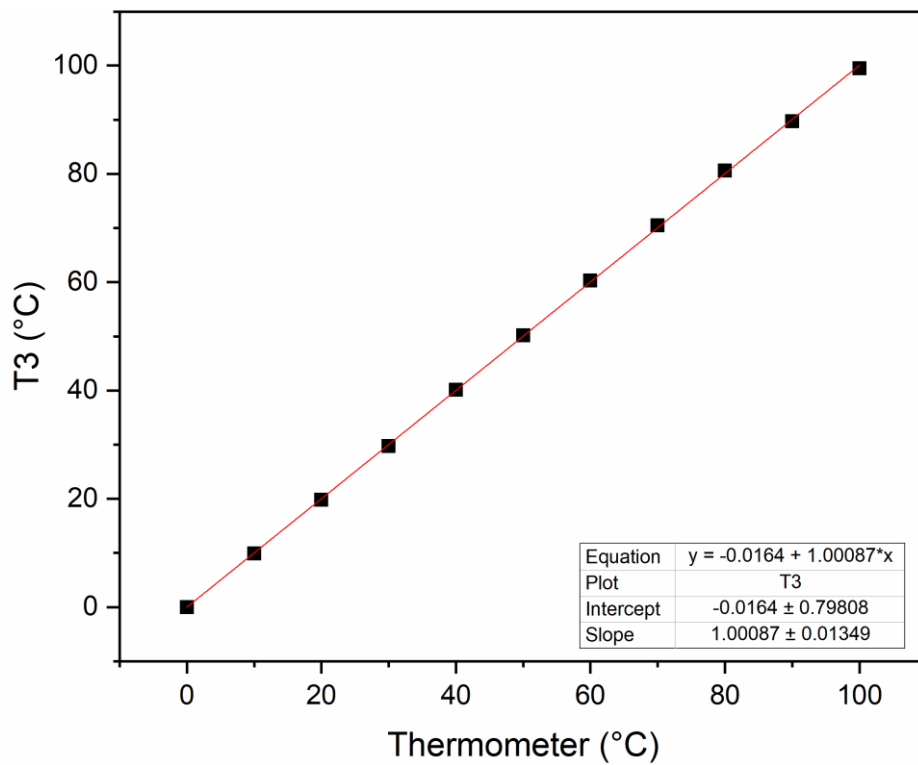


Figure A5. T3 thermocouples calibration

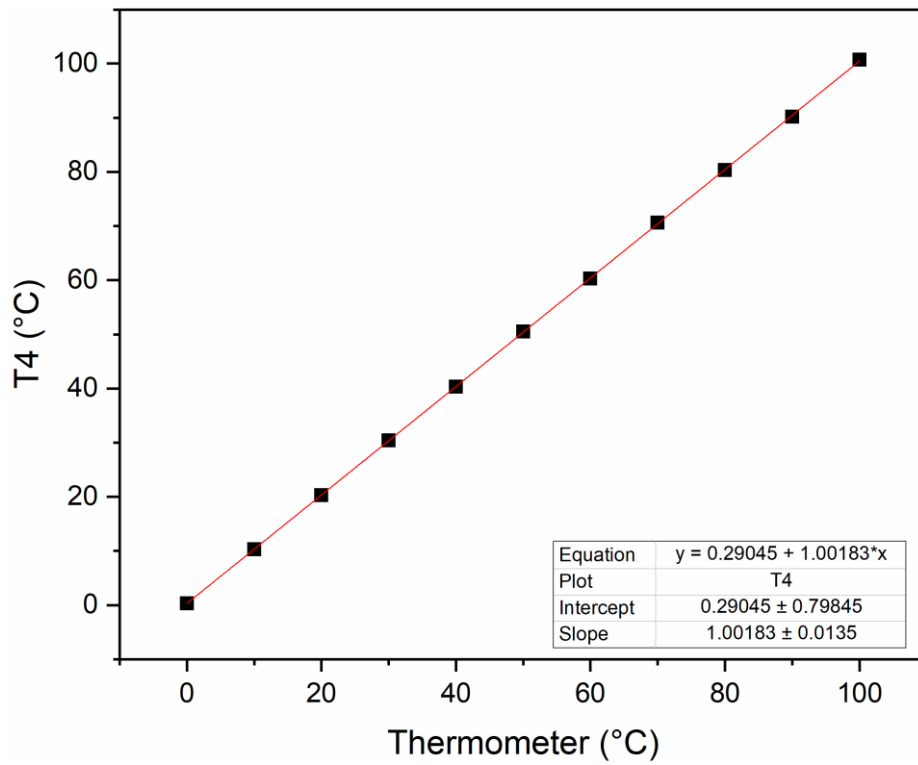


Figure A6. T4 thermocouples calibration

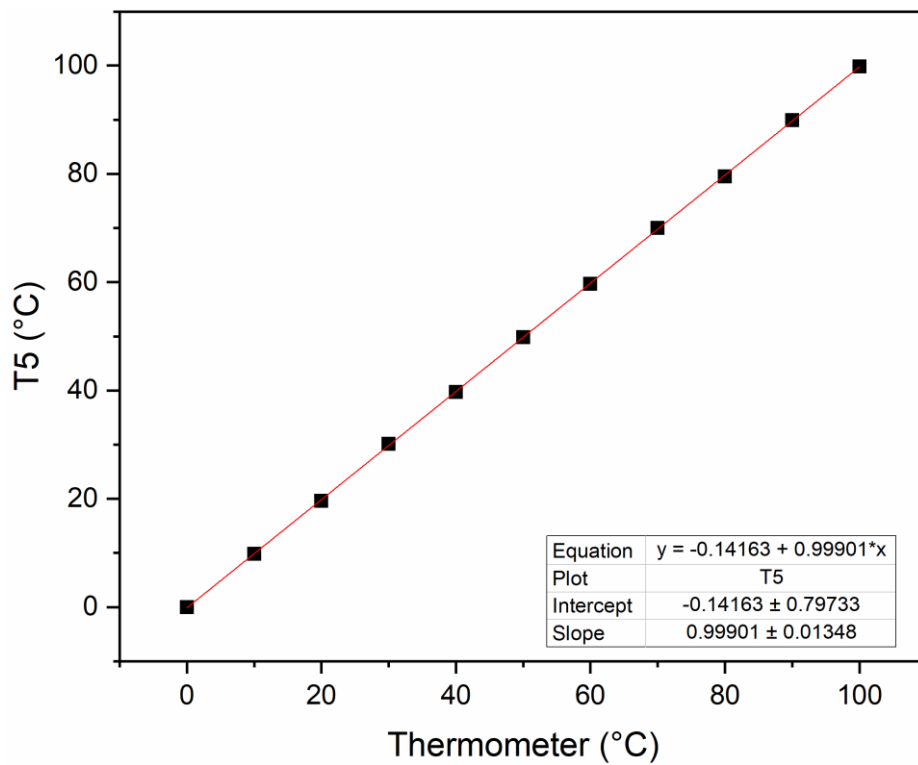


Figure A7. T5 thermocouples calibration

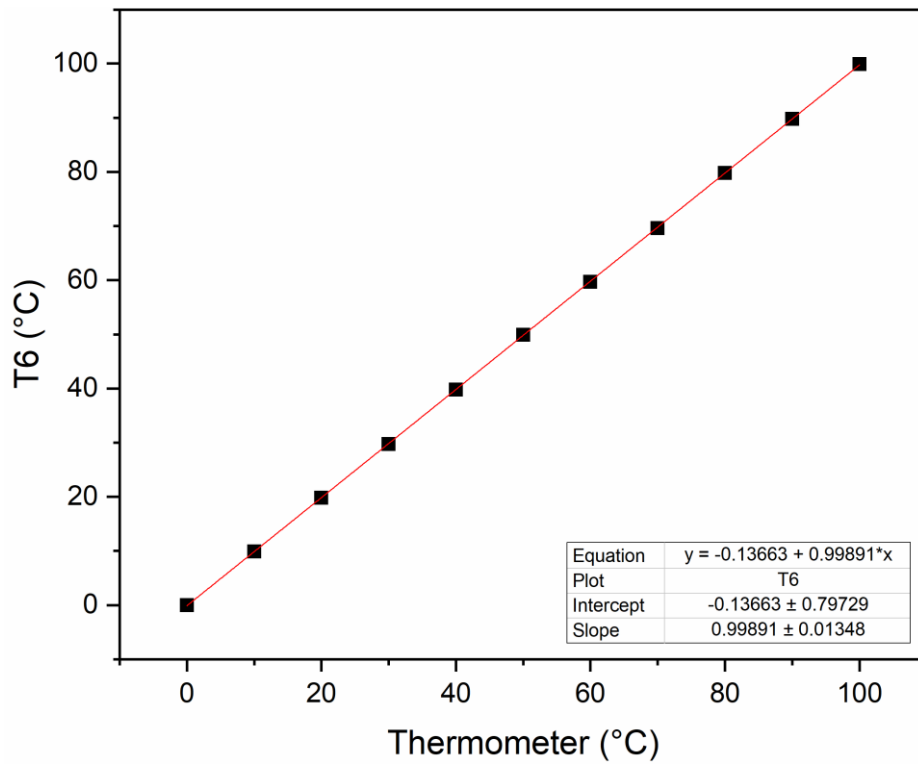


Figure A8. T6 thermocouples calibration

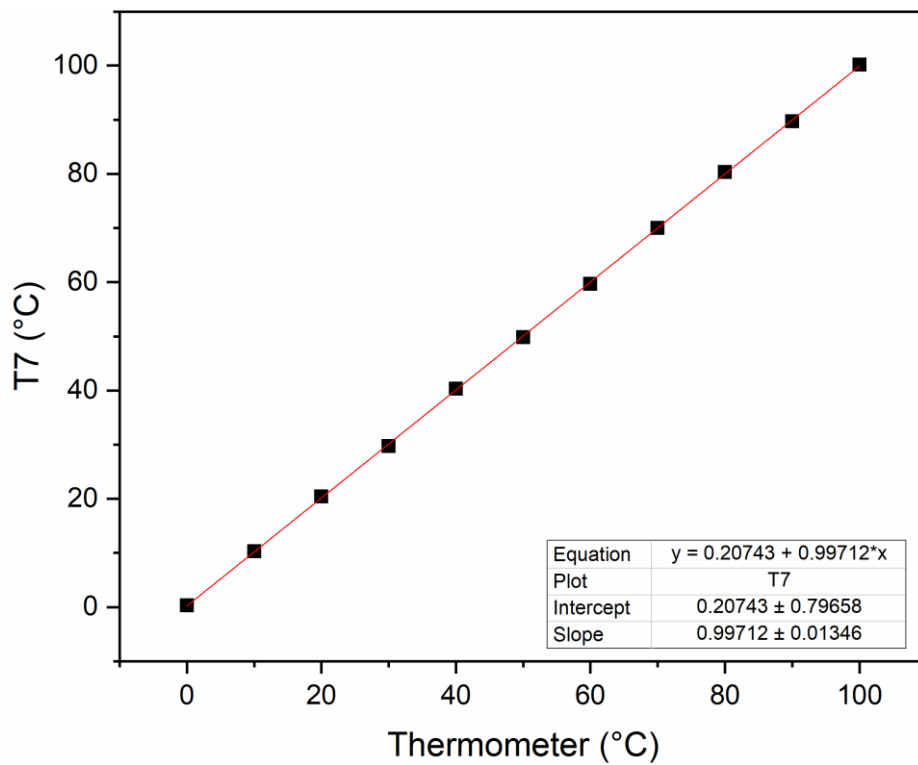


Figure A9. T7 thermocouples calibration

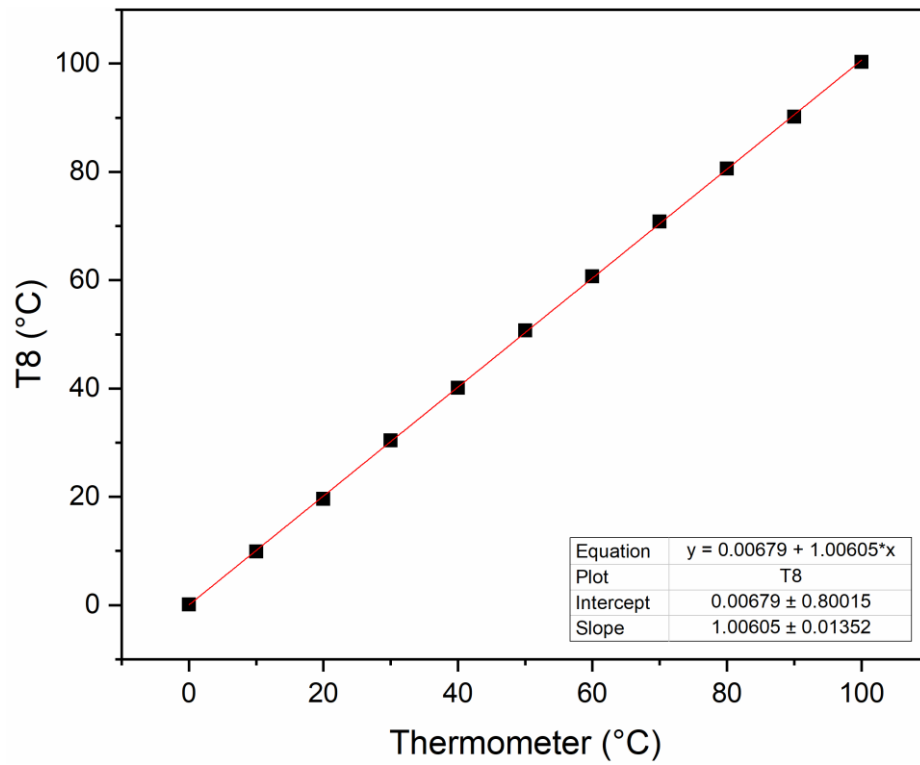


Figure A10. T8 thermocouples calibration

APPENDIX – B

NANOPARTICLE'S PROPERTIES

Nanoparticles Specifications

All nanoparticles (manufactured by Guangzhou Hongwu Material Technology Co., Ltd.) were used to prepare the nanofluids. The properties of nanoparticles are listed in Table B1. Figure (B1, B2, B3) shows scanning electron microscopy (SEM) for all nanomaterials used in the study with a certificate originating from the manufacturer.

Table B1 details and properties of nanoparticles

Details	Al ₂ O ₃	CuO	MWCNT
Appearance	White powder	Dark brown powder	Black powder
Purity	99.99%	99%	99%
Size (nm)	D: 20-30 nm	D: 30-50 nm	D: 30-60 nm L: 5-20 um
Thermal conductivity (W/m. K)	46	76.5	3000
Density (kg/m ³)	3890	6400	2100
Specific heat (j/kg. K)	778	531	769

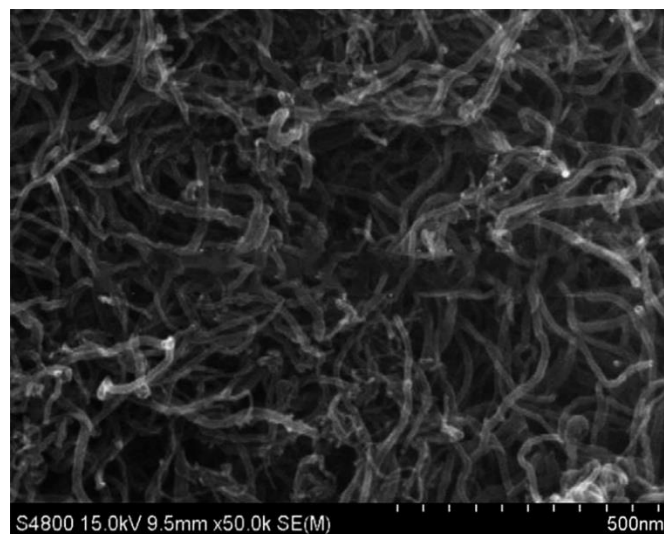


Figure B1. SEM images for MWCNT

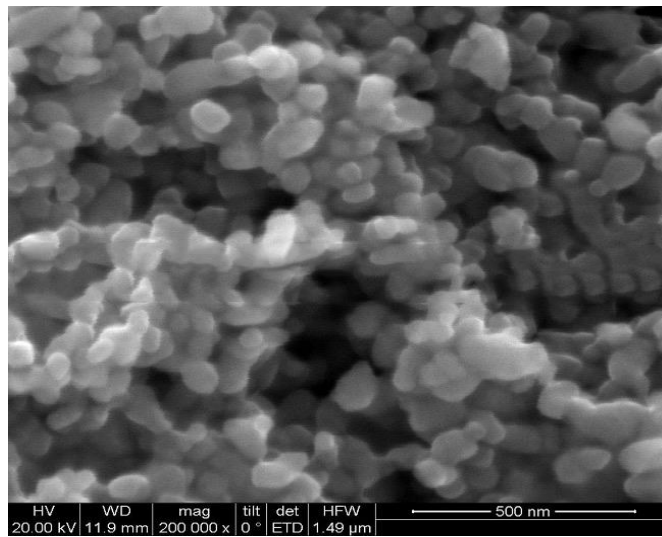


Figure B2. SEM images for CuO

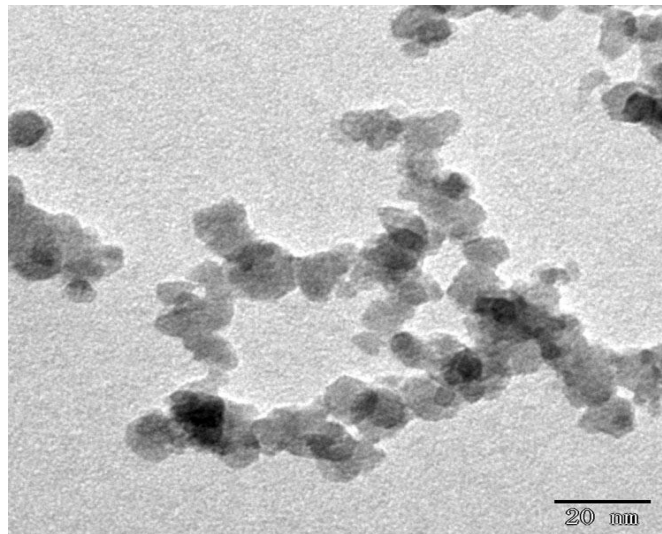


Figure B3. SEM images for Al₂O₃

Product Name	Multi-Walled Carbon Nanotube (多壁碳纳米管)	copper oxide (氧化铜)	aluminum oxide (氧化铝)	
Electrical resistivity	965.4 $\mu\Omega\cdot m$	60.6 $\mu\Omega\cdot m$	104.9 $\mu\Omega\cdot m$	合格 Conform
Electric conductivity	1035.840066 S/m	0.18 - 0.39 S/m	1*10 ⁻¹² S/m	合格 Conform
Specific surface area	90-130 m ² /g	99.67 m ² /g	118 m ² /g	合格 Conform
Bulk density	0.22g/cm ³	0.35 g/cm ³	0.355 g/cm ³	合格 Conform
True density	2.1g/cm ³	6.4 g/cm ³	3.850 g/cm ³	合格 Conform
Thermal conductivity	3000 W/m. K	76.5 W/m. K	46 W/m. K	合格 Conform

For and on behalf of
HONGWU INTERNATIONAL GROUP LTD
宏武國際集團有限公司



.....
Authorised Signature(s)

Tel: (86) 20-87226359, (86) 20-87748917

Website: www.xuzhounano.com

E-mail: hwnano@xuzhounano.com

APPENDIX – C

Uncertainty In Measurement

All quantities measured to estimate the Nusselt number and the coefficient of friction are subject to uncertainty due to errors in measurement. Quantities such as hydraulic diameter (D_h), length of tube (L), wall temperature (T_w), average fluid temperature (T_b), velocity of fluid flow (U), are measured and calculated. Possible errors in each for estimating uncertainties associated with the experimental data for heat transfer rate, Nusselt number and Reynold number. The experimental uncertainty was calculated according to ANSI/ASME standards. Uncertainties associated with the experimental data are calculated based on a 96% confidence level. Calculations indicated that the uncertainties involved in the measurements are about $\pm 4\%$ and $\pm 4.5\%$, respectively for the heat transfer coefficient and the Nusselt number. As in the following equations can be used to calculate the uncertainty of experimental data:

$$w_r = \sqrt{\sum_0^i \left(\frac{\partial R}{\partial X_i} * W_{xi} \right)^2} \quad (C-1)$$

Where

W_R = Uncertainty of the result

C1. Reynold Number Uncertainty

$$Re = \frac{\rho * v * D_h}{\mu} \quad (C-2)$$

$$\Delta Re = \left[\left(\frac{\partial Re}{\partial v} * \Delta v \right)^2 + \left(\frac{\partial Re}{\partial d} * \Delta d \right)^2 \right]^{0.5} \quad (C-3)$$

$$\Delta Re = \left[\left(\frac{\rho d}{\mu} * \Delta v \right)^2 + \left(\frac{\rho v}{\mu} * \Delta d \right)^2 \right]^{0.5} \quad (\text{C-4})$$

$$\Delta Re = \left[\left(Re * \frac{\Delta v}{v} \right)^2 + \left(Re * \frac{\Delta d}{d} \right)^2 \right]^{0.5} \quad (\text{C-5})$$

$$\frac{\Delta Re}{Re} = \left[\left(\frac{\Delta v}{v} \right)^2 + \left(\frac{\Delta d}{d} \right)^2 \right]^{0.5} \quad (\text{C-6})$$

C2. Nusselt Number Uncertainty

$$Nu = \frac{h * D_h}{k} \quad (\text{C-7})$$

$$\Delta Nu = \left[\left(\frac{\partial Nu}{\partial h} * \Delta h \right)^2 + \left(\frac{\partial Nu}{\partial d} * \Delta d \right)^2 \right]^{0.5} \quad (\text{C-8})$$

$$\Delta Nu = \left[\left(\frac{d}{k} * \Delta h \right)^2 + \left(\frac{h}{k} * \Delta d \right)^2 \right]^{0.5} \quad (\text{C-9})$$

$$\Delta Nu = \left[\left(Nu * \frac{\Delta h}{h} \right)^2 + \left(Nu * \frac{\Delta d}{d} \right)^2 \right]^{0.5} \quad (\text{C-10})$$

$$\frac{\Delta Nu}{Nu} = \left[\left(\frac{\Delta h}{h} \right)^2 + \left(\frac{\Delta d}{d} \right)^2 \right]^{0.5} \quad (\text{C-11})$$

C-3. heat transfer coefficient Uncertainty

$$Q = h * A_s * (T_w - T_b) \quad (\text{C-11})$$

$$h = \frac{Q}{A_s * \Delta T} \quad (\text{C-12})$$

$$\Delta h = \left[\left(\frac{\partial h}{\partial Q} * \Delta Q \right)^2 + \left(\frac{\partial h}{\partial A_s} * \Delta A_s \right)^2 + \left(\frac{\partial h}{\partial \Delta T} * \Delta(\Delta T) \right)^2 \right]^{0.5} \quad (\text{C-12})$$

$$\Delta h = \left[\left(\frac{1}{A_s \Delta T} * \Delta Q \right)^2 + \left(\frac{Q}{A_s \Delta T} * \Delta A_s \right)^2 + \left(\frac{Q}{A_s \Delta T} * \Delta(\Delta T) \right)^2 \right]^{0.5} \quad (\text{C-13})$$

$$\Delta h = \left[\left(h * \frac{\Delta Q}{Q} \right)^2 + \left(h * \frac{\Delta A_s}{A_s} \right)^2 + \left(h * \Delta \frac{(\Delta T)}{\Delta T} \right)^2 \right]^{0.5} \quad (\text{C-14})$$

$$\frac{\Delta h}{h} = \left[\left(\frac{\Delta Q}{Q} \right)^2 + \left(\frac{\Delta A_s}{A_s} \right)^2 + \left(\Delta \frac{(\Delta T)}{\Delta T} \right)^2 \right]^{0.5} \quad (\text{C-16})$$

C-4. Heat Transfer rate Uncertainty

$$Q = h * A_s * \Delta T \quad (\text{C-15})$$

$$\Delta Q = \left[\left(\frac{\partial Q}{\partial h} * \Delta h \right)^2 + \left(\frac{\partial Q}{\partial A_s} * \Delta A_s \right)^2 + \left(\frac{\partial Q}{\partial \Delta T} * \Delta(\Delta T) \right)^2 \right]^{0.5} \quad (\text{C-16})$$

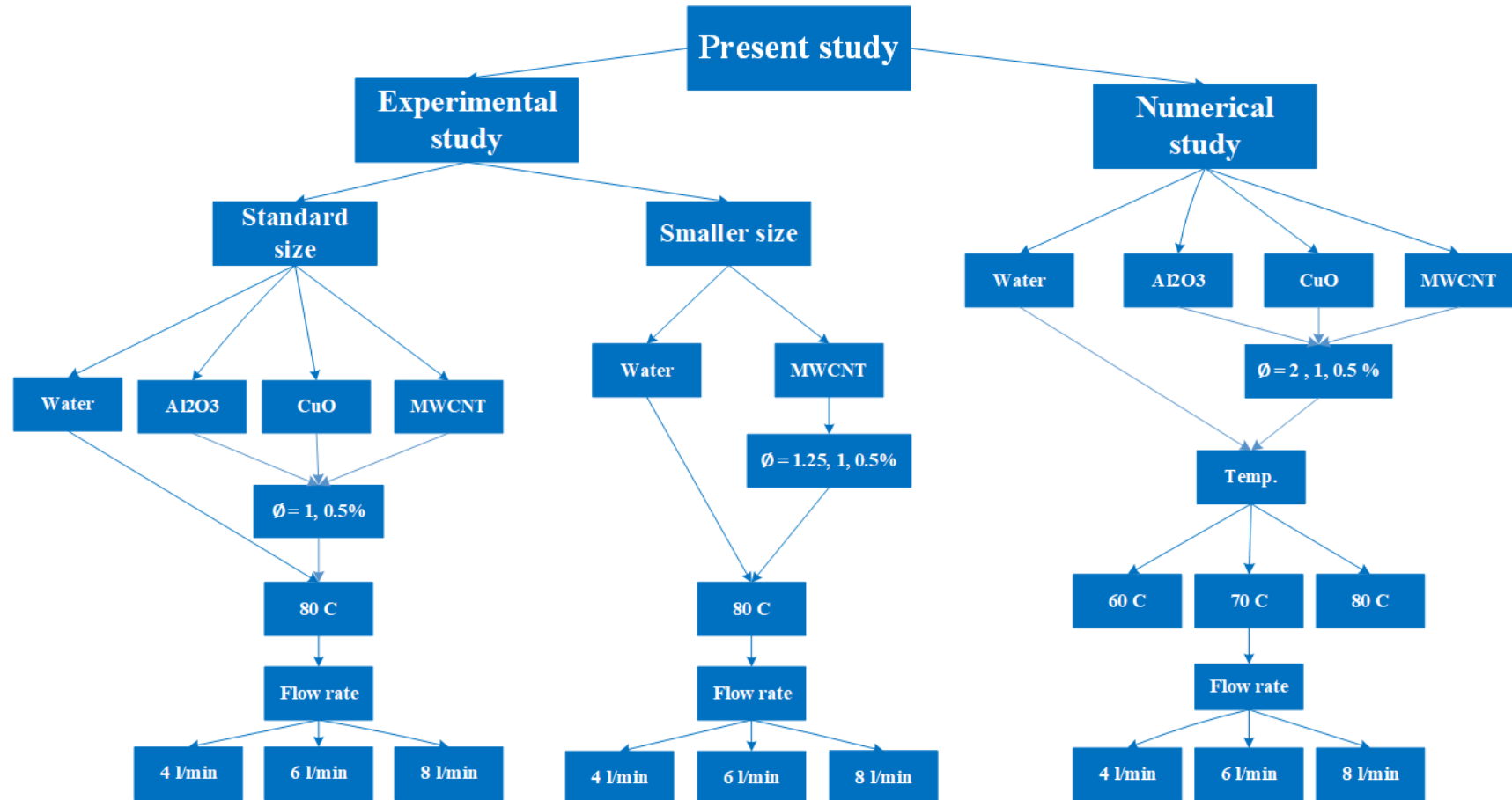
$$\Delta Q = \left[(A_s * \Delta T * \Delta h)^2 + (h * \Delta T * \Delta A_s)^2 + (h * v * \Delta(\Delta T))^2 \right]^{0.5} \quad (\text{C-17})$$

$$\Delta Q = \left[\left(Q * \frac{\Delta h}{h} \right)^2 + \left(h * \frac{\Delta A_s}{A_s} \right)^2 + \left(Q * \Delta \frac{(\Delta T)}{\Delta T} \right)^2 \right]^{0.5} \quad (\text{C-18})$$

$$\frac{\Delta Q}{Q} = \left[\left(\frac{\Delta h}{h} \right)^2 + \left(\frac{\Delta A_s}{A_s} \right)^2 + \left(\Delta \frac{(\Delta T)}{\Delta T} \right)^2 \right]^{0.5} \quad (\text{C-19})$$

APPENDIX – D

BLOCK DIAGRAM FOR OUR STUDY



APPENDIX - E

WIND SPEED CALIBRATION

In this study, an AM-4206M anemometer was used to measure wind speed. It was calibrated with the Davis standard weather station installed above the ground in the Technical College of Engineering in Najaf / Iraq. Figure D1 shows the results of the calibration.

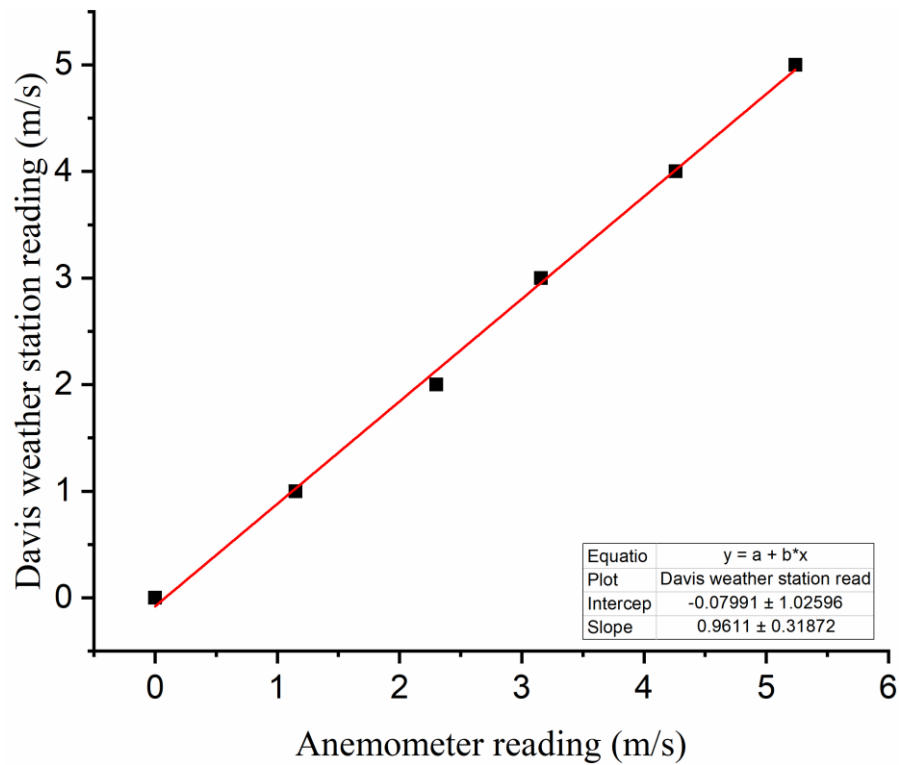


Figure D1 Anemometer Calibration

APPENDIX – F

LIST OF PUBLICATIONS

1-Karaar Mahdi Al-Araji, Dhafer Manea Hachim, Almoussawi M A, “Nano-Fluids as a Coolant for Automotive Engine Radiators: Review Study” Al-Furat Journal of Innovations in Mechanical and Sustainable Energy Engineering FJIMSE, Volume 1, Issue 2, 13 February 2021

<https://journals.atu.edu.iq/index.php/fjimse/article/view/86>



Al-Furat Journal of Innovations in Mechanical and Sustainable Energy Engineering (FJIMSE) Published by Al-Furat Al-Awsat Technical University (ATU) / Iraq



Nano-Fluids as a Coolant for Automotive Engine Radiators: Review Study

Karaar Mahdi Al-Araji^{1, a,*}, Dhafer Manea Hachim^{1, b} & Almoussawi M A^{1, c}

¹Department of Power Mechanics Engineering, Engineering Technical Collage / Al-Najaf, Al-Furat Al-Awsat Technical University (ATU), Najaf, Iraq

^akaraar.mahdi@student.atu.edu.iq

^bcoj.dfr@atu.edu.iq

^cinj.mun@atu.edu.iq

*Corresponding Contact: karaar.mahdi@student.atu.edu.iq

<https://dx.doi.org/10.52262/130221-05>

Abstract. Low-efficiency crossflow heat exchangers which are used as radiators in the automotive sector may cause engine damage. Nano-fluids are ideal coolants due to their high heat diffusion coefficient and can be added to almost any process that requires a fast reaction to thermal performance, such as the automobile. The nanofluid's thermal conductivity is greater than that of the base fluid such as water and ethylene glycol and can achieve more than 40% and enhance the heat transfer coefficient by more than 50%. The best results for heat transfer were to use carbon nanoparticles with base fluid. This article reviews previous research investigating the effect of nano-fluid in automotive radiators in which nanoparticles such as Al₂O₃, CuO, TiO₂, and MWCNT are used. The preparation and application of nano-fluid and measurement of thermal properties and the effect of volume fraction on efficiency are discussed. The review also is focused on the numerical and experimental studies of previous work related to nano-fluid performance in automobile radiators.

2- Karaar Mahdi Al-Araji, Almuoussawi M A, Kareem J. Alwana, “The Heat Transfer Performance of MWCNT, CuO, and Al₂O₃ Nanofluids in an Automotive Engine Radiator” E3S Web Conf. Volume 286, 2021 (10th International Conference on Thermal equipment’s, Renewable Energy and Rural Development) (TE-RE-RD 2021) DOI: <https://doi.org/10.1051/e3sconf/202128601009>.

The Heat Transfer Performance of MWCNT, CuO, and Al₂O₃ Nanofluids in an Automotive Engine Radiator

Karaar Mahdi Al-Araji^{1*}, M. A. Almuoussawi¹ and Kareem J. Alwana²

¹Department of Power Mechanics Engineering, Engineering Technical Collage / Al-Najaf, Al-Furat Al-Awsat Technical University (ATU), 31001 Najaf, Iraq

²Al-Furat Al-Awsat Technical University, Najaf Technical Institute, 31001, Iraq

Abstract. The effect of enhancing heat transfer using three nanofluids, Multi-Walled Carbon Nanotubes MWCNT, Copper oxide CuO, and aluminum oxide Al₂O₃, have been experimentally studied on the automotive radiator with a concentration of 1% vol and different flow rates (4-8) l/min, air velocity of 3 m/s and inlet temperatures range (60-80) °C. The results showed that the use of nanofluids improved the thermal performance compared to the base fluid. Using the (MWCNT-Water) achieved 41.7% of Nusselt number where as, copper oxide (CuO) and aluminum oxide (Al₂O₃) have improved the Nusselt number by 31.7 % and 12.3 % respectively. The Nusselt number showed an increase with the increase in the flow rate and the inlet temperature.

Keywords: Nanofluid, Al₂O₃, CuO, MWCNT, Automotive engine radiator, Nusselt number.

الخلاصة

يمكن تحسين أداء محركات السيارات عن طريق إزالة كمية الحرارة المتولدة من الاحتراق الداخلي من خلال المشعات عن طريق تعزيز سائل التبريد. كان استخدام الموائع النانوية أحد أسباب تقليل كمية الحرارة وزيادة الأداء الحراري للمحرك. تتمتع معظم السوائل الأساسية بأداء حراري منخفض. ومع ذلك ، يمكن زيادة كفاءتها الحرارية باستخدام الجسيمات النانوية ، والسوائل النانوية عبارة عن سوائل غروانية تتكون من جسيمات بحجم النانو >100 نانومتر ممزوجة بسائل أساسي. الهدف من الدراسة هو تقليل حجم المبرد ودراسة التحليل الاقتصادي لاستخدام الموائع النانوية في مشعات السيارات. في هذا العمل ، تمت دراسة تأثير السوائل النانوية على الأداء الحراري لمشعات السيارات عدديًا وتجريبيًا. تم إجراء الدراسة العددية باستخدام برنامج (COMSOL Multiphysics V.5.4) على ثلاثة أنواع من السوائل النانوية (MWCNT, CuO, Al₂O₃) بتركيزات حجم مختلفة (2,1,0.5%) ومعدل تدفق مختلف (4 ، 6 ، 8) لتر / دقيقة ودرجة حرارة دخول (60 ، 70 ، 80) درجة مئوية. تم إجراء التجارب على اثنين من مشعات السيارات المختلفة ، الحجم العادي مع 60 أنبوبًا والحجم الأصغر بنسبة 35٪ من حجم المبرد العادي. تم اختبار الأنواع الثلاثة من الموائع النانوية على المبرد لمقارنة أدائها الحراري فيما يتعلق بالسائل الأساسي. تمت مقارنة النتائج الحالية بالدراسات السابقة بدرجة عالية من الرصانة للتحقق من النتائج العددية ، حيث وجدنا توافق جيد بنسبة 6.2٪ تقريبًا ، وللتحقق من النتائج التجريبية ، تمت مقارنة النتائج مع الارتباطات التي تمثل التدفق الصفحي داخل الأنابيب ، و أظهرت النتائج توافقًا جيدًا بنسبة 6.7٪ تقريبًا. أظهرت النتائج العددية أن أفضل أداء حراري كان سائل نانوي انابيب الكربون متعدد الجدران النانوية ، حيث تم الحصول على أعلى نسبة تحسن لعدد نسلت 25.83٪ ، 42.37٪ ، 59.7٪ بتركيز حجم 0.5 ، 1 ، 2٪ على التوالي. . أظهرت نتائج التجربة أن الموائع النانوية تعمل بأداء

حراري أعلى من السوائل الأساسية. أعلى رقم لـ Nusselt عند استخدام انابيب الكربون متعدد الجدران النانوية كان 26.6% ، 42% بتركيز حجمي 0.5 ، 1% مقارنة بالسائل الأساسي. أظهر التحليل الاقتصادي للدراسة التجريبية أنه من الممكن تقليل حجم مشعاع السيارة بنسبة 35% ، وكذلك إعطاء مساحة إضافية وتقليل كمية سائل التبريد عند استخدام انابيب الكربون متعدد الجدران النانوية بمعدل تدفق 4 لتر / دقيقة و 80 درجة مئوية.



تطبيقات السوائل النانوية في مشعات محركات السيارات

رساله مقدمه الى

قسم هندسه تقنيات ميكانيك القوى كجزء من متطلبات نيل درجه ماجستير تقني في
هندسة الحرارية

تقدم بها

كرار مهدي صالح مهدي

اشراف

أ.د. ظافر مانع حاجم

أ.م.د. منتظر عبودي محمد

آب 2021